Vol. 133 No. 1, February 1, 1981 ISSN 0378-4304
(Computer Techniques and Optimization, Vol. 5 No. 1)

ANALYTICA CHIMICA ACTA

International journal devoted to all branches of analytical chemistry

COMPUTER TECHNIQUES AND OPTIMIZATION

ELSEVIER SCIENTIFIC PUBLISHING COMPANY

ANALYTICA CHIMICA ACTA

International journal devoted to all branches of analytical chemistry
Revue internationale consacrée à tous les domaines de la chimie analytique
Internationale Zeitschrift für alle Gebiete der analytischen Chemie

PUBLICATION SCHEDULE FOR 1981 (incorporating the section on Computer Techniques and Optimization).

	J	F	M	A	M	J	J	A	S	O	N	D
Analytica Chimica Acta	123	124/1	124/2	125	126	127	128	129	130/1	130/2	131	132
Section on Computer Techniques and Optimization		133/1			133/2			133/3			133/4	

Scope. *Analytica Chimica Acta* publishes original papers, short communications, and reviews dealing with every aspect of modern chemical analysis, both fundamental and applied. The section on *Computer Techniques and Optimization* is devoted to new developments in chemical analysis by the application of computer techniques and by interdisciplinary approaches, including statistics, systems theory and operation research. The section deals with the following topics: Computerized acquisition, processing and evaluation of data. Computerized methods for the interpretation of analytical data including chemometrics, cluster analysis, and pattern recognition. Storage and retrieval systems. Optimization procedures and their application. Automated analysis for industrial processes and quality control. Organizational problems.

Submission of Papers. Manuscripts (three copies) should be submitted as designated below for rapid and efficient handling:

Papers from the Americas to: Professor Harry L. Pardue, Department of Chemistry, Purdue University, West Lafayette, IN 47907, U.S.A.

Papers from all other countries to: Dr. A. M. G. Macdonald, Department of Chemistry, The University, P.O. Box 363, Birmingham B15 2TT, England.

For the section on *Computer Techniques and Optimization:* Dr. J. T. Clerc, Universität Bern, Pharmazeutisches Institut, Sahlistrasse 10, CH-3012 Bern, Switzerland.

American authors are recommended to send manuscripts and proofs by INTERNATIONAL AIRMAIL.

Information for Authors. Papers in English, French and German are published. There are no page charges. Manuscripts should conform in layout and style to the papers published in this Volume. Authors should consult Vol. 121, p. 353 for detailed information. Reprints of this information are available from the Editors or from: Elsevier Editorial Services Ltd., Mayfield House, 256 Banbury Road, Oxford OX2 7DE (Great Britain).

Reprints. Fifty reprints will be supplied free of charge. Additional reprints (minimum 100) can be ordered. An order form containing price quotations will be sent to the authors together with the proofs of their article.

Advertisements. Advertisement rates are available from the publisher.

Subscriptions. Subscriptions should be sent to: Elsevier Scientific Publishing Company, P.O. Box 211, 1000 AE Amsterdam, The Netherlands. The section on *Computer Techniques and Optimization* can be subscribed to separately.

Publication. *Analytica Chimica Acta* (including the section on *Computer Techniques and Optimization*) appears in 11 volumes in 1981. The subscription for 1981 (Vols. 123–133) is Dfl. 1639.00 plus Dfl. 198.00 (postage) (total approx. U.S. $942.00). The subscription for the *Computer Techniques and Optimization* section only (Vol. 133) is Dfl. 149.00 plus Dfl. 18.00 (postage) (total approx. U.S. $86.00). Journals are sent automatically by airmail to the U.S.A. and Canada at no extra cost and to Japan, Australia and New Zealand for a small additional postal charge. All earlier volumes (Vols. 1–121) except Vols. 23 and 28 are available at Dfl. 164.00 (U.S. $84.00), plus Dfl. 13.00 (U.S. $6.50) postage and handling, per volume.

Claims for issues not received should be made within three months of publication of the issue, otherwise they cannot be honoured free of charge.

Customers in the U.S.A. and Canada who wish to obtain additional bibliographic information on this and other Elsevier journals should contact Elsevier/North Holland Inc., Journal Information Center, 52 Vanderbilt Avenue, New York, NY 10017. Tel: (212) 867-9040.

ANALYTICA CHIMICA ACTA
VOL. 133 (1981)
(Computer Techniques and Optimization, Vol. 5)

ANALYTICA CHIMICA ACTA

International journal devoted to all branches of analytical chemistry

COMPUTER TECHNIQUES AND OPTIMIZATION

VOL. 5 1981

ELSEVIER SCIENTIFIC PUBLISHING COMPANY

Anal. Chim. Acta, Vol. 133 (1981)

Printed in The Netherlands

Analytica Chimica Acta, 133 (1981) 1—18
Computer Techniques and Optimization

APPLICATION OF PATTERN RECOGNITION FOR DISCRIMINATION BETWEEN ROUTINE ANALYTICAL METHODS USED IN CLINICAL LABORATORIES

ROB. T. P. JANSEN*

Department of Internal Medicine, Laboratory for Clinical Chemistry, St. Radboud Hospital, Geert Grooteplein Zuid 16, Nijmegen (The Netherlands)

FRANS W. PIJPERS and GEERT A. J. M. DE VALK

Department of Analytical Chemistry, Catholic University, Toernooiveld, Nijmegen (The Netherlands)

(Received 19th June 1980)

SUMMARY

Patterns of analytical methods, obtained from the Dutch coupled external/internal quality control program for clinical laboratories, can be described by four features: accuracy, precision, tendency to give erroneous results, and tendency to give systematically different results in different laboratories. The data base provided a maximum of six patterns per analytical method for the determination of a serum component. Unsupervised pattern recognition revealed clusters formed by the patterns in a four-dimensional space for each of the three serum components considered (inorganic phosphate, glucose and cholesterol). The detected clusters were defined as classes. Supervised techniques based on these classes showed that not all descriptors are equally important in discriminating between the clusters for different serum components. Patterns for a particular analytical method often clustered in the same class. The numerical values of the features of the patterns belonging to such a class are measures of the quality of that class. Pattern recognition provides an objective assessment of analytical methods used routinely in clinical laboratories.

In clinical chemistry, the performance of an analytical method must be studied before the method can be applied routinely to specimens from patients. The selection of a method and the criteria considered in making a decision are therefore of fundamental importance [1].

The features that describe important characteristics of an analytical method are its practicability (speed, cost, technical skill requirement, dependability and laboratory safety) and reliability (specificity, accuracy, precision and detection limit). Information is required about all these features in considering the suitability of a method. Usually information about the practicability of a method is readily available and depends on the environment of the laboratory.

Objective information about the reliability (ruggedness) of an analytical method is often difficult to obtain. If this information is not available, it

must be acquired by well-defined procedures in order to make an objective assessment.

In each trial of the national coupled external/internal quality control program in the Netherlands [2], participants submit results based on the analysis of a number of serum components in a lyophilized serum five times per week for eight weeks. To establish a "reference" overall mean value and a "reference" day-to-day standard deviation, results are removed if they contribute significantly to sources of error detected in a two-way analysis of variance with replicates [2]. After this removal, mean values for the various analytical methods are computed from the mean values of the results accepted. The day-to-day standard deviations of the analytical methods are computed from the algorithm $s_m^2 = \Sigma \phi_i s_i^2 / \Sigma \phi_i$. Here s_m is the standard deviation of method m, ϕ_i is the number of accepted results minus 1 for lab i applying method m, and s_i^2 is the variance of the accepted results from lab i.

Apart from the inaccuracy and imprecision, the percentage of removed results for a particular method is considered as a third descriptive feature. Systematic differences between users of the same analytical method is considered as a fourth feature.

Thus the national coupled external/internal program gives information about four characteristics of the analytical methods: (1) inaccuracy, i.e. the tendency of the method to give results deviating systematically from the true value; (2) imprecision, i.e. the tendency of the method to give different results for replicate measurements on the same specimen; (3) the tendency of the method to give erroneous results, e.g. values increasing or decreasing with time, weekly means deviating significantly from the overall mean, an overall mean deviating by more than 2.5 "reference" standard deviations from the "reference" value, etc. [2]; (4) the tendency of the method to give systematically different results for different users, because of differences in laboratory procedures.

An analytical method is defined here according to the method codes of the Stichting Kwaliteitsbewaking Klinisch Chemische Ziekenhuis Laboratoria (Foundation for Quality Control in Clinical Chemistry Hospital Laboratories) [3]. Two descriptive parameters are used: (a) the principle of the chemical reaction, and (b) the instrumental methodology (manual, continuous flow, discrete, centrifugal analyzer, etc.). One of the goals of this National Foundation for Quality Control is the objective assessment of analytical methods with regard to reliability. The Foundation should be able to recommend, approve or disapprove of analytical methods objectively. Accordingly, the information content of the four features describing the analytical methods must be investigated.

Pattern recognition techniques have proved useful tools for solving multidimensional problems [4]. This suggested their use in the detection of different behaviour by analytical methods. For this purpose, the computer program ARTHUR [5] was applied to the analytical methods that have been

described by the four characteristics mentioned. In this investigation, methods for the determination of three serum components, namely inorganic phosphate, glucose and cholesterol, in use by participants in the above-mentioned control program, were studied. Participants in this program submit for each trial the results for a lyophilized serum assayed five times per week during eight weeks. The results of six trials were used to obtain a maximum of six patterns per method per serum component. Patterns of analytical methods applied by less than four participants were not included in the calculations, because the statistics produce less reliable results. Pattern recognition provides information for classification of the various patterns, defines the relative importance of the four descriptors, and gives numerical correlations between the descriptors. The frequency of appearance of the patterns of an analytical method in a particular class gives information about the quality of that method. This paper presents the procedures applied.

EXPERIMENTAL

The data base was taken from a previous paper [6]. The pattern recognition techniques applied were the Zahn minimal spanning tree construction (TREE) [7] and hierarchal or Q-mode clustering (HIER) [8, 9] for unsupervised learning, and the nearest neighbor classification (KNN) and linear pattern classification (PLANE) [10—12] for supervised learning. The features of the data base were preprocessed by SCALE [8, 9], which is a method for the production of unbiased features, CORREL [13], which is a method for the detection of inter-feature correlation, WEIGHT [8, 9, 14], which deals with feature ranking, and KARLOV [15] which calculates eigenvalues and eigenvectors based on feature variances. The patterns were projected on a plane defined by the two eigenvectors with the highest amounts of information by the plotting routine VARVAR for each of the serum components. These methods of calculation are all part of the ARTHUR program [5] and are denoted by the names used there.

RESULTS AND DISCUSSION

The descriptors

Four features were used to describe the patterns (for a more detailed description of the features, see [6]): (1) the mean value of a method relative to the "reference" value (RELMV) in a trial of the external/internal quality control program [2]; (2) the day-to-day standard deviation of a method relative to the "reference" standard deviation (RELSD) in a trial; (3) the percentage of removed values for a method in a trial (PERCREM); (4) the mean relative deviation of the mean values of laboratories applying a given method from the mean value for that method in a particular trial (LABDEV) computed from the formula: $100 * \Sigma_{i=1}^{N} \{(X_i - X_m)/X_m\}/N$, where X_i is the mean value of lab i applying method m before any removal of values; X_m is

the mean value of method m after removal of erroneous results; N is the number of laboratories.

All descriptors $X_{i,j}$ (feature i of pattern j) were autoscaled to a mean of zero and a normalized standard deviation according to

$$X'_{i,j} = (X_{i,j} - \bar{X}_i)/\{\sigma_i (N-1)^{1/2}\}$$

where $X'_{i,j}$ is the new autoscaled descriptor value of feature i (i = 1—4) for pattern j, $\bar{X}_i$ is the average value of descriptor i, σ_i is the standard deviation of the i-th descriptor and N is the number of patterns in the training set. The correlation between the various features, COR(i,j), was calculated for the three serum components by the equation

$$\mathrm{COR}(i,j) = \sum_{k=1}^{N} (X_{i,k} - \bar{X}_i)(X_{j,k} - \bar{X}_j) \Big/ \left\{ \sum_{k=1}^{N} (X_{i,k} - \bar{X}_i)^2 \sum_{k=1}^{N} (X_{j,k} - \bar{X}_j)^2 \right\}^{1/2}$$

The correlation coefficients thus obtained are listed in Table 1. For glucose and cholesterol, the correlations between the features were found to be less than 0.4. For phosphate, PERCREM and LABDEV were correlated (COR = 0.6) as were RELMV and RELSD (COR = 0.6). However, in order to preserve as much information as possible, none of the features was eliminated even when the phosphate data were considered.

Unsupervised clustering

The abbreviations used for the various analytical methods are explained in Table 2. In order to find clusters, the HIER and TREE methods were applied

TABLE 1

Correlations between the features for the determinations of inorganic phosphate, glucose and cholesterol

	RELMV	RELSD	PERCREM	LABDEV
Inorganic phosphate				
RELMV	—	0.571	0.312	0.179
RELSD		—	0.227	—0.020
PERCREM			—	0.614
LABDEV				—
Glucose				
RELMV	—	—0.028	—0.019	—0.138
RELSD		—	—0.042	—0.153
PERCREM			—	0.314
LABDEV				—
Cholesterol				
RELMV	—	—0.178	—0.105	0.172
RELSD		—	—0.184	0.056
PERCREM			—	0.396
LABDEV				—

TABLE 2

Abbreviations used for the notation of the patterns of the various methods applied in the various trials

Serum component	Abbreviation	Principle of the analytical method
Inorganic phosphate	FStn[a]	automatic, continuous flow system, $SnCl_2$ reduction
	FNtn	automatic, continuous flow system, no reduction
	MFtn	manual, Fe(II) salt reduction
	MOtn	manual, organic reducing agent
Glucose	FHtn	automatic, continuous flow system, hexokinase
	DHtn	automatic, discrete, hexokinase
	MGtn	manual, glucose oxidase
	FGtn	automatic, continuous flow system, glucose oxidase
	MTtn	manual, *o*-toluidine
	APtn	automatic, polarographic
	FOtn	automatic, continuous flow system, oxidizing agent
Cholesterol	FEtn	automatic, continuous flow system, enzymatic
	DEtn	automatic, discrete, enzymatic
	CEtn	automatic, centrifugal fast analyser, enzymatic
	MEtn	manual, enzymatic

[a]tn = Trial number.

in an unsupervised fashion to training sets of 22, 40, and 24 patterns of the methods for the determination of inorganic phosphate, glucose and cholesterol, respectively. Similarity values, $S_{i,j}$, based on their mutual distances $D_{i,j}$, are defined as: $S_{i,j} = 1 - D_{i,j}/D_{max}$. The $D_{i,j}$ are Euclidean distances in the four-dimensional space spanned by the features RELMV, RELSD, PERCREM and LABDEV. For each of the three serum components studied, the patterns of the analytical methods were grouped at levels of similarity, $S_{i,j}$, in HIER, and were linked in branched chains based on the distances $D_{i,j}$ in TREE. For all three serum components, TREE could detect only one cluster of patterns. For phosphate, HIER calculated three major clusters at similarity level 0.50 (Table 3). For glucose three major clusters were detected by HIER at similarity level 0.62 (Table 4). For cholesterol also, three clusters were calculated at similarity level 0.60 (Table 5).

Feature weighting

In order to establish the relative importance of the features for classification, the autoscaled descriptors were weighted with Fisher weighting factors based on the mean values and standard deviations within each class.

TABLE 3

Hierarchal clustering of the patterns for inorganic phosphate based on the unweighted descriptors

Cluster defined as class	Pattern	Similarity values 1.0 — 0.5 — 0.0
3	MO04	0.86
	FS06	0.59
	MO06	0.50
	MF04	0.84
	MO02	0.78
	MF02	
2	MF03	0.85
	MF05	0.83
	MO05	0.74
	MF06	0.60
	MO01	0.83
	MO03	0.73
	FN01	0.69
	MF01	0.38
1	FN02	0.88
	FN04	0.77
	FS02	0.63
	FS01	0.83
	FN03	0.57
	FS05	0.73
	FS03	0.65
	FS04	0.32

The Fisher weighting factor $W(F)_{j,m,n}$ for separating class m from class n by means of descriptor j is $W(F)_{j,m,n} = \{(\overline{X'_m})_j - (\overline{X'_n})_j\}^2/(N_m\sigma^2_{m,j} + N_n\sigma^2_{n,j})$, in which $(\overline{X'_i})_j$ denotes the mean value of the autoscaled descriptor j in class i, N_i is the number of patterns in class i, and $\sigma_{i,j}$ is the standard deviation of the autoscaled descriptor j in class i. The Fisher weighting factor of descriptor j for all linear class separations, $W(F)_j$ is $W(F)_j = 2\,(\Sigma_{m=1}^{M-1}\,\Sigma_{n=m+1}^{M} W(F)_{j,m,n})/\{M(M-1)\}$, in which M denotes the number of classes.

Initial training sets

Based on the results of the hierarchal clustering without supervision, initial training and evaluation sets were formed for the three serum components. The clusters found in Tables 3—5 are now defined as classes. Patterns not clearly clustering in a particular class were put in an evaluation set.

In order to visualize the classes and possible intra-class pattern distributions, Karhunen—Loève transformations were performed, which constructed eigenvectors from linear combinations of the four descriptors, Fisher-weighted for the various classes of Tables 3—5. These eigenvectors are

TABLE 4

Hierarchal clustering of the patterns for glucose based on the unweighted descriptors

Cluster defined as class	Pattern	Similarity values 1.0 — 0.5 — 0.0
1	FG01	0.93
	FG03	0.85
	MG01	
	AP02	0.80
	MT04	0.93
	MG06	0.87
	MG02	0.72
	MG05	0.87
	MG03	0.82
	FG04	0.88 0.70
	AP03	0.77
	AP04	
	DH05	0.88 0.68
	DH06	0.78
	DH03	
	AP01	
2	FO01	0.85
	FO03	0.73
	FO02	0.58
	FO05	0.87 0.70
	FO06	0.82
	MT01	0.75 0.67
	MT06	
	MT03	0.65
	FH04	0.83
	FH06	0.77 0.52
	FO04	
3	MG04	0.92
	FG06	0.78
	FG05	0.73
	FH03	0.70
	DH04	0.62 0.48
	AP05	0.68
	AP06	0.57
Evaluation set	MT05	0.35
	FH01	0.75
	FG02	0.67
	FH02	0.38
	FH05	
	MT02	

TABLE 5

Hierarchal clustering of the patterns for cholesterol based on the unweighted descriptors

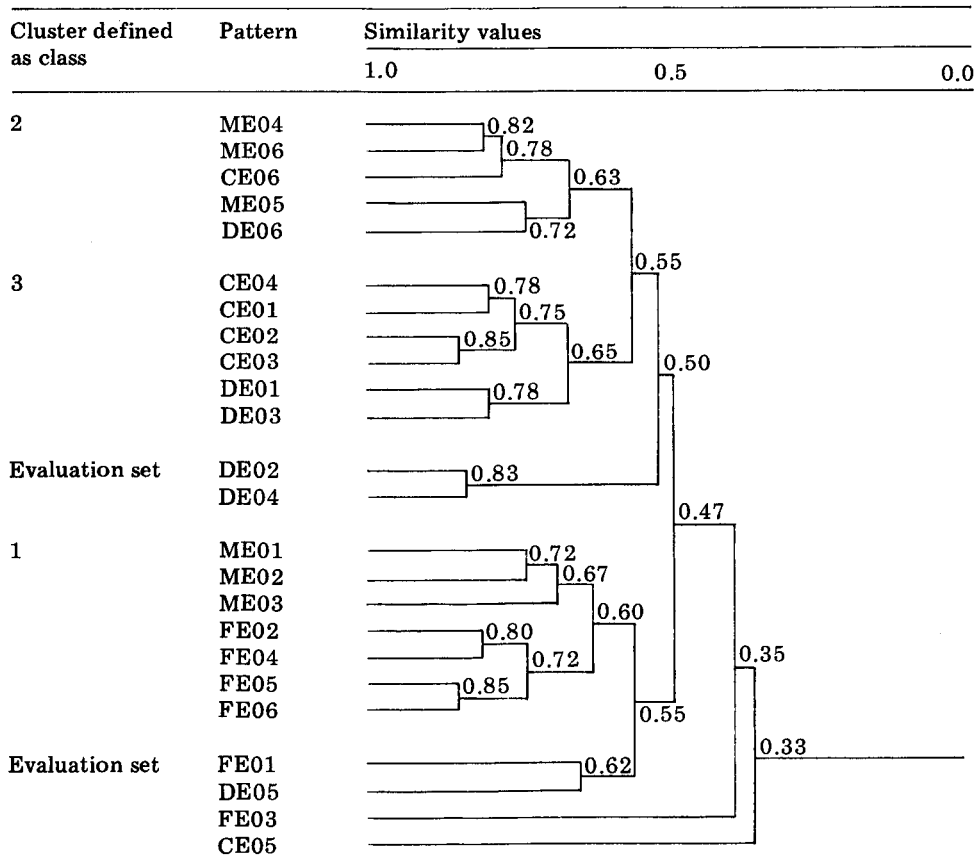

ranked on the base of their information content. The percentage amounts of information comprised in the k-th eigenvector, $\mathrm{Info}(E)_k$, the eigenvectors and the descriptor weightings are listed in Tables 6—8 for phosphate, glucose and cholesterol, respectively. For all three serum components the first two eigenvectors yielded more than 90% of all information. Figures 1—3 present the projections of the patterns of the training and evaluation sets on planes defined by their first two eigenvectors of $W(F)_{j,m,n}$ for inorganic phosphate, glucose and cholesterol, respectively.

For phosphate, Fig. 1 reveals that the classes formed in Table 3 needed no further adaptation. For glucose, Fig. 2 shows that the cluster defined as class 1 in Table 4 is separated into two classes. Three patterns of class 1 are misclassified (patterns MG04, MG05, and FO04), and two patterns of class 2 are misclassified (patterns FH06, MT06), as is one pattern of class 3 (pattern FG05). The patterns of the evaluation set all obviously belong to a

TABLE 6

Fisher weightings and eigenfunctions based on the Fisher-weighted features for the descriptors of the training set for inorganic phosphate

Descriptor	$W(F)_j \times 10^2$	% of total	Eigenvectors of the $W(F)_{j,m,n}$ matrix (columns)			
RELMV	11.60	6.9	0.0296	−0.1539	−0.0085	−0.9876
RELSD	43.39	25.7	0.0084	−0.9543	−0.2578	−0.1512
PERCREM	34.55	20.5	0.2897	−0.2414	0.9254	−0.0383
LABDEV	78.98	46.9	0.9566	0.0863	−0.2778	−0.0176
Eigenvalues Info$(E)_k$ (% of total) of $W(F)_{j,m,n}$ matrix			71.4	21.4	6.3	0.9

TABLE 7

Fisher weightings and eigenfunctions based on the Fisher-weighted features for the descriptors of the initial training set for glucose

Descriptor	$W(F)_j \times 10^2$	% of total	Eigenvectors of the $W(F)_{j,m,n}$ matrix (columns)			
RELMV	36.15	50.3	0.9705	−0.2400	−0.0211	0.0027
RELSD	1.33	1.8	−0.0001	0.0069	0.0447	0.9990
PERCREM	15.99	36.1	−0.2334	−0.9582	0.1654	−0.0008
LABDEV	8.45	11.8	−0.0600	−0.1555	−0.9850	−0.0452
Eigenvalues Info$(E)_k$ (% of total) of $W(F)_{j,m,n}$ matrix			65.6	31.8	2.5	0.1

TABLE 8

Fisher weightings and eigenfunctions based on the Fisher-weighted features for the descriptors of the initial training set for cholesterol

Descriptor	$W(F)_j \times 10^2$	% of total	Eigenvectors of the $W(F)_{j,m,n}$ matrix (columns)			
RELMV	62.69	44.7	−0.0933	−0.9956	−0.0031	0.0021
RELSD	0.47	0.4	0.0012	0.0020	0.0236	0.9997
PERCREM	4.96	3.5	0.0285	−0.0059	0.9993	−0.0236
LABDEV	72.09	51.4	0.9952	−0.0932	−0.0289	−0.0003
Eigenvalues Info$(E)_k$ (% of total) of $W(F)_{j,m,n}$ matrix			57.0	42.8	0.2	0.0

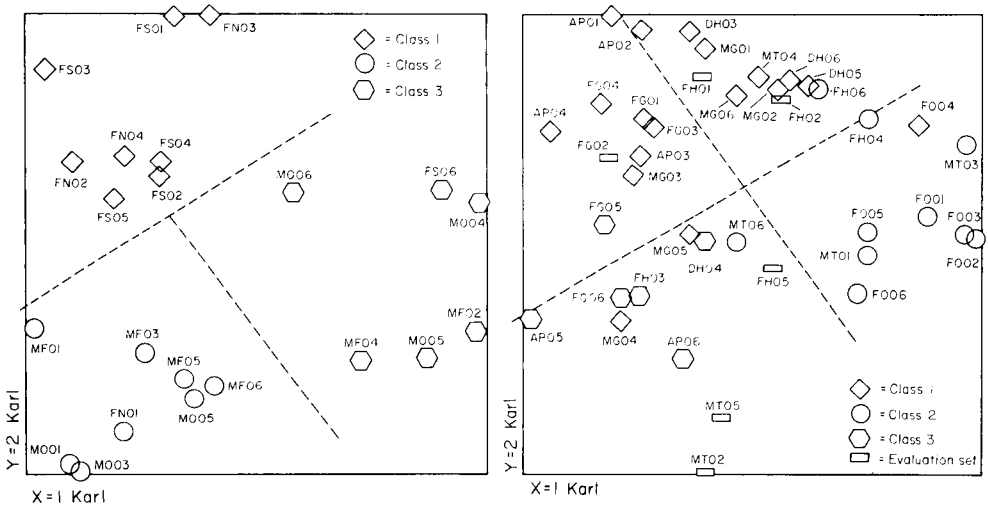

Fig. 1. Projection of the training set for inorganic phosphate on a plane defined by the most important eigenvectors of the Karhunen—Loève transformation listed in Table 6. Patterns are indicated by the abbreviations defined in Table 2. Patterns of classes defined in Table 3 are depicted by the indicated symbols. Classes detected in the KARLOV projection are depicted by lines.

Fig. 2. Projection of the initial training and evaluation set for glucose on a plane defined by the most important eigenvectors of the Karhunen—Loève transformation listed in Table 7. Patterns are indicated by the abbreviations defined in Table 2. Patterns of classes defined in Table 4 are depicted by the indicated symbols. Classes detected in the KARLOV projections are depicted by lines.

distinct class. Based on this KARLOV projection, a new training set and a new evaluation set were formed (Table 9). For cholesterol, Fig. 3 reveals that two patterns of the evaluation set and one pattern of class 2 do not definitely belong to class 1 or class 2. All other patterns of the evaluation set classify obviously in a category. For cholesterol, a new training set and a new evaluation set were also formed (Table 9).

Final training sets of phosphate, glucose and cholesterol

The descriptor weightings for the final training sets for phosphate, glucose and cholesterol are listed in Tables 6 and 10. After the relative importance of the features for classification had been determined, the classifications based on the hierarchal clustering and on the minimal spanning tree were re-evaluated in a supervised calculation by using the four descriptors Fisher-weighted for the various classes for the three serum components. The results are presented in Tables 11—13 for HIER, and Fig. 4 for TREE, for phosphate, glucose and cholesterol.

HIER. For glucose (Table 12) class 1 is separated into two smaller classes both combined at similarity level 0.72. For phosphate and cholesterol, the classes are not further subdivided.

TABLE 9

Composition of the classes of the final training set and the evaluation set for glucose and cholesterol based on the KARLOV projections of Figs. 2 and 3, respectively

	Class	Patterns
Glucose		
Training set	1	FH01, FH02, FH06, DH03, DH05, DH06, MG01, MG02, MG06, MT04
	2	FH03, FH05, DH04, MG04, MG05, MT02, MT05, MT06, AP06, FG06
	3	FG01, FG02, FG03, FG04, FG05, AP03, AP04, MG03
	4	FO01, FO02, FO03, FO04, FO05, FO06, MT01, MT03
Evaluation set	?	FH04, AP01, AP02, AP05
Cholesterol		
Training set	1	FE02, FE04, FE05, FE06, ME01, ME02, ME03, DE05
	2	MA05, MA06, CA06, DI06
	3	CE01, CE02, CE03, CE04, CE05, DE01, DE02, DE03, DE04
Evaluation set	?	FE01, FE03, ME04

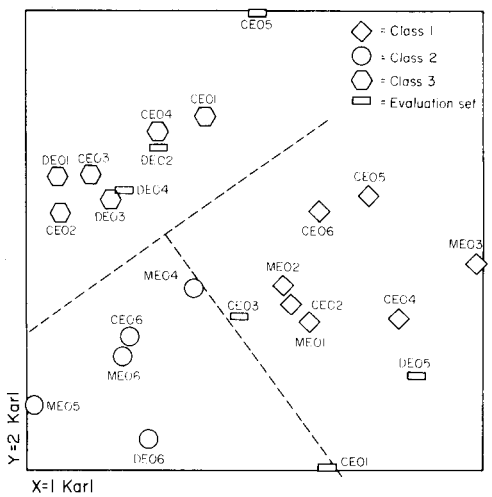

Fig. 3. Projection of the initial training and evaluation set for cholesterol on a plane defined by the most important eigenvectors of the Karhunen—Loève transformation listed in Table 8. Patterns are indicated by the abbreviations defined in Table 2. Patterns of classes defined in Table 5 are depicted by the indicated symbols. Classes detected in the KARLOV projection are depicted by lines.

TABLE 10

Fisher weightings and eigenfunctions based on the Fisher-weighted features for the descriptors of the final training set for glucose and cholesterol

Descriptor	$W(F)_j \times 10^2$	% of total	Eigenvectors of the $W(F)_{j,m,n}$ matrix (columns)			
Glucose						
RELMV	100.10	65.6	0.9999	−0.0122	−0.0035	−0.0002
RELSD	1.83	1.1	0.0017	0.0021	0.4377	0.8991
PERCREM	53.79	32.0	−0.0122	−0.9998	0.0127	−0.0039
LABDEV	2.15	1.3	−0.0032	−0.0130	−0.8990	0.4377
Eigenvalues Info$(E)_k$ (% of total) of $W(F)_{j,m,n}$ matrix			80.7	19.3	0.0	0.0
Cholesterol						
RELMV	58.16	46.8	0.3582	−0.9337	−0.0044	0.0001
RELSD	0.02	0.1	−0.0000	0.0001	0.0030	1.0000
PERCREM	1.53	1.2	0.0078	0.0077	−0.9999	0.0030
LABDEV	64.47	51.9	0.9336	0.3581	0.0101	−0.0001
Eigenvalues Info$(E)_k$ (% of total) of $W(F)_{j,m,n}$ matrix			56.9	43.1	0.0	0.0

TREE. For all three constituents the patterns of the analytical methods are arranged according to the classes formed. Fig. 4A shows the spanning tree for phosphate in which the lengths of the interconnecting lines between the patterns represent distances $D_{i,j}$; in this supervised method, TREE calculated a single cluster. Figure 4B shows the tree for glucose; TREE calculated three clusters combining class 1 and 3. For cholesterol (Fig. 4C) TREE calculated three clusters in accordance with the three classes.

KARLOV projections. The Karhunen—Loève projections of the patterns of the final training set for phosphate have been presented in Fig. 1. For glucose and cholesterol the first two eigenvectors of the Fisher-weighted data of the respective final training sets yield 100% of all information, as can be seen from Table 10. Figure 5 presents the projections of the patterns of the final training sets and the evaluation sets on planes defined by the first two eigenvectors for glucose and cholesterol, respectively. The results improve the class separation given by HIER and TREE for glucose in separating classes 1 and 3, and confirm the classes of phosphate and cholesterol.

Other supervised classification methods

Supervised classification methods were applied to the training and evaluation sets of the various serum constituents. One of those methods is based on the nearest neighbor of a Fisher-weighted pattern vector in the n-dimensional space by using distances $D_{i,j}$ as previously defined. The results of 1—5 nearest neighbor classifications are considered here.

TABLE 11

Hierarchal clustering of the patterns of the final training set for inorganic phosphate based on the Fisher-weighted descriptors

Class	Pattern	Similarity values
		1.0 0.5 0.0
1	FS04	
	FN04	
	FN02	
	FS02	
	FS05	
	FS01	
	FN03	
	FS03	
2	MF05	
	MF06	
	MO05	
	MF03	
	MO01	
	MO03	
	FN01	
	MF01	
3	MF04	
	MO02	
	MF02	
	MO04	
	FS06	
	MO06	

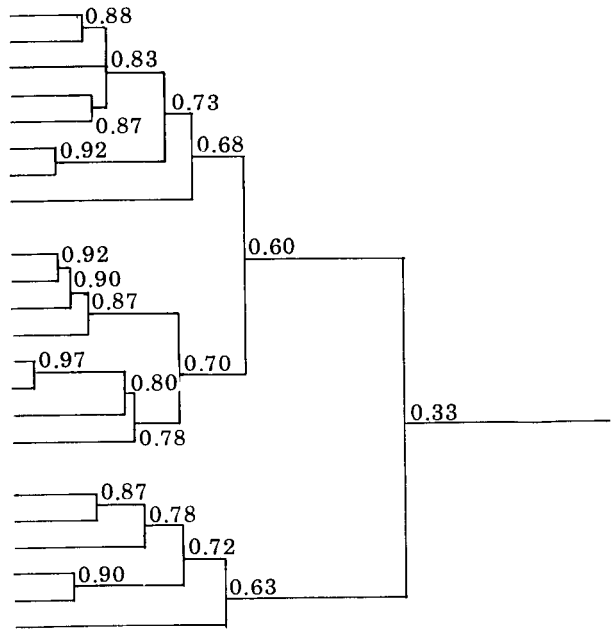

For glucose, DH03 was misclassified once in class 3. All other patterns of phosphate, glucose and cholesterol were unequivocally correctly classified by their neighbors. A second classification with supervision was based on the binary classifier PLANE, that separates all possible pairs of classes by using negative feedback training. The classification with PLANE indicates the quality of the training set because, when one or more class separations are unsuccessful, the quality of the training set classification is usually poor and its success as a classifier is limited. The separation with PLANE was 100% successful for all pairs of classes for all three serum components.

The classification by the various methods of the members of the evaluation sets are summarized in Table 14. Even though the classification of these patterns is not as explicit as the classification of the members of the training sets, it can be observed that the patterns of the various analytical methods usually are classified in the classes where the patterns of the corresponding methods of the training sets cluster.

TABLE 12

Hierarchal clustering of the patterns of the final training set for glucose based on the Fisher-weighted descriptors

Class	Pattern	Similarity values
		1.0 0.5 0.0
3	FG01	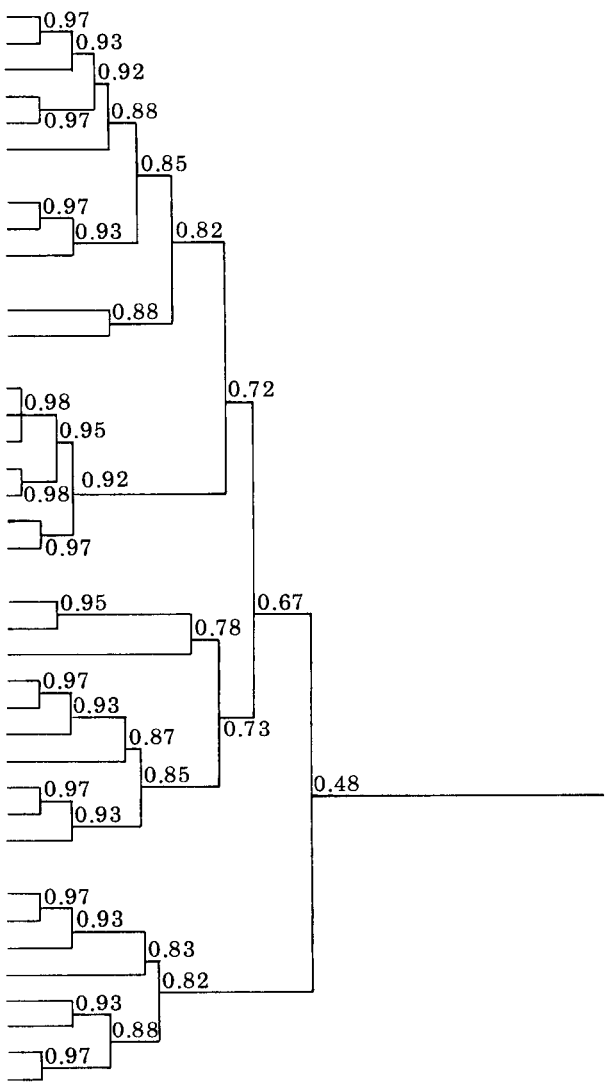
	FG03	
	FG02	
	MG03	
	AP03	
	FG05	
1	MG01	
	FH01	
	DH03	
3	FG04	
	AP04	
1	FH02	
	DH06	
	MG02	
	FH06	
	DH05	
	MG06	
	MT04	
2	MT02	
	MT05	
	FH05	
	MG05	
	DH04	
	MT06	
	AP06	
	MG04	
	FG06	
	FH03	
4	MT01	
	FO05	
	FO06	
	FO04	
	FH03	
	FO01	
	FO02	
	FO03	

TABLE 13

Hierarchal clustering of the patterns of the final training set for cholesterol based on the Fisher-weighted descriptors

Class	Pattern	Similarity values
		1.0 0.5 0.0
3	CE03	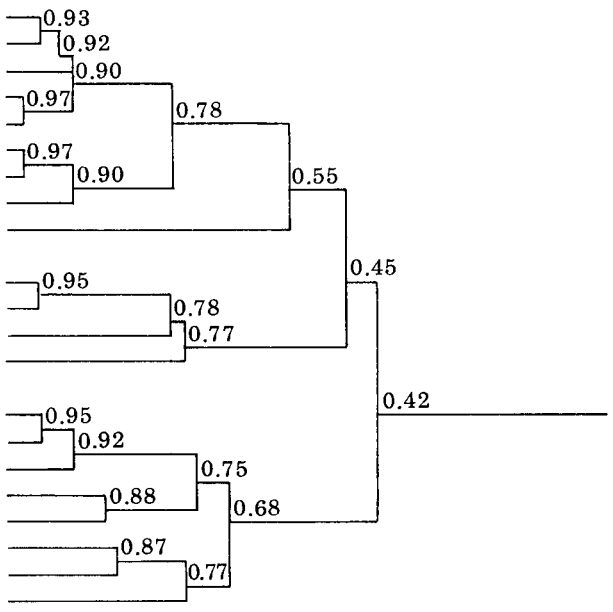
	DE01	
	CE02	
	DE03	
	DE04	
	CE04	
	DE02	
	CE01	
	CE05	
2	ME06	
	CE06	
	DE06	
	ME05	
1	FE02	
	ME02	
	ME01	
	FE05	
	FE06	
	FE04	
	DE05	
	ME03	

CONCLUSIONS

From the results presented, it can be concluded that the strategy followed in applying the various pattern recognition techniques can be successful for discrimination between analytical methods that are described by the four features used above. The detected clusters, defined as classes, often contain a majority of the patterns of one single method or are formed by patterns of analytical methods based on similar techniques (see Tables 3 and 9 in combination with Table 2). Another merit of the pattern recognition techniques is the revelation that, for different serum components, the four features alternately are of importance in discriminating between the clusters. The feature values of the various classes are measures of the quality of these classes. The frequency of appearance of the patterns of an analytical method in a particular class can be correlated with the performance of that method. If most of the patterns of an analytical method cluster in the class with the best feature values, this analytical method can be recommended. If the patterns of an analytical method belong to many different classes or to no

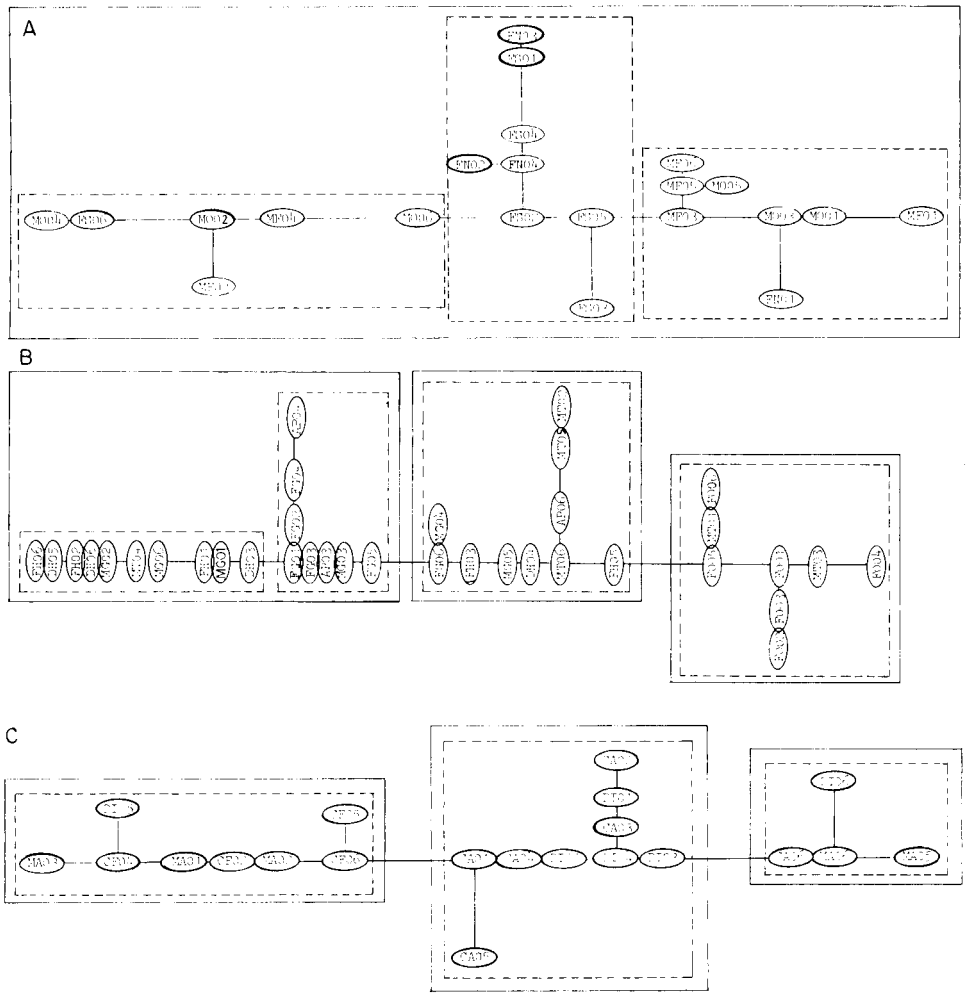

Fig. 4. Zahn minimal spanning tree of the final training set patterns based on Euclidean distances and Fisher-weighted descriptors. (—) cluster calculated by TREE; (- - - -) class defined in Tables 3 and 9. (A) Inorganic phosphate; (B) glucose; (C) cholesterol.

class at all, the method can be disapproved. Other analytical methods can be approved, if necessary, with annotations concerning the feature values to be expected. Thus pattern recognition offers the possibility of assessing analytical methods objectively.

The number of patterns is still limited, but as a practical example, the following recommendations can be made tentatively for glucose. Both automatic hexokinase techniques considered can be recommended as the majority of their patterns classify in the best category (category 1: no bias; lowest PERCREM values). The continuous flow—glucose oxidase techniques

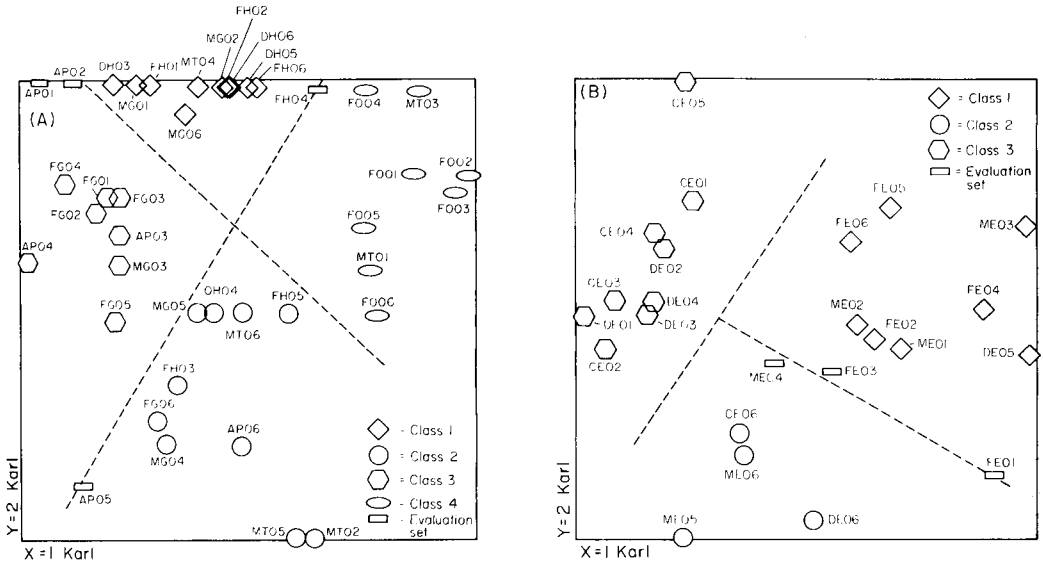

Fig. 5. Projection of the final training set and evaluation set for (A) glucose and (B) cholesterol, on a plane defined by the most important eigenvectors of the Karhunen—Loève transformation listed in Table 10. Patterns are indicated by the abbreviations defined in Table 2. Patterns of classes defined in Table 9 are depicted by the indicated symbols. Classes detected in the KARLOV projection are depicted by lines.

TABLE 14

Classification of the members of the evaluation sets for glucose and cholesterol by various classification methods

	Pattern	KARLOV projection 1—2	KNN	PLANE
Glucose	FH04	1 (4)	1 (4)	4
	AP01	3 (1)	3	3
	AP02	3 (1)	3 (1)	3
	AP05	2 (3)	3 (2)	3
Cholesterol	FE01	1 (2)	1	1 (2)
	FE03	1 (2)	1	1
	ME04	1 (2)	1 (2)	1

can also be approved, as well as the automatic polarographic techniques; both would have the annotation: slight negative bias. The continuous flow—aspecific oxidizing agent techniques should be approved also (annotation: positive bias). Both manual techniques should be disapproved because the patterns considered are classified in three categories.

We thank Prof. G. Kateman and Prof. A. P. Jansen for their critical remarks, and Prof. B. R. Kowalski for making the computer program ARTHUR available.

REFERENCES

1 J. Büttner, R. Borth, J. H. Boutwell, P. M. G. Broughton and R. C. Bowyer, Clin. Chim. Acta, 98 (1979) 145F.
2 R. T. P. Jansen and A. P. Jansen, Clin. Chim. Acta, 107 (1980) 185.
3 A. P. Jansen, E. J. van Kampen, B. Leijnse, C. A. M. Meijers and P. J. J. van Munster, Clin. Chim. Acta, 74 (1977) 191.
4 F. W. Pijpers, H. L. M. van Gaal and J. G. M. van der Linden, Anal. Chim. Acta, 112 (1979) 199.
5 D. L. Duewer, J. R. Koskinen and B. R. Kowalski, Laboratory for Chemometrics, Department of Chemistry BG-10, University of Washington, Seattle, WA.
6 R. T. P. Jansen, F. W. Pijpers and G. A. J. M. de Valk, Ann. Clin. Biochem., submitted for publication.
7 H. C. Andrews, Introduction to Mathematical Techniques in Pattern Recognition, Wiley-Interscience, New York, 1972.
8 B. R. Kowalski and C. F. Bender, J. Am. Chem. Soc., 94 (1972) 5632.
9 P. C. Jurs and T. L. Isenhour, Chemical Applications of Pattern Recognition, Wiley, New York, 1975.
10 D. R. Preus and P. C. Jurs, Anal. Chem., 46 (1974) 520.
11 T. L. Isenhour, B. R. Kowalski and P. C. Jurs, C. R. C. Crit. Rev. Anal. Chem., 4 (1974) 1.
12 P. C. Jurs, B. R. Kowalski, T. L. Isenhour and C. N. Reilly, Anal. Chem., 41 (1969) 69.
13 O. L. Davies and P. L. Goldsmith, Statistical Methods for Research and Production, Hafner, New York, 1972, p. 234.
14 R. A. Fisher, Ann. Eugen., 7 (1936) 179.
15 B. R. Kowalski and C. F. Bender, J. Am. Chem. Soc., 95 (1973) 686.

Analytica Chimica Acta, 133 (1981) 19—29
Computer Techniques and Optimization

A COMPUTER-AIDED SYSTEM FOR ORGANIC FUNCTIONAL GROUP DETERMINATIONS*

M. FARKAS*, J. MARKOS, P. SZEPESVÁRY, I. BARTHA, G. SZALONTAI and Z. SIMON

Research Institute for Heavy Chemical Industries NEVIKI, H-8201 Veszprém (Hungary)

(Received 9th November 1979)

SUMMARY

The computerized system ASSIGNER is designed to assist in structure elucidation of organic compounds. The system can operate in both on-line and off-line modes, yielding a list of possible functional groups consistent with the measured data and with the stored spectroscopic and chemical information.

Pesticide research is the main field of activity of this Institute, so that the main analytical load is the identification and/or structure determination of new synthetic organic compounds, metabolites and decomposition residues. The practical aim of the computerized analytical system ASSIGNER, which has been developed in recent years, is to provide support for the general work of structure elucidation of organic compounds. Several methods are known for computer-aided structure recognition from spectroscopic data. These methods can be divided into two types, which use fundamentally different approaches. In the first type of method, stored spectra of chemical compounds are compared with the measured spectra of unknown compounds using different search strategies [1—7]. The output is usually a ranked list of reference compounds similar to the unknown, or if the unknown compound is present in the reference collection, a reference compound identical to the unknown. Methods belonging to the second class are based on correlations of spectral features and structural elements. The output is initially a list of possible structural fragments, and then the molecular structures are constructed from the fragments with due regard to empirical formula and other chemical evidence [8—19]. The number of the candidate structures can be decreased either by reduction of the number of possible functional groups based on chemical and spectroscopic evidence, or by comparison of the artificially generated and measured spectra.

BASIC DESCRIPTION OF THE SYSTEM

The ASSIGNER system is designed to determine the presence or absence of chemical functional groups in organic compounds. Solution of the problem

*This paper was presented at the International Conference on Computer-based Analytical Chemistry, Portorož, Yugoslavia, September 1979.

is based on comparison of experimentally determined properties of particular structural fragments with those stored in the computer memory. It should be emphasized that complete spectra are not compared.

Essential steps in the structural fragment search

A system suitable for undertaking the work outlined above must have the following features. First, it must be capable of executing some hardware operations, such as collecting, converting, transmitting and storing the analytical signals of the unknown sample investigated. Secondly, it must perform data-processing functions. This includes the transformation of analytical signals to valuable information, i.e. properties ($A \rightarrow P$ transformation), the inference of structural fragments (functional groups) from properties, reduction of the number of candidate functional groups on the basis of additional information, harmonization of the inferences obtained from different types of spectra ($P \rightarrow F$ transformation), and construction of possible molecular structures from the set of functional groups found ($F \rightarrow S$ transformation). Finally, the system must ensure strict control of data. These activities are possible with the ASSIGNER system, except for the $F \rightarrow S$ transformation, which has not yet been implemented.

The logic scheme of the operational steps is shown in Fig. 1. Detailed discussion of these steps requires some definitions. The unknown compound (the sample investigated) is always considered as a chemically pure compound. Analytical signals (A) are defined as the measurable and recordable information obtained by the analytical instruments; e.g., data sets which represent infrared spectra are considered as signals. Properties (P) are the characteristic effects produced by some fragments of the chemical structure. In the ASSIGNER system, chemical and spectroscopic properties are defined. Functional groups (F) are fragments of a chemical structure, and are often defined simply by their properties; in any case, suitable properties are essential for inferring the presence of a functional group. Possible structures (S) can be constructed from the presumed functional groups in any allowed way, taking into account the empirical formula, valences, etc. Information arising from other sources can be used to filter this set, giving acceptable chemical structures.

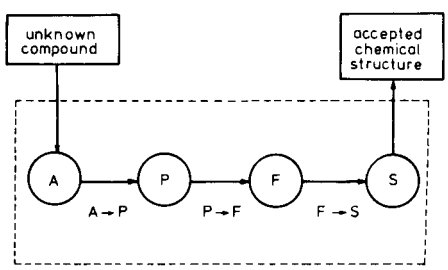

Fig. 1. Logic scheme of the system: A, set of analytical signals; P, set of properties; F, set of possible functional groups; S, set of possible chemical structures.

Principles of the inference process

The essential feature of a search system is obviously the mode by which functional groups and properties are related ($P \rightarrow F$).

The set of functional groups included in the data base of the system can be defined as F: $\{f_1, f_2, \ldots, f_n\}$, and the set of their properties can be defined as P: $\{p_1, p_2, \ldots, p_m\}$. Then the statement that the properties belong to the functional groups implies a relationship between sets F and P. With regard to this relationship, one condition is essential: properties must be additive, i.e., no property may vanish in any combination of functional groups.

Graphical examples of the relation between the two sets are given in Fig. 2. The edges of the graph connect elements of the sets belonging to the relation. The boundary around the F set (groups included in the system) borders the set of all conceivable functional groups (F_{TOTAL}). Suppose that a subset of the properties P_J has been derived from the analytical signals observed ($P_J \in P$). The problem is how to infer the logical value of the statement "f_i is present" from the actual logical value of the statement "properties of f_i are present".

Basically, it is necessary to distinguish two definitely different situations. In the first case (case 1, Fig. 2), the possibility that the sample contains functional groups that are not included in the system but contribute to P_J is not excluded. In such cases, it can be stated only that the presence of a particular functional group without the appearance of its properties is impossible:

$$(f_i \text{ is present}) \wedge (\text{properties of } f_i \text{ are absent}) = 0 \qquad (1)$$

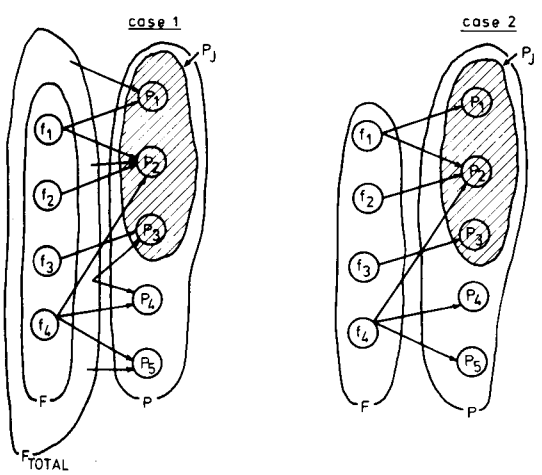

Fig. 2. Examples of the $F \rightarrow P$ and $P \rightarrow F$ relation. Solutions are as follows. Case 1: $f_1 \leqslant$ true, $f_2 \leqslant$ true, $f_3 \leqslant$ true, f_4 = false. Case 2: f_1 = true, $f_2 \leqslant$ true, f_3 = true, f_4 = false.

Possible answers are then given by the inference:

(f_i is present) $\leqslant$ (properties of f_i are present) (2)

i.e. the logical value of the statement "f_i is present" is less than or equal to the logical value of the statement "properties of f_i are present". Thus if the properties of f_i are present, f_i is possible; otherwise, f_i is absent.

In the second case (case 2, Fig. 2), it is true (or tentatively assumed) that the sample contains only functional groups that are included in the system. This case would require the solution of a system of Boolean equations, i.e. equations representing the inverse of the $F \rightarrow P$ relation [21]. Depending on the actual observed values of properties, the solution designates logical values for the statements "f_i is present": true, false or both (i.e., possible). Obviously, the true answer postulates at least one specific property.

In the ASSIGNER system, essentially case 1 is considered; thus false or possible are the alternative answers. Roughly speaking, the strategy is screening out. The observed property set, refined from the analytical signals, is compared with the stored property sets belonging to the individual functional groups. According to the logical equations (eqn. 1), all groups whose properties have not been recognized will be omitted from the possible functional group list. This time-consuming procedure can be and is shortened by utilization of common properties, which allow an optimal hierarchical search. Details of this procedure are discussed below.

Refinement of the results

The number of chemical structures that can be constructed from the presumed functional groups, increases greatly with increasing number of groups. It is therefore very important to diminish the number of possible functional groups. Spectroscopic and chemical information is used for this reduction. First, the separate functional group lists relevant to each spectroscopic technique are shortened; then these lists are harmonized, resulting in a coherent common list.

The chemical information used here consists of the elemental constituents of functional groups given by their atomic numbers, the number of free valences with their type, and some chemical features of the functional groups, e.g. whether or not it contains a carbon—carbon double or triple bond, whether or not it can participate in building an aromatic or a heterocyclic ring. The chemical features stored allow the use of information given by the chemist, who usually knows the type of molecule sent for analysis or at least the kind of compound he intended to make.

The defined and stored spectroscopic information is used to avoid contradictions in the set of functional groups found. Thus, if one of the functional groups requires the presence of one or more other functional groups, a condition is prescribed that these two (or more) functional groups must be shown as possible simultaneously. For example, an olefinic carbon can be present only if there is at least one other group that can be attached to the

double bond. If the answers given by different spectroscopic techniques are contradictory with respect to the absence of a group, the answer accepted will be the one obtained by the technique most selective for the given group. There are some functional groups, the possible presence of which forces their appearance on at least two lists originating from different spectroscopic techniques. If such a group is absent from one of the lists, it will be cancelled from the common list.

CONSTRUCTION OF THE SYSTEM

The system developed to realize the principles outlined above, operates basically in an on-line mode but can also be used off-line. In the present state of development, it yields a list of possible functional groups for a given sample. The scheme of the analytical system is shown in Fig. 3. The analog or digital signals coming from the analytical instruments are converted and temporarily stored in a special unit. The digital data are transmitted to the computer, where the respective properties are determined ($A \rightarrow P$ transformation). This is followed by $P \rightarrow F$ transformation (search) and by refinement of the set of F, both using the data bases. The results are obtained as printed output sheets.

When this system is used off-line, the properties (P) obtained from measured data or from atlases can be input-punched on cards.

Hardware implementation

The hardware representation of the system is shown in Fig. 4. The central processor unit of the system is a Hungarian minicomputer EC-1010 with 32K words core memory (16 bits/word). More instruments may be connected to the computer through special units (interfaces, DOUBLER). The DOUBLER is a piece of hardware programmed to do data logging, temporary data storage and transference of stored data. The data sources whose data can be collected by the DOUBLER comprise instruments having electronic analog or digital output, and keyboards for typing in optional digital data. In the

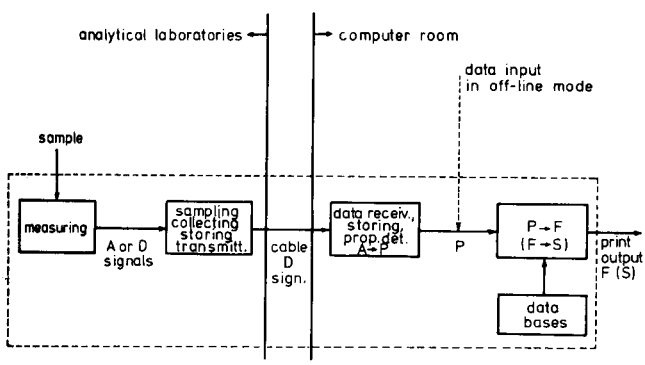

Fig. 3. Scheme of the analytical system.

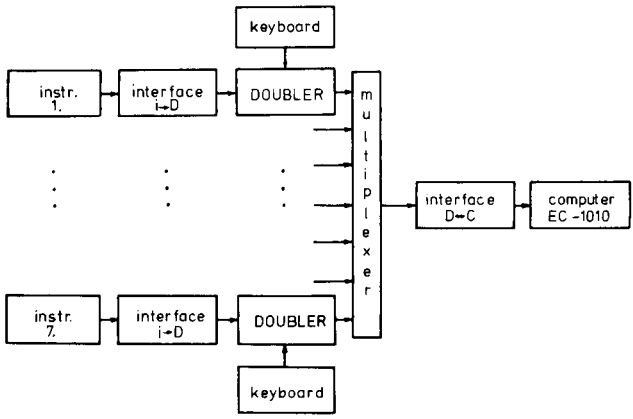

Fig. 4. Hardware representation of the analytical system.

case of instruments having analog and or digital outputs, data input is automated. If they have no electronic output, data are input manually from the keyboard. For instruments with electronic output, an interface is needed between the instrument and the DOUBLER; its construction depends on the output signals of the instrument, on the chosen frequency of scanning and on the input characteristics of the DOUBLER. From the data source, data arrive at the DOUBLER memory, directly in the case of digital signals and after conversion in the case of analog signals.

Leaving a multiplexer, data arrive at the computer memory via a common data path and the DOUBLER/computer interface. Its construction depends on the input features of the data processing unit and the output signals of the DOUBLER. The DOUBLER can also receive and display those check messages which indicate normal operation or possible errors of the processing unit.

The memory of the DOUBLER unit is a twin-buffer with a capacity of 1K words each (12 bits/word). From the point of view of data transfer, the two stores are the same. If one store becomes full, the data line carrying instrumental or keyboard data is switched over automatically to the other store, and simultaneously a computer interrupt is initialized. From this moment, the computer can read the full store. At the end of the data transfer, this buffer may store data again. This operation is cyclic, so that the capacity of the DOUBLER memory is very greatly extended. For practical reasons, the DOUBLER and interfaces were developed and made in this Institute.

Software implementation

The software representation of the system is shown in Fig. 5. Most of the programs are written in FORTRAN, but some parts of the system, e.g. subroutines for bit handling, were worked out in assembly language. The pro-

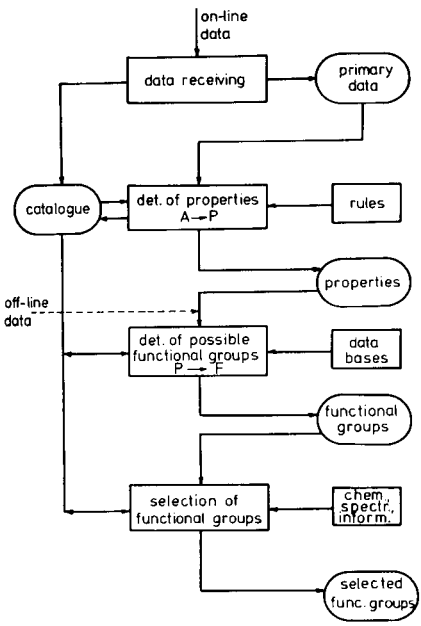

Fig. 5. Data processing.

gram system was developed as an overlay structure.

Data receival. The first part of the program is the data receiver. This checks the data arriving from the DOUBLER memory for syntactic correctness; any error messages are displayed on the DOUBLER. The data receiver also organizes data storage, produces a catalog for recording of data packs, and saves the data packs on magnetic tapes. The actions of this program result in the stored primary data and the catalog.

Property formulation. The second part of the program formulates the derived subset of properties, using the primary data and a set of rules describing the $A \rightarrow P$ transformation. Data reduction involves noise and spike screening, curve smoothing, peak searching, and $A \rightarrow P$ transformation. The results from this program are the stored properties extracted from every experimental data set of each spectroscopic technique.

Functional group search. The next part of the software determines the empirical formula of the sample and performs the functional group search. The empirical formula is made available either by computation from measured data, or by typing in on the keyboard of the DOUBLER. The functional group search includes performance of the $P \rightarrow F$ transformation, using the properties obtained, the data bases and, of course, the empirical formula. The result is a list containing the possible functional groups.

The last step is reduction of the list of functional groups according to the principles described above. This activity also requires use of the data bases (see below). The result of this last operation is the final, concise,

harmonized common set of possible functional groups.

As already mentioned, the system currently contains no program for construction of possible chemical structures based on the possible functional groups, i.e., for the $F \rightarrow S$ transformation.

Data bases and representation of functional groups

The data bases are essential in the inference process. The elements of the set of functional groups are characterized by their spectroscopic and chemical properties. As every technique gives specific information for particular structural elements of organic compounds, separate property collections have been defined for each technique.

All property sets must of course be assigned unambiguously to the relevant groups. A description of how the groups themselves are represented follows. Each group is represented by a numeric group identifier. The identifier is not chosen arbitrarily but is calculated from four indices I, J, K, L, which carry pragmatic information allowing an optional hierarchical search, so as to render a search over the whole file unnecessary.

The index I indicates one particular element of the power set of the 10 chemical elements included in the system (C, H, O, N, S, P, Cl, Br, I, F). Chemical element subsets up to four elements can be distinguished. Functional groups built up from more than four elements are designated by $I = 32$. The power set of the chemical elements belonging to the different indices I is shown in Table 1.

Indices J, K, L indicate classes of functional group which have certain common properties. All the functional groups having the same index in position J have at least one common property. Within this class, subclasses are defined. Functional groups with the same J and the same K have the property of the higher-level J class as well as at least one further common property, etc. It is obvious that such indexing can save computer time. If certain properties are missing in the first step of the search, then those functional groups designated with index J pertaining to the missing properties will not be sought in the second step. For groups with an allowed index J, missing $P(K)$ properties are sought, which exclude functional group classes in the third search level.

TABLE 1

Assignment of I value to different power sets of chemical elements[a]

		∅	O	N	S	P	Cl	Br	I	F
C + H +	∅	1	2	3	4	5	6	7	8	9
	O			10	11	12	13	14	15	16
	N				17	18	19	20	21	22
	S					23	24	25	26	27
	P						28	29	30	31

[a]Otherwise $I = 32$.

The properties of the functional groups, including inherent chemical information, and the information required for reducing the list, are stored in data bases called matrices.

The property matrices contain the i.r., ^{13}C-n.m.r. and ^{1}H-n.m.r. spectral feature of functional groups. Most of their elements define property ranges. The spectral features of a functional group are as follows.

I.r. spectra: wavenumber ranges, peak intensity ranges, allowed peak shapes (classified according to predefined criteria), minimum number of peaks which must be present together with pointers to compulsory peaks.

^{13}C-n.m.r. spectra: chemical shift ranges, line multiplicity, coupling constant ranges, carbon assignment.

^{1}H-n.m.r. spectra: chemical shift ranges, line multiplicity ranges, coupling constant ranges, peak intensities.

In addition to these data, the property matrices contain the identifier numbers and the names of the functional groups in text form. The chemical matrices contain the information used for coherence inferences as described previously. For every functional group, they contain the atomic numbers of chemical elements in the fragment, the number and type of the free valences, and chemical information about the possible environment of the group.

The coherence information is stored in condition matrices which contain logical expressions representing a logical function. This function designates a value for the presence of the functional groups actually considered, depending on the presence of other groups influencing the presence of groups considered. The dependence may be represented by any combination of Boolean operations. Such a condition matrix exists both for the separate technique lists and for the common list.

Data control

To organize the processing of the measured data, it is necessary to have precise information referring to the sample and the measurement, and sometimes to the measuring conditions. Each sample to be analysed is given an identifying character string and each analytical method is given an identifying number. The identifiers and other necessary data are input on the keyboards of the DOUBLERs. The identifying numbers of on-line linked instruments are given by the interface. The sample identifier is attached to the data pack during the whole data processing. This allows randomly arriving data to be linked to the respective samples. The method identifier is required for selecting the appropriate subroutine for evaluation of the data. Because of the limited capacity of our computer memory, only data aquisition and primary data storage are done in real time, the actual data processing being done in work-free periods, e.g. at night.

Testing and modification

In addition to checking hardware performance, a further aim of on-line testing is to compare the properties produced by the computer from measured data to those inferred by the analysts. Experience has shown that more peaks are identified by the computer than by the analysts. The aim of the off-line testing is to check and modify the data bases. Here, the properties are formulated by the analyst and input to the program at the appropriate point (see Figs. 3 and 5). The results from processing these data are thus in no way affected by the spectra-processing section, so flaws in the data bases may easily be identified. Off-line tests have shown that the number of groups reported as possibly present is in general about twice the number of groups actually present. However, none of the groups actually present is lost.

For the time being, the analytical system accepts as input data the molecular weight, elemental constituents, i.r. spectra and n.m.r. spectra (the 30-MHz ^{1}H-n.m.r. spectrometer available has low resolution so that the data are not very informative).

Further development of the system will involve linking further instruments into the system, since additional techniques would permit a better selection of functional groups provided that proper software is constructed. It is also intended to adapt a model and produce a program for solving the problem of structure generation, based on the possible functional groups, the free valences, the molecular weight and the elemental composition.

A detailed description of the system from the analytical point of view and an example are given in another paper [20].

The authors acknowledge the valuable contributions of E. Hunya, J. Nagy, Z. Csapó, Zs. Récsey, I. Nagy, A. Fodor, B. Gombás, E. Bokor, and discussions with Gy. Pfeifer. This work was financially supported in part by the National Council for Research and Development (OMFB).

REFERENCES

1 F. Erni and J. T. Clerc, Chimia, 24 (1970) 388; Helv. Chim. Acta, 55 (1972) 489.
2 S. R. Heller, Anal. Chem., 44 (1972) 1951.
3 P. R. Naegeli and J. T. Clerc, Anal. Chem., 46 (1974) 739A.
4 E. C. Penski, D. A. Padowski and J. B. Bouck, Anal. Chem., 46 (1974) 955.
5 V. A. Koptjug, Z. Chem., 15 (1975) 41.
6 K. Tanabe and S. Saeki, Anal. Chem., 47 (1975) 118.
7 R. Schwarzenbach, J. Meili, H. Könitzer and J. T. Clerc, Org. Magn. Reson., 8 (1976) 11.
8 J. Lederberg, G. L. Sutherland, B. G. Buchanan, E. A. Feigenbaum, A. V. Robertson, A. M. Duffield and C. Djerassi, J. Am. Chem. Soc., 91 (1969) 2973.
9 A. M. Duffield, A. V. Robertson, C. Djerassi, B. G. Buchanan, G. L. Sutherland, E. A. Feigenbaum and J. Lederberg, J. Am. Chem. Soc., 91 (1969) 2977.
10 G. Schroll, A. M. Duffield, C. Djerassi, B. G. Buchanan, G. L. Sutherland, E. A. Feigenbaum and J. Lederberg, J. Am. Chem. Soc., 91 (1969) 7440.
11 J. Lederberg, in G. R. Waller (Ed.), Biochemical Application of Mass Spectrometry, Interscience-Wiley, 1972, p. 193.

12 N. A. B. Gray, Anal. Chem., 47 (1975) 2426.
13 V. V. Serov, M. E. Elyashberg and L. A. Gribov, J. Mol. Struct., 31 (1976) 381.
14 H. B. Woodruff and M. E. Munk, Anal. Chim. Acta, 95 (1977) 13.
15 L. A. Gribov, M. E. Elyashberg and V. V. Serov, Anal. Chim. Acta, 95 (1977) 75.
16 T. Yamasaki, H. Abe, Y. Kudo and S. Sasaki, in D. H. Smith (Ed.), Computer-Assisted Structure Elucidation, ACS Symposium Series 54, Washington, D.C., 1977, p. 108.
17 C. A. Shelley, H. B. Woodruff, C. R. Snelling and M. E. Munk, in D. H. Smith (Ed.), Computer-Assisted Structure Elucidation, ACS Symposium Series 54, Washington, D.C., 1977, p. 92.
18 R. E. Carhart, T. H. Varkony and D. H. Smith, in D. H. Smith (Ed.), Computer-Assisted Structure Elucidation, ACS Symposium Series 54, Washington, D.C., 1977, p. 126.
19 C. A. Shelley, T. R. Hays, M. E. Munk and R. V. Roman, Anal. Chim. Acta, 103 (1978) 121.
20 G. Szalontai, Z. Simon, Z. Csapó, M. Farkas and Gy. Pfeifer, Anal. Chim. Acta, 133 (1981) 31.
21 G. G. Székely and P. Szepesváry, Anal. Chim. Acta, 122 (1980) 257.

Analytica Chimica Acta, 133 (1981) 31—40
Computer Techniques and Optimization

USE OF IR AND ^{13}C-NMR DATA IN THE RETRIEVAL OF FUNCTIONAL GROUPS FOR COMPUTER-AIDED STRUCTURE DETERMINATION

G. SZALONTAI*, Z. SIMON, Z. CSAPÓ, M. FARKAS and Gy. PFEIFER
Research Institute for Heavy Chemical Industries NEVIKI, Veszprém (Hungary)
(Received 9th November 1979)

SUMMARY

Computer-aided interpretation of ^{13}C-n.m.r. and i.r. spectra of organic molecules (m.w. $\leqslant$ 500) is done by an artificial intelligence approach. The output of the proposed ASSIGNER system is a list of functional groups which are reasonable candidates for the final structural isomers. The procedure of finding possible functional groups and the main features of the filtering steps are outlined. One search is worked out in detail to demonstrate the capability of the system.

Structural analysis of new, probably bio-active, organic compounds in the molecular weight range 250—500 is regularly needed in many areas, e.g. in pesticide chemistry. In dealing with this problem, the artificial intelligence method [1—4] seems likely to be flexible and efficient, in that it attempts to parallel human reasoning as much as possible. Only a few published systems [5—7] interpret spectroscopic data in this manner. These programs usually include the interpretation of i.r., u.v., m.s., and ^{1}H-n.m.r. data. Yamasaki et al. [8] described the first program that also included the interpretation of ^{13}C-n.m.r. spectra.

These systems work in two cycles: first, a list of possible structural fragments (functional groups) consistent with the molecular formula and spectroscopic data is formed; secondly, on the basis of this list, those molecular structures are constructed which fit all the requirements. As the number of structural isomers increases proportionally to n (n being the number of possible fragments) [9] the reduction of possible groups is critical from the point of view of the final result. The immediate conclusions are that the larger the identifiable fragment and the more reasonable the filtering step incorporated, the better the system will be. This paper presents a discussion of the first cycle.

THE ASSIGNER SYSTEM

A flow chart of the ASSIGNER system is shown in Fig. 1. The results presented here were obtained in off-line operation. The required inputs [10] are as follows.

^{13}C-n.m.r.: empirical formula, chemical shifts (ppm), line multiplicities (1—4), carbon allocations.
I.r.: empirical formula, wavenumbers (cm^{-1}), peak intensities (0—1000), peak shape codes (1—5).
During the functional group analysis (see Fig. 1) functional groups consistent with the spectroscopic data are selected. This process yields two sets of groups, one each from i.r. and ^{13}C-n.m.r. data interpretation. To reduce the number of possible groups, different filters are used.

^{13}C-n.m.r. data interpretation

The program for analysis of ^{13}C-n.m.r. spectra contains the following filtering elements: (a) chemical matrix comprising molecular formula and chemical features; (b) property matrix comprising chemical shifts, line multiplicity and carbon allocations; (c) condition matrix; (d) information from the chemist.

Chemical matrix. This matrix contains the elemental compositions of the functional groups (the atoms of the neighbouring groups are also considered) and a few properties relevant to the chemical features of the groups. Some examples are given in Table 1.

Property matrix. The selection according to the chemical shifts, line multiplicities and carbon allocations is included in the matrix. The chemical shift ranges are based mainly on literature data [11, 12], but in some cases were modified through experience. A few examples of the total 160 ^{13}C-n.m.r. correlations are shown in Table 2. The use of the multiplicity data usually eliminates about 65% of the list obtained on the base of chemical shift

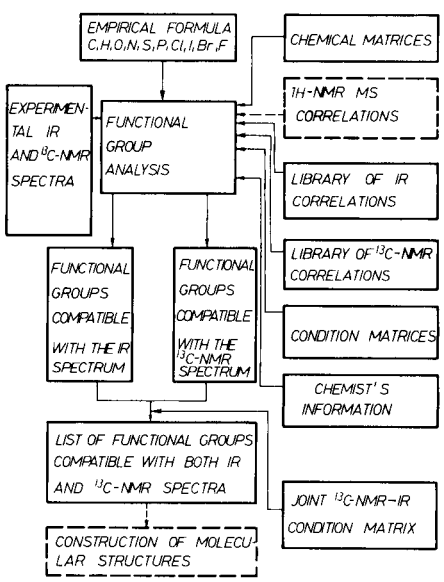

Fig. 1. Flow chart of the ASSIGNER system. Blocks enclosed in dashed lines are not yet operational.

TABLE 1

Partial list of the ^{13}C-n.m.r. chemical matrix

Identifier number	Functional group	Composition	Free valences	Chem. features				
				A	B	C	D	E[a]
2540	$=\overset{*}{C}H-O-$[b]	C_1 H_1 O_1	3/2,1/	0	1	0	0	0
2330	$-O-C=\overset{*}{C}-$	C_2 O_1	3/111/	0	1	0	0	0
2320	$-O-C=\overset{*}{C}H_2$	C_2 H_2 O_1	1/1	0	1	0	0	0

[a] A contains atom(s) of an aromatic ring. B contains an sp^2 olefinic carbon atom. C contains an *sp*-carbon (acetylenic only). D contains carbon, possibly part of a heterocyclic ring. E contains C=X double or triple bond (X = O, S or N).
[b] The asterisk indicates the carbon in question. Unmarked carbon atoms are the expected environments; the number of hydrogens attached to them is undefined.

data alone (see below). Unfortunately, the off-resonance experiments are time-consuming and sometimes it is not possible to achieve precise real multiplicities. The carbon allocations usually do not reduce the list drastically but, of course, are essential in the construction of molecular structures.

Condition matrix. This matrix consists of logical expressions. The functions included comprise the commonest logical steps in human interpretation of spectroscopic data. Some of the logical expressions of the matrix are illustrated in Table 3. For example, to confirm or to diminish the probability of a $=\overset{*}{C}H-O-$ group, (Table 3; identifier 2540) the program looks for other sp^2-carbons consistent with the environment of the carbon in question. If at least one of the groups listed in the first row of Table 3 is also among the possible groups, the existence of the $=\overset{*}{C}H-O-$ group as part of a $-C=\overset{*}{C}H-O-$ or $-CH=CH-O-$ or $CH_2=CH-O-$ fragment is possible. If a $-\overset{*}{C}=C-O-$ group (identifier 2330) is also listed, then the presence of a $-C=CH-O-$ fragment is suggested. Of course, if more than one condition is fulfilled, e.g. both the $-\overset{*}{C}=C-O-$ and the $-\overset{*}{C}H=C-O-$ groups are listed as possible functional groups, the number of fragments will increase, i.e. here the $-CH=CH-O-$ and the $-C=CH-O-$ fragments will be allowed. Insofar as there is no reason to cancel either, these are informational homologs. Simi-

TABLE 2

Partial list of the ^{13}C-n.m.r. property matrix containing 160 entries

Identifier number	Functional group[a]	Chemical shift range (ppm)	Line multiplicity (1—4)	Carbon assignment
2540	$=\overset{*}{C}H-O-$	138.5—152.0	2	1
2330	$-O-C=\overset{*}{C}-$	94.5—107	1	1
2320	$-O-C=\overset{*}{C}H_2$	80.0—97.0	3	1

[a] Asterisks indicate the carbon to which the chemical shift range refers.

TABLE 3

Partial list of the ^{13}C-n.m.r. condition matrix

Identifier number	Functional group x_1[a]	$x_2, x_3, x_4 \ldots x_n$ functional groups required to verify the presence of x_1
2540	$=\overset{*}{C}H-O-$	$-O-C=\overset{*}{C}-$ or $-O-C=\overset{*}{C}H-$ or $-O-C=\overset{*}{C}H_2$
2520	$=\overset{*}{C}-O-$	$-O-C=\overset{*}{C}-$ or $-O-C=\overset{*}{C}H-$ or $-O-C=\overset{*}{C}H_2$
2330	$-\overset{*}{C}=C-O-$	$=\overset{*}{C}H-O-$ or $=\overset{*}{C}-O-$
2610	$=C-\overset{*}{C}O-O-R$	(=C— or =CH— or $=CH_2$...) and ($-O-CH_2-$ or .., etc.)

[a]See footnote to Table 2.

larly, the verification of a $=C-\overset{*}{C}O-R$ fragment (identifier 2610; Table 3) requires, in addition to the $=C-\overset{*}{C}O-O-R$ carbon, the presence of an olefinic double bond and an —O—R group (R = —C—, —CH—, $-CH_2-$...etc.).

Information from the chemist. This step was not originally included in the program, but it became apparent that, despite the above filtering steps, there remained too many possible functional groups. An important reason for this is that ^{13}C-n.m.r. chemical shift ranges often overlap, particularly for aromatic and other sp^2-carbons. The A, B, C, D and E chemical features of functional groups stored in the chemical matrix (see Table 1) make it possible to incorporate information from the chemist who can provide at least some data on the chemical nature of the molecule synthesized. In its present state, the program can handle the following yes/no information: aromatic, olefinic double bond(s), acetylenic triple bond, heterocyclic ring.

These data can reduce the size of the property matrix. According to the yes/no answers, a bit vector is formed, e.g. for structure I (see later) this vector is (1 0 0 0), which means that it is probably aromatic, without carbon—carbon double or triple bonds and heterocyclic rings. If for some reason the original hypothesis (bit vector) proves to be bad, the operator can repeat the search with a new vector.

Summarising the above functions of the ^{13}C-n.m.r. interpretation program, the result is a list of functional groups (see Fig. 1) consistent with the ^{13}C-n.m.r. data and assumptions based on synthesis of the sample compound.

TABLE 4

An example of the i.r. property matrix[a]

Identifier number	Functional group	Wavenumber ranges (cm^{-1})	Peak intensities ranges	Band shape codes
1120	CH_3—(C)	1. 2985—2960	200—1000	1 v 2 v 3
		2. 2895—2850	100—900	1 v 2 v 3
		3. 1485—1440	200—900	1 v 2 v 3
		4. 1390—1360	200—900	1 v 2

[a]There are 260 entries in the property matrix. For the set given here, the maximum condition number is 4 and the minimum condition number is 3.

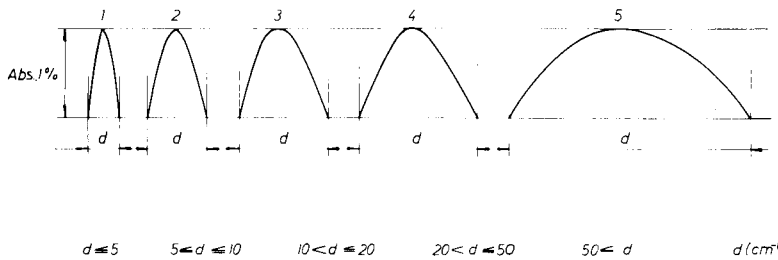

Fig. 2. Illustration of band shape codes used in i.r. data interpretation.

I.r. data interpretation

The techniques for i.r. data interpretation are quite similar to those for the ^{13}C-n.m.r. interpretation. The program is composed of the following filtering elements: chemical matrix, property matrix, condition matrix; information from the chemist is not yet implemented.

The chemical and condition matrices have the same role as in ^{13}C-n.m.r. Features included in the property matrix (see Table 4 and Fig. 2) are as follows: wavenumber range (cm^{-1}) which is based mainly on the CRC Atlas [13], peak intensity (0—1000) as absolute intensity, band shape (see Fig. 2), and maximal and minimal number of conditions; the minimal number of conditions is required to declare a functional group possible while an asterisk indicates indispensable conditions.

The matrix contains 260 i.r. correlations but during the joint ^{13}C-n.m.r.—i.r. interpretation only some of them are active. However, if ^{13}C-n.m.r. data are not available for solubility or other reasons, all the 260 i.r. correlations are used.

Joint ^{13}C-n.m.r.—i.r. interpretation

The results of the processes outlined above are two separate lists of functional groups (one each from i.r. and ^{13}C-n.m.r.). If data coming from different spectroscopic sources but carrying information about the same or similar functional groups are compared, the question of priority arises. Accordingly, the functional groups are divided into three classes as follows.

Class I. Carbon-containing groups from the ^{13}C-n.m.r. list, e.g., —CH_2—C—, —CH—N—, CH_3—S—, etc.

Class II. Carbon-containing groups coming from the ^{13}C-n.m.r. list, which are filtered with i.r. data. Those carbon-containing and hetero atom(s)-containing groups which have highly characteristic i.r. bands belong to this class. Examples are —N=C=O, —N=C=S, —S—C≡N, etc.

Class III. Pure hetero groups coming from the i.r. list, e.g. —NH—, —NH_2, —OH, —SO_2—, etc.

In the joint ^{13}C-n.m.r.—i.r. interpretation, only those i.r. correlations which are highly characteristic are considered (106 of the total 260). In addition, the environment of i.r. groups is neglected; e.g., the program will add only a —NH— group to the ^{13}C-n.m.r.—i.r. common result even if two or

more —NH— groups with different chemical environments are found on the i.r. list. Examples are

—NH— (sec-amine): (Al)—NH—(Ar), (Al)—NH—CH_2, (Ar)—NH—(Ar).

R—COOH: (Al)—COOH, (—CH_2—)—COOH, (—C=C)—COOH

This implies that the strategy is based on ^{13}C-n.m.r. data rather than on i.r. data. This is a straightforward consequence of the fact that ^{13}C-n.m.r. spectral lines give exact information on the nature (primary, secondary, etc.) and the number of carbon atoms, i.e. blocks of organic molecules are identified. The frequently overlapping i.r. absorption bands give less certain information; indeed, the absence of characteristic i.r. bands can be more useful, e.g., in filtering steps, than their presence. Of course, in the case of hetero groups, the i.r. data have an unquestionable role.

EXAMPLES OF APPLICATION

The output of the ASSIGNER program is a list of functional groups which are reasonable candidates for the final structural isomers. Examples of its application are given below.

Example 1

The first example relates to structure I; the results and ^{13}C-n.m.r. spectral data are given in Tables 5 and 6, whereas full i.r. spectral data are omitted to save space.

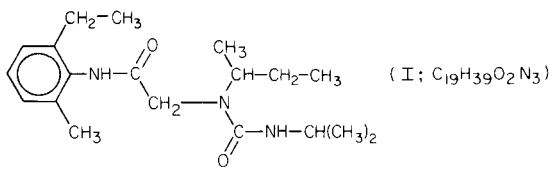

(I; $C_{19}H_{39}O_2N_3$)

The i.r.-output (Table 5) contains 17 possible functional groups, 10 of which belong to class I (these are omitted in the joint interpretation), 2 of which belong to class II thus confirming the presence of the —C=N— and —N—CO—N— groups (see Table 6), and 5 of which belong to class III thus

TABLE 5

Surviving groups of compound I through i.r. interpretation (chemical, property and condition matrices)[a]

Class I.	CH_3—(R), $(CH_3)_2$—(CH—R), $(CH_3)_3$—(C—R), CH_3(U), CH_3—(Ar), benzene-1,4(U), (—C=C)—CO—(C=C—), (Ar)—CO—(Ar), CH_3—(CO—O—), —CH_2—(CO—)
Class II.	—C=N— → —C=N— (^{13}C-n.m.r.) (R, R)—N—CO—N(R, R) → —N—CO—N— (^{13}C-n.m.r.)
Class III.	(Al)—NH—(Ar), (Ar)—NH—(Ar), (—C)=N—NH—(Ar), (—C=)N—NH—(Ar), (R)—CO—NH—(Ar)

[a]R, hydrocarbon group; U, any atom(s); Ar, aromatic carbon; Al, aliphatic hydrocarbon.

TABLE 6

^{13}C-n.m.r. input data and the surviving functional groups of compound I through ^{13}C-n.m.r. and ^{13}C-n.m.r.—i.r. joint interpretation

Line No.	Input data (^{13}C-n.m.r.)			Possible functional groups	
	Chem. shift (ppm)	C	Line multiplicity	^{13}C-n.m.r. alone	Joint ^{13}C-n.m.r.—i.r.
1	170.2	1	1	—COOR	—
				Ar—COOH	—
				—CO—N—	—CO—N—
2	159.0	1	1	1O—Ar—C1	—
				—C=N—	—C=N—
				C(−)...N(+)	—
				—C=N—OH	—
				—N—CO—O—	—
				—N—CO—N—	—N—CO—N—
3	141.0	1	1	1C—Ar—C1	1C—Ar—C1
				1N—Ar—C1	1N—Ar—C1
4	135.7	1	1	1C—Ar—C1	1C—Ar—C1
5	133.5	1	1	1C—Ar—C1	1C—Ar—C1
6	128.2	1	2	1H—Ar—C1	1H—Ar—C1
7	127.4	1	2	1H—Ar—C1	1H—Ar—C1
8	126.3	1	2	1H—Ar—C1	1H—Ar—C1
9	53.6	1	2	—CH—OH	—
				—CH—N—	—CH—N—
				—N—$\overset{*}{C}$H—COO—	—
10	46.8	1	3	—C—$\overset{*}{C}H_2$—C—	—C—$\overset{*}{C}H_2$—C—
				—CH_2—OH	—
				—CH_2—N—	—CH_2—N—
				—CH_2—N—NO	—CH_2—N—NO
11	42.9	1	2	—C—$\overset{*}{C}$H—C—	—C—$\overset{*}{C}$H—C—
12	28.0	1	3	—C—$\overset{*}{C}H_2$—C—	—C—$\overset{*}{C}H_2$—C—
13	24.9	1	3	—C—$\overset{*}{C}H_2$—C—	—C—$\overset{*}{C}H_2$—C—
14	23.3	2	4	—C—$\overset{*}{C}H_3$	—C—$\overset{*}{C}H_3$
15	18.7	1	4	—C—$\overset{*}{C}H_3$	—C—$\overset{*}{C}H_3$
16	18.6	1	4	—C—$\overset{*}{C}H_3$	—C—$\overset{*}{C}H_3$
17	14.5	1	4	—C—$\overset{*}{C}H_3$	—C—$\overset{*}{C}H_3$
18	11.2	1	4	—C—$\overset{*}{C}H_3$	—C—$\overset{*}{C}H_3$
—					—NH—

adding a —NH— group to the common list as all of them suggest the presence of this group. The absence of further class II groups from the i.r. list results in the elimination of an additional 8 functional groups from the ^{13}C-n.m.r. list (Table 6). The results of the ^{13}C-n.m.r. and the ^{13}C-n.m.r.—i.r. joint interpretation are given in Table 6. The common list contains 23 functional groups; none of the expected 19 is lost, so that the relative excess of groups is low. As the —NH— group is originated from the i.r. data alone, it does not contain quantitative information. To demonstrate the efficiency of different

filtering steps, the results of the consecutive steps in the case of structure I are presented in Fig. 3.

Example 2

For comparison, the results obtained for structure II are also presented.

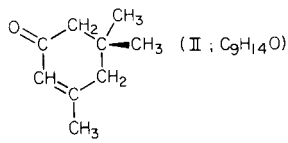

(II ; $C_9H_{14}O$)

For ^{13}C-n.m.r. interpretation, the chemical shift data of Yamasaki et al. [8] were used; unfortunately i.r. data were not available. The results for this compound based on ^{1}H-n.m.r., i.r. and ^{13}C-n.m.r. data have been reported [8, 14]; at the end of the first cycle, the CHEMICS output contained 29 surviving groups [8]. The results obtained by the present method are shown in Table 7. In this case the only information from the chemist used was that no aromatic was present. The list contains 11 different groups (without the loss of the true ones) on the basis of ^{13}C-n.m.r. spectrum alone. This improvement can be attributed to the different data base and to the operation of the condition matrix.

CONCLUSIONS

The system developed is capable of printing a list of functional groups that may be present in an unknown organic molecule on the basis of i.r.

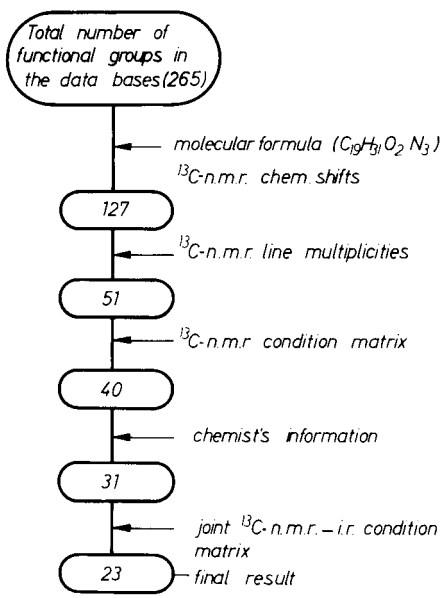

Fig. 3. Reduction of the number of functional groups through consecutive filtering steps for compound I.

TABLE 7

Surviving functional groups of structure II through ^{13}C-n.m.r. analysis

^{13}C-n.m.r. lines	Chemical shift (ppm)[a]	Carbon assignment	Multiplicity	Assigned possible groups (^{13}C-n.m.r.)
1	199.2	1	1	=C—$\overset{*}{C}$O—C— —C—$\overset{*}{C}$O—C—(ketone)
2	159.9	1	1	—$\overset{*}{C}$=C—
3	125.4	1	2	—$\overset{*}{C}$H=C— 1H—Ar—Cl
4	50.8	1	3	—C—$\overset{*}{C}$H$_2$—C— —C—$\overset{*}{C}$H$_2$—OH
5	45.0	1	3	—C—$\overset{*}{C}$H$_2$—C— —C—$\overset{*}{C}$H$_2$—OH —$\overset{*}{C}$H$_2$—CO—
6	33.5	1	1	—C—$\overset{*}{C}$—C—
7	28.3	1	4	—C—$\overset{*}{C}$H$_3$ —CO—$\overset{*}{C}$H$_3$
8	24.4	2	4	—C—$\overset{*}{C}$H$_3$

[a]Data from ref. 8.

and ^{13}C-n.m.r. spectra and the empirical formula. The program has been operational since the middle of 1979 and has been tested on 170 molecules. On average, the output contains 1.5—2.5 times more functional groups than are really present, in most cases without loss of the groups actually present. These results are promising. The ideas of condition matrices, the use of information from the chemist synthesizing the sample, and the strategy of the joint ^{13}C-n.m.r.—i.r. interpretation proved to be useful.

It is necessary to indicate the limitations of the program. Because of spin—spin couplings, results obtained from molecules containing phosphorus, fluorine or other $I = 1/2$ nuclei, can be misleading. There is no direct information on aromatic rings, unsaturated rings and their substitutions, and symmetric molecules are often misinterpreted because of the operation of the ^{13}C-n.m.r. condition matrix. To overcome these problems and to incorporate ^{1}H-n.m.r. and m.s. data interpretation into the system require further study. Nevertheless, the relatively low excess of possible functional groups is encouraging from the point of view of generation of molecular structures which is planned for the future. A list of the ^{13}C-n.m.r. and i.r. correlations is available from the authors on request.

This work was financially supported in part by the National Council for Research and Development (OMFB).

REFERENCES

1 J. Lederberg, G. L. Sutherland, B. G. Buchanan, E. A. Feigenbaum, A. V. Robertson, A. M. Duffield and C. Djerassi, J. Am. Chem. Soc., 91 (1969) 2973.

2 A. M. Duffield, A. V. Robertson, C. Djerassi, B. G. Buchanan, G. L. Sutherland, E. A. Feigenbaum and J. Lederberg, J. Am. Chem. Soc., 91 (1969) 2977.
3 G. Schroll, A. M. Duffield, C. Djerassi, B. G. Buchanan, G. L. Sutherland, E. A. Feigenbaum and J. Lederberg, J. Am. Chem. Soc., 91 (1969) 7440.
4 G. Sutherland, Heuristic Dendral: A Family of LISP Programs, appeared in D. Bobrow (Ed.), LISP Applications (also Stanford, Artificial Intelligence Project Memo. No. 80).
5 N. A. Gray, Anal. Chem., 47 (1975) 2426.
6 L. A. Gribov, M. E. Elyasberg and V. V. Serov, Anal. Chim. Acta, 95 (1977) 75.
7 C. A. Shelley, H. B. Woodruff, C. R. Snelling and M. E. Munk, in D. H. Smith (Ed.), Computer-Assisted Structure Elucidation, ACS Symposium Series 54, Washington, D.C., 1977, p. 92.
8 T. Yamasaki, H. Abe, Y. Kudo and S. Sasaki, in D. H. Smith (Ed.), Computer-Assisted Structure Elucidation, ACS Symposium Series 54, Washington, D.C., 1977, p. 108.
9 J. Zupan, Anal. Chim. Acta, 103 (1978) 273.
10 M. Farkas, J. Markos, P. Szepesvary, I. Bartha, G. Szalontai and Z. Simon, Anal. Chim. Acta, 133 (1980) 19.
11 F. W. Wehrli and T. Wirthlin, Interpretation of Carbon-13 NMR Spectra, Heyden, London, 1976.
12 G. W. A. Milne, J. Zupan, S. R. Heller and J. A. Miller, Org. Magn. Reson., 12 (1979) 289.
13 J. G. Grasselli and W. M. Ritchey (Eds.), Atlas of Spectral Data and Physical Constants for Organic Compounds, CRC Press, Cleveland, 1975.
14 S. Sasaki, I. Fujiwara, H. Abe and T. Yamasaki, Anal. Chim. Acta, 122 (1980) 87.

Analytica Chimica Acta, 133 (1981) 41—49
Computer Techniques and Optimization

EFFIZIENZ DER REGRESSION IN DER RÖNTGENSPEKTROMETRIE

R. PLESCH

Siemens AG, Bereich Meß- und Prozeßtechnik, 7500-Karlsruhe-21 (Bundesrepublik Deutschland)

(Eingegangen den 28. April 1980)

SUMMARY

(*The efficiency of regression calculations in x-ray spectrometry*)

Regression fitting by the least-squares technique minimizes analytical errors. Examples in the literature indicate the possible errors of the method with regard to overfitting, extrapolation and gaps in the concentration range of the standard samples. Strict consideration shows that in practice such errors are insignificant. The problem of unnecessary parameters is discussed; it is shown that regression fitting can cope with such parameters without increased error. The method can also provide a criterion for the necessity of parameters in calibration functions. The most important sources of error in x-ray spectrometry, which are enumerated, do not include the regression calculations.

ZUSAMMENFASSUNG

Die Regressionsrechnung auf der Grundlage der kleinsten Fehlerquadratsumme führt auf den minimalen Analysenfehler. Kürzlich wurden Beispiele angegeben, die auf Fehlermöglichkeiten der Methode hinweisen. Es handelt sich dabei um Überkorrektur, Extrapolation und Lücken im Konzentrationsbereich der Standardproben. Eine genauere Betrachtung der Probleme zeigt aber, daß mit solchen Fehlern in der Praxis nicht gerechnet werden muß. Weiterhin wird auch noch auf das Problem der überflüssigen Parameter eingegangen und an einem Beispiel gezeigt, daß die Regressionsrechnung in der Lage ist, auch solche Parameter ohne gravierenden Fehler zu bewältigen und außerdem ein Kriterium für die Notwendigkeit von Parametern in Eichfunktionen zu liefern Schließlich werden noch die wichtigsten Fehlerquellen der Röntgenspektrometrie aufgezählt. Die Regressionsrechnung gehört nicht dazu.

Wie überall in Naturwissenschaft und Technik besteht auch in der Röntgenspektrometrie die Auswertung von Meßergebnissen darin, eine geeignete mathematische Funktion zu finden und deren Koeffizienten so zu bestimmen, daß die Summe der Abweichungsquadrate der Messungen von der Funktion ein Minimum bildet (kurz, aber nicht ganz treffend, seit den Zeiten von Gauss als Methode der kleinsten Quadrate bezeichnet). Die Koeffizienten werden auf dieser Basis mit Hilfe der Regressionsrechnung bestimmt. Für eine gewählte Funktion ergibt sich dadurch ein optimaler Ausdruck, der ohne neue Messungen nicht mehr verbessert werden kann. Dies schließt

natürlich nicht aus, daß durch die Wahl einer anderen Funktion eine noch bessere Anpassung der Meßwerte möglich ist.

In der Röntgenanalyse kommen nur wenige Funktionen infrage. Als beste Auswertefunktion ergibt sich aus der Theorie eine hyperbolische Beziehung zwischen der Konzentration C_i und der gemessenen Intensität I_i [1, 2]. Aus rechnertechnischen Gründen wird die Hyperbel durch ein Polynom angenähert, das vielfach nach dem linearen Glied bereits abgebrochen werden kann, was zu einer Geraden als Eichfunktion führt. In selteneren Fällen benötigt man ein quadratisches Polynom und kann alle höheren Glieder vernachlässigen. Andere mathematische Funktionstypen sind in der Praxis weder im Allgemeinen notwendig noch werden sie benützt, wenn auch ein kubisches Polynom in seltenen Fällen vielleicht noch eine geringe Verbesserung zu bewirken vermag.

Die Forderung nach der kleinsten Summe der Abweichungsquadrate ist identisch mit der Forderung nach dem kleinsten Analysenfehler. Bezeichnet man nämlich mit C_i die gegebenen Konzentrationen (Massengehalte) der Standards, mit C_i' die Konzentrationswerte aus der Funktion $C = f(I)$, so gilt für die Standardabweichung S_e:

$$S_e = [\sum (C_i' - C_i)^2/(n - p)]^{1/2} \qquad (1)$$

In Gl. (1) bedeuten n die Anzahl der Standards und p die Anzahl der in $f(I)$ bestimmten Koeffizienten. Der Zähler enthält unter dem Wurzelzeichen nichts anderes als die Summe der Abweichungsquadrate. Ihre Minimierung führt daher auch auf den kleinsten Wert von S_e, der mit der gewählten Funktion und den vorliegenden Standards zu erreichen ist. Da auch der Analysenfehler (Standardabweichung) für die unbekannten Proben in guter Näherung mit S_e übereinstimmt, führt die Regressionsrechnung demnach auf diejenigen Werte der Koeffizienten, die den kleinsten Analysenfehler zur Folge haben. Hat man mit Matrixeffekten zu rechnen, so müssen dadurch noch Korrekturen vorgesehen werden, daß in $f(I)$ zusätzlich die Konzentrationen oder Intensitäten der Matrixelemente eingeführt werden [3]. Die Anzahl der neuen Koeffizienten muß ebenfalls in p enthalten sein.

Es ist unbestreitbar und wird auch nicht bestritten, daß die Regressionsrechnung auf die besten Werte der Koeffizienten führt. Auf der anderen Seite aber tritt gelegentlich ein gewisses Mißtrauen gegen die Methode auf. Das Ablaufen eines mathematischen Vorgangs im Rechner läßt die Frage nach den Grenzen des Verfahrens entstehen, die von der praktischen Seite her vermutet werden, und nach den Fehlern, die durch eine kritiklose Anwendung entstehen können. In [4] wird diese Thematik besonders deutlich angesprochen. Die Bedenken konzentrieren sich auf vier Sachverhalte, die stichwortartig etwa lauten: (1) Überkorrektur, (2) Extrapolation, (3) Lücken, und (4) Überflüssige Parameter.

ÜBERKORREKTUR

Wenn man bei gegebener Anzahl n der Standards die Anzahl p der Koeffizienten erhöht, so wird die Differenz $n - p$ in Gl. (1) kleiner. Man

bezeichnet sie als die Anzahl der Freiheitsgrade. Ihre Verringerung bedeutet, daß S_e in Gl. (1) zunehmen kann. In diesem Falle ist es nicht mehr nützlich, die Anzahl der Koeffizienten zu erhöhen, wie ausführlich gezeigt wurde [5]. Die Standardabweichung S_e kann daher als Kriterium dafür dienen, wie weit eine Vermehrung der Koeffizienten noch analytisch sinnvoll ist.

Die Abb. 1 zeigt dafür ein einfaches Beispiel. Sie enthält vier Meßpunkte, die sich auf die Analyse von Al_2O_3 in einer oxidischen Matrix beziehen. In [6] sind 36 Meßergebnisse von Standards angegeben, aus denen die vier Werte der Abb. 1 entnommen wurden. Mit C_i ist der relative Massengehalt und mit I_i die relative Nettointensität bezeichnet, die auf die Intensität des reinen Oxids bezogen wurde. Die Messungen wurden an Aufschlußproben 1:9 vorgenommen. Für die Auswertung wurde ein Polynom dritter Ordnung verwendet, das in Abb. 1 angegeben ist. Damit liegt die höchste mögliche Überkorrektur vor, die Zahl der Freiheitsgrade hat den geringsten möglichen Wert, nämlich eins, und S_e nach Gl. (1) ergab sich zu 0,029 rel. Massengehalt. Hätte man linear nach $C_i = a_1 I_i$ ausgewertet, so hätte man $S_e = 0{,}016$ erhalten. Eine lineare Auswertung wäre demnach besser gewesen, was man allerdings erst weiß, wenn man beide Auswertungen durchgeführt hat.

In Abb. 2 [4] wird eine funktionelle Darstellung gezeigt, die ebenfalls als Überkorrektur bezeichnet wird. Wie man sieht, ist es nicht möglich, zwischen den Meßpunkten zu interpolieren. Dazu ist allerdings zu sagen, daß es sich hier nicht um eine statistische Auswertung mit Hilfe der Regressionsrechnung handeln kann. Die Ausgleichskurve geht exakt durch jeden Punkt hindurch. Eine solche Kurve bezeichnet man aber als Interpolationskurve. Sie ist nicht anwendbar für die Auswertung von Meßwerten, die einem zufälligen Fehler unterliegen und erlaubt keine Bestimmung des Analysenfehlers [7].

Weiterhin handelt es sich um eine periodische Funktion, wie sie durch die Verwendung trigonometrischer Funktionen gewonnen werden kann. Um dies zu zeigen, wurden in Abb. 3 die ersten vier Meßwerte aus Abb. 2 mittels

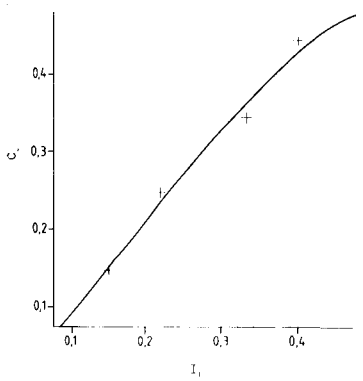

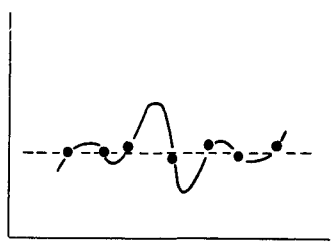

Abb. 1. Maximale Überkorrektur. $C = a_1 I + a_2 I^2 + a_3 I^3$; $S_e = 0{,}029$.

Abb. 2. Vermutete Fehler durch Überkorrektur [4].

einer Fourier-Funktion interpoliert, die Funktion ist ebenfalls angegeben. Wie man erkennt, hat sie denselben Charakter wie die Kurve in Abb. 2. Mehr läßt sich nicht sagen, da es unendlich viele Möglichkeiten gibt, die vier Punkte durch eine trigonometrische Kurve zu verbinden. Man muß aber festhalten, daß in der Analytik die Interpolation nicht anwendbar ist und trigonometrische Eichfunktionen nicht angewandt werden. Der Abb. 2 kommt daher keine Beweiskraft zu.

Wie Abb. 1 zeigt, kommen die hier dargestellten Fehlermöglichkeiten auch bei extremer Überkorrektur in der Praxis nicht vor.

EXTRAPOLATION

Die Abb. 4 [4] soll zeigen, welche Fehler entstehen können, wenn man eine durch Regression gewonnene Eichkurve außerhalb des Bereiches verwendet, der durch die Meßwerte der Standards gekennzeichnet ist. Es ist jedem Lehrbuch der Mathematik zu entnehmen, daß die Eigenschaften von Funktionen immer nur in einem bestimmten Intervall gültig sind, dessen Grenzen genau angegeben werden müssen. Das gilt selbstverständlich auch für analytische Eichfunktionen. Wenn der Gültigkeitsbereich erweitert werden soll, müssen zusätzliche Standards ausgewertet werden. Diese Notwendigkeit darf man aber nicht als Nachteil der Ausgleichsrechnung auffassen, denn es handelt sich um eine allgemeine mathematische Gesetzmäßigkeit.

Im übrigen wird der steile Abfall und Anstieg der Eichkurve außerhalb der Meßpunkte, wie er in Abb. 4 dargestellt ist, in der Praxis nicht gefunden. In Abb. 5 sind ebenfalls 8 Meßpunkte eingetragen, die sich auf Nickel in hochlegiertem Stahl beziehen. Es sind aus simulierten Standards berechnete Werte [8]. Die Auswertung erfolgte nach einem quadratischen und kubischen Polynom, deren Koeffizienten a_1, a_2 und a_3 durch Regressionsrechnung ermittelt wurden.

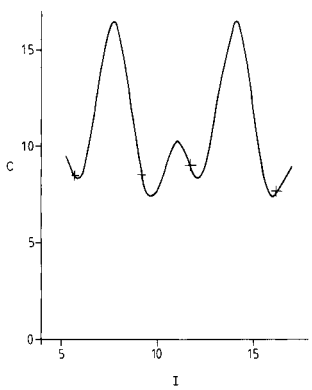

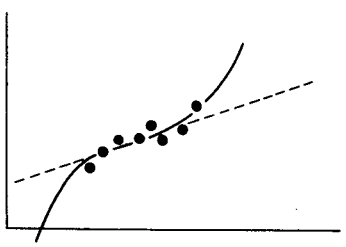

Abb. 3. Fourier-Interpolation durch die ersten vier Meßpunkte der Abb. 2. $C = 10{,}92 + 0{,}46 \cos I + 3{,}12 \sin I - 2{,}43 \cos 2I$.

Abb. 4. Vermutete Fehler durch Extrapolation [4].

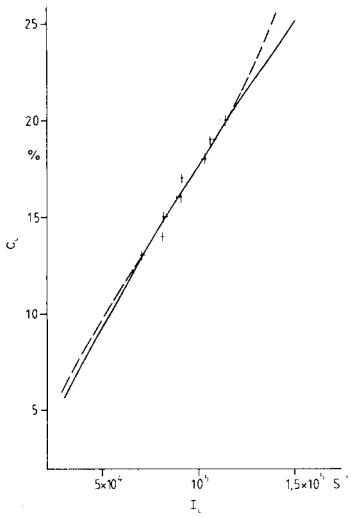

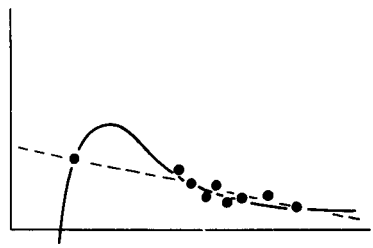

Abb. 5. Zur Extrapolation. (—) $C = a_1 I + a_2 I^2$; (---) $C = a_1 I + a_2 I^2 + a_3 I^3$.

Abb. 6. Vermutete Fehler durch eine Konzentrations-Lücke [4].

LÜCKEN

In Abb. 6 [4] wird angedeutet, welcher große Fehler bei der Regressionsrechnung entstehen kann, wenn der Konzentrationsbereich der Standards größere Lücken aufweist. Die Eichkurve erhält dann eine Ausbuchtung in dieser Lücke und ist in diesem Bereich analytisch nicht mehr brauchbar. Zur Überprüfung dieser Verhältnisse sind in Abb. 7 ebenfalls 9 Meßpunkte eingetragen, die eine ähnlich große Lücke enthalten. Es handelt sich wieder um das Beispiel des Nickels in Stahl [8]. Die Auswertung erfolgte linear,

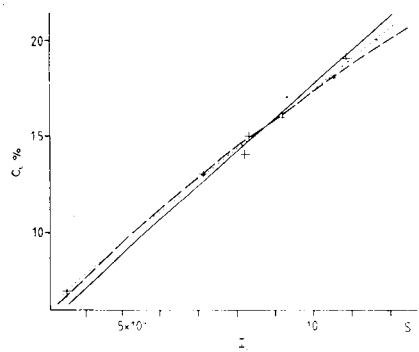

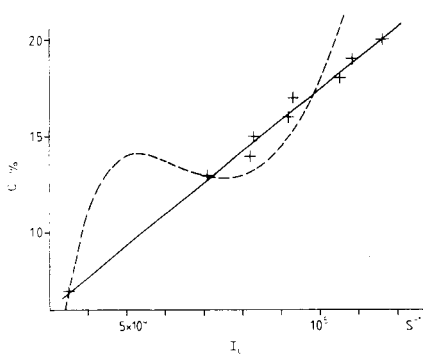

Abb. 7. Zur Auswertung mit Konzentrations-Lücke. (...) $C = a_1 I + a_2 I^2 + a_3 I^3$; (---) $C = a_1 I + a_2 I^2$; (—) $C = a_1 I$.

Abb. 8. Auswertung mit ungewöhnlicher Eichfunktion. (—) $C = 1{,}84 \times 10^{-4} I - 1{,}13 \times 10^{-6} I^2 + (2{,}39 \times 10^{-4}/I)$.

quadratisch und kubisch. In keinem Falle wurde eine Ausbuchtung der Funktionswerte wie in Abb. 6 gefunden. Da andere Funktionen in der Analytik nicht verwendet werden, ist in der Praxis diese Erscheinung auch nicht zu erwarten.

Zur weiteren Klärung des Sachverhalts soll noch kurz untersucht werden, wie eine Funktion aussehen müßte, die in einer Lücke zwischen zwei Meßpunkten zu einem Maximum wie in Abb. 6 führt. Die Abb. 8 enthält dieselben Meßpunkte wie die Abb. 7. Die Funktion der gestrichelten Kurve vom Typ $C = a_0 + a_1 I + a_2 I^2 + a_3/I$ wurde so berechnet, daß sie durch die beiden ersten Meßpunkte hindurchgeht und zwischen ihnen ein Maximum bildet. Es handelt sich dabei um eine rein mathematische Konstruktion ohne Bezug zur Analytik.

Anschließend wurde dieselbe Funktion zur Regressionsrechnung über alle 9 Meßpunkte verwendet, das Ergebnis ist in Abb. 8 eingetragen. Nach dieser Rechnung hat die Funktion das Maximum völlig verloren, wie die ausgezogene Kurve zeigt. Die Regressionsrechnung hat also selbst bei dieser ungewöhnlichen Eichfunktion, die aus einer quadratischen Parabel und einer Hyperbel zusammengesetzt ist, zu Koeffizienten geführt, die dem quadratischen Polynom in Abb. 7 entsprechen. Dies ist ein weiterer Beweis dafür, daß ein Maximum zwischen zwei Meßpunkten, wie in Abb. 6 dargestellt, in der Praxis nicht auftreten kann, auch wenn man eine Funktion verwendet, die aus mathematischen Gründen ein solches Maximum theoretisch zuließe. Daß in der Analytik solche Funktionen nicht verwendet werden, sei nur noch am Rand vermerkt.

In [4] wird noch auf Fehler hingewiesen, die entstehen, wenn nur am Anfang und am Ende des Konzentrationsbereiches Meßwerte vorhanden sind, während sie im gesamten Zwischenraum fehlen. Hier handelt es sich aber nicht um Fehler der Methode. Wo keine Meßwerte vorhanden sind, kann weder eine Auswertung durch Regressionsrechnung noch irgend eine andere durchgeführt werden.

ÜBERFLÜSSIGE PARAMETER

Der besondere Vorteil von Polynomen als Eichfunktionen besteht vor allem darin, daß zusätzliche Einflußgrößen (Parameter) einfach additiv hinzugefügt werden können. Ihr Koeffizient errechnet sich dann durch eine erneute Anwendung der Regressionsrechnung. Desgleichen kann man auch einfach auf nicht mehr benötigte Parameter verzichten.

Damit ist aber auch die Möglichkeit gegeben, irrtümlicherweise eigentlich nicht benötigte Parameter in die Auswertung einzuführen. Dadurch wird die Anzahl p der Koeffizienten in Gl. (1) unnötig erhöht und es besteht die Gefahr einer Vergrösserung des Analysenfehlers nach Gl. (1). Das Thema sei an einem einfachen Beispiel behandelt.

In Tabelle 1 sind die Massengehalte C_i in % des Elements Chrom in 7 Proben aus rostfreiem Stahl eingetragen, zusammen mit den durch Messung

TABELLE 1

Ohne Einfluß von t_i (vgl. Text)

Probe Nr.	C_i (Massen-%)	I_i (s^{-1})	t_i (min)
1	21	1,469 + 5	3
2	25	1,760 + 5	9
3	17	1,205 + 5	12
4	13	0,925 + 5	14
5	15	1,055 + 5	17
6	23	1,632 + 5	19
7	19	1,322 + 5	24

erhaltenen Bruttointensitäten I_i. In der letzten Spalte ist mit t_i die Uhrzeit bezeichnet, die für die Messung der jeweiligen Probe zutrifft. Diese Angabe ist so zu verstehen, daß die Probe Nr. 1 beispielsweise um 9.03 Uhr gemessen wurde, die Probe Nr. 2 um 9.09 Uhr und so fort.

Der Analytiker möge nun das Gefühl haben, seine Meßwerte hingen auch von der Uhrzeit ab, beispielsweise infolge einer Drift seines Analysengerätes. Aus diesem Grund bezieht er die Uhrzeit in seine Auswertung mit ein und setzt die folgende Eichfunktion an:

$$C_i = a_0 + a_1 I_i + a_2 t_i \tag{2}$$

Die Auswertung der Tabellenwerte mit Hilfe der Regressionsrechnung anhand des Ansatzes (2) führt dann auf

$$C_i = -\,0{,}13 + 1{,}43 \times 10^{-4}\, I_i + 1{,}16 \times 10^{-3}\, t_i \tag{3}$$

und aus Gl. (1) ergibt sich eine Standardabweichung S_e = 0,18 Massen-%. Da der mittlere Massengehalt aller Standardproben nach Tabelle 1 den Wert von 19% hat, liegt demnach der Analysenfehler knapp unterhalb eines Prozents dieses Wertes. Falls der Analytiker mit diesem Ergebnis zufrieden ist, glaubt er die Erkenntnis gewonnen zu haben, daß er die Uhrzeit als zusätzlichen Parameter in die Auswertung einführen muß. Trotzdem hat er sich getäuscht. Führt er nämlich als Gegenprobe die Auswertung ohne die Uhrzeit als zusätzlichen Parameter durch, so ergibt sich

$$C_i = -\,0{,}10 + 1{,}43 \times 10^{-4}\, I_i \tag{4}$$

und die Standardabweichung errechnet sich nach Gl. (1) zu 0,16 Massen-%. Sie ist also geringer geworden und damit ist erwiesen, daß eine zeitliche Abhängigkeit der Messungen nicht besteht, das Spektrometer arbeitet einwandfrei.

Zur Abrundung des Beispiels sei nun angenommen, das Analysengerät weise eine Drift von −1% pro Minute auf (selbstverständlich eine völlig unrealistische Annahme, aber das Rechenbeispiel verlangt deutliche Änderungen). Mit dieser Annahme ergeben sich die Werte der Tabelle 2.

TABELLE 2

Mit Einfluß von t_i (vgl. Text)

Probe Nr.	C_i (Massen-%)	I_i (s^{-1})	t_i (min)
1	21	1,469 + 5	3
2	25	1,654 + 5	9
3	17	1,097 + 6	12
4	13	0,823 + 5	14
5	15	0,907 + 5	17
6	23	1,371 + 5	19
7	19	1,044 + 5	24

Die Regressionsrechnung führt auf

$$C_i = -3{,}33 + 1{,}60 \times 10^{-4} I_i + 0{,}23\, t_i \qquad (5)$$

und nach Gl. (1) ergibt sich eine Standardabweichung von 0,14 Massen-%.

Würde man jetzt die Auswertung ohne t_i als Parameter durchführen, erhielte man eine Standardabweichung von 0,58 Massen-%, ein sehr deutlicher Hinweis auf die nunmehr bestehende Abhängigkeit von der Uhrzeit (und auf die Notwendigkeit, den Wartungsdienst zu bemühen).

Die Bedeutung eines Auswerteparameters erkennt man sofort am zahlenmäßigen Betrag, den er bei der Berechnung der ausgeglichenen Konzentration C_i' leistet. Setzt man z.B. in Gl. (3) die Werte der Probe 3 aus Tabelle 1 ein, so erhält man

$$C_i' = -0{,}13 + 17{,}23 + 0{,}0014 = 17{,}10 \qquad (6)$$

und man erkennt die Bedeutungslosigkeit von t_i an der Kleinheit des Beitrags.

Entsprechend findet man aus Gl. (5) und Tabelle 2 für das Beispiel mit der Drift:

$$C_i' = -3{,}33 + 17{,}55 + 2{,}76 = 16{,}98 \qquad (7)$$

Die Bedeutung des Parameters t_i ist in Gl. (7) nicht mehr zu übersehen.

Aus diesem Beispiel lassen sich zwei Schlüsse ziehen. (a) Wenn ein überflüssiger Parameter in die Auswertung eingeführt wird, dann sorgt die Regressionsrechnung dafür, daß sein Beitrag in der Eichfunktion verschwindend gering bleibt, gemessen am Beitrag der notwendigen Parameter, wie Gl. (3) und (6) zeigen. Die Mathematik besitzt hier die Eigenschaft der "Selbstheilung", das heißt, sie sorgt dafür, daß ein überflüssiger Parameter keinen großen Schaden anrichten kann. Dies ist der Grund dafür, warum der Eindruck entstehen kann, ein überflüssiger Parameter sei sinnvoll. (b) Als objektives Kriterium zur Beurteilung eines Parameters dient die Standardabweichung S_e der Eichung nach Gl. (1). Bewirkt ein neuer Parameter eine sichtbare Verringerung von S_e, so ist er sinnvoll. Auch dieser Sachverhalt wird aus dem zweiten Teil des gewählten Beispiels deutlich. Daraus folgt aber auch, daß ein neuer Parameter nur dann als notwendig betrachtet werden darf, wenn er diesem Kriterium genügt.

SCHLUßBEMERKUNGEN

Wenn in [4] gefordert wird, die Güte der Auswertung mit der Regressionsrechnung müsse überprüft werden, so ist dies im Prinzip richtig. Die Rechenmethode als solche bedarf aber keiner Überprüfung, da sie den Analysenfehler nach Gl. (1) per definitionem zu einem Minimum macht.

Bei einem unbefriedigendem Ergebnis muß man sich vielmehr folgende Fragen vorlegen.

(a) Wurde die am besten geeignete Eichfunktion gewählt (Polynom 1. oder 2. Ordnung, Ratiomethoden, Verwendung einer Streulinie oder des Untergrunds als innerer Standard [2, 8])?
(b) Sind im Falle einer Matrixkorrektur alle notwendigen Matrixelemente in der Eichfunktion berücksichtigt worden?
(c) Entsprechen die Standards in ihrer Güte (Homogenität, Oberflächenbeschaffenheit, Konzentrationsfehler) den Anforderungen des Analysenproblems?
(d) Besteht die Möglichkeit von Fehlereinflüssen aus anderen Ursachen (Probenahme, Präparations- und Meßfehler)?
(e) Sind die verwendeten Standards nach Konzentrationsbereich, Art und Beschaffenheit repräsentativ für die zu erwartenden unbekannten Proben?

Mit anderen Worten: die Verringerung des Analysenfehlers kann auf vielen Wegen möglich sein, nur nicht auf dem Wege einer Verbesserung der Rechenmethode als solcher.

LITERATUR

1 R. Plesch, Fresenius Z. Anal. Chem., 272 (1974) 262.
2 R. Plesch, Fresenius Z. Anal. Chem., 296 (1979) 266.
3 R. Plesch und B. Thiele, Anal. Chim. Acta, 112 (1979) 75.
4 R. Jenkins, XXI Colloquium Spectroscopicum Internationale, Cambridge, July 1—6, 1979, Keynote Lectures, Heyden, London, 1980, S. 37.
5 R. Plesch, X-Ray Spectrom., 5 (1976) 142.
6 D. A. Stephenson, Anal. Chem., 43 (1971) 310.
7 R. Plesch, X-Ray Spectrom., 5 (1976) 204.
8 R. Plesch, Fresenius Z. Anal. Chem., 302 (1980) 393.

Analytica Chimica Acta, 133 (1981) 51—66
Computer Techniques and Optimization

EINSATZ VON RECHENANLAGEN IN DER EMISSIONSSPEKTROCHEMIE FÜR AUFSTELLUNG, BEWERTUNG UND LINEARISIERUNG DER ANALYTISCHEN EICHGERADEN

MIKULÁŠ MATHERNY*

Lehrstuhl für Chemie der Hüttenmännischen Fakultät der Technischen Hochschule, Švermova 9, CS-043 85 Košice

JOZEF ONDÁŠ

Ostslowakische Eisenwerke VEB, Abt. Rechenzentrum, CS-044 54 Košice (Tschechoslowakei)

(Eingegangen den 9. Februar 1980)

SUMMARY

(The use of computers in emission spectrometry for the establishment, evaluation and linearization of analytical calibration curves)

The problems of establishing optimum linear calibration lines for atomic emission spectrometry are discussed, with emphasis on use of photographic recording techniques. The calculation procedure, which is based on the least-squares method, generates additional statistical values which permit the linearity to be checked. As the desired linearity is not always achieved at the first attempt, the process is repeated after unreliable input data have been removed.

ZUSAMMENFASSUNG

Die vorliegende Arbeit beschäftigt sich mit den Problemen der Aufstellung von optimalen, linearverlaufenden analytischen Eichgeraden für die atomare Emmisionsspektrochemie, die die photographische Registrierung bevorzugt. Bei der Berechnungsprozedur, die auf der Methode der kleinsten Quadrate beruht, werden auch weitere statistische Hilfswerte ermittelt die letztlich auch die Prüfung der Linearität erlauben. Da aber in der ersten Berechnungsstufe nicht immer die gewünschte Linearität erreicht wird, ist der Rechengang durch eine weitere Prozedur ergänzt, die nichtzuverlässige Eingangsdaten ausschliesst.

Beim Aufstellen von analytischen Eichkurven ist die Gerade der gewünschte Spezialfall. Dementsprechend sollen alle vernünftige Bestrebungen unternommen werden um diesen Spezialfall zu erreichen. Der Vorteil der analytischen Eichgeraden gegenüber einer Eichkurve liegt darin, dass diese bessere Kontrollmöglichkeiten ihres Verlaufs bietet [1, 2], und gleichzeitig auch die Ermittlung der Nachweisgrenzen [3] erlaubet. Die experimentelle Vorbereitung der Grundeingangsdaten für die analytischen Eichgeraden fusst entweder in synthetischen Modellmischungen (Eichmischungen, Etalons usw.), die auch Neben- sowie Spurenelemente beinhalten, oder aber man

verwendet natürliche Eichproben (Bezugsproben), die meistens durch nasschemische Methoden auf die Neben- und Spurenelemente analysiert wurden. Dieser letztgenannte Weg ist nur dann zu empfehlen, wenn die Modellierung des krystallochemischen Charakters der Eichmatrixes bedeutende Schwierigkeiten bereitet. In jeden Fall sind aber die Bezugsproben sowie einige typische analytische Proben, unabhängig von der Art der Vorbereitung und Bestimmung der Konzentrationswerte der Neben- und Spurenelemente, auf die Eliminierung der Matrixeffekte zu prüfen [4]. Für eine Eichprozedur sind prinzipiell nur solche Proben zugelassen, die dieselben Matrixeffekte aufweisen wie die typischen Analysenproben.

ALLGEMEINE THEORETISCHE GEDANKENGÄNGE

Eine analytische Eichgerade (Abb. 1) muss immer und ausschliesslich für eine bestimmte Spannweite der Konzentrationswerte $\langle c_{X,\min} - c_{X,\max} \rangle$ aufgestellt werden [5]. Die entsprechende Formel für die emissionsspektrochemischen Methoden stützt sich auf die Arbeiten von Lomakin [6], Scheibe und Schnettler [7]. Für die Bezugslinienmethode hat aber diese empirische Formel ganz konsequent nur Malpica [8] angewendet. Sie wird meistens in einer logarithmischen Form verwendet (die angewendeten Symbole sind in Tabelle 1 erklärt):

$$\Delta Y_{X,R} = A_{X,R} + B_X \cdot \log c_X \qquad (1)$$

Kaiser [3] hat nachdrücklich betont, dass trotz des empirischen Charakters der diskutierten Formel eine direkte Proportionalität zwischen den Logarithmen der analytischen Konzentrationswerte und den auf Messungen beruhenden ΔY-Werten ein logischer Zusammenhang besteht.

Die Aufstellungsprozedur [1, 5, 9] verlangt eine Anfangsmatrix der experimentellen Angaben $\{\Delta Y_{X,R,i,j}, \log c_{X,j}\}$, mit $i = 1, \ldots, K$, $K \in \langle 3, 15 \rangle$ und $j = 1, \ldots, M$, $M \in \langle 4, 20 \rangle$. K stellt dabei die Zahl der wiederholten Spektren für einen gewissen analytischen Konzentrationswert $c_{X,j}$ und M die Gesamtzahl der zur Eichung angewendeten Bezugskonzentrationswerte dar. Die $\Delta Y_{X,R,i,j}$-Werte ergeben sich immer aus der Differenz zweier Y-Werte, die aber von den gemessenen Schwärzungswerten S, oder von den den Transparenzwerten proportionalen a_i-Werten ($a_i = T.\ a_{max}$) abgeleitet werden müssen. Der ΔY-Differenzwert kann prinzipiell auf vier Wege gebildet werden, abhängig davon, ob und wie man die Untergrundkorrektur [10] vornimmt. Die vier möglichen Eingabematrices, von den die Y- und schliesslich auch die ΔY-Werte abgeleitet werden, finden sich in Tabelle 2. Die Schwärzungswerte sind erstens zwangsläufig in die Y-Werte und teilweise auch in die relativen Intensitätswerte I ($I = 10^Y$) umzusetzen. Für diese komplexe Operation eignet sich das Unterprogram TRANSL [11] falls man die l-Transformation [12] bevorzugt, oder aber das Unterprogramm TRANSP [11], falls sich die allgemeine P-Transformation [13] besser für die angewendete Emulsion eignet.

TABELLE 1

Erläuterung der angewendeten Symbole

c_X	Analytischer Konzentrationswert
$A_{X,R}$	Parameter der analytischen Eichgerade; Schnittpunkt der Eichgerade mit der Y-Achse für $c_X = 1$
B_X	Parameter der analytischen Eichgerade; Richtungstangente der Eichgerade; relative Empfindlichkeit der Methode
S	Schwärzungswert
a_i	Transparenzwert ($a_i = T \times 10^3$)
I	Relativer Intensitätswert einer Spektrallinie oder des Untergrundes
Y	$= \log I$
ΔY	$= Y_X - Y_R$
r	Korrelationskoeffizient
R	Bestimmtheitsmass in %
s	Standardabweichung
t_c	Testwert, abgeleitet von experimentellen Angaben
t_{tab}	Tabellierter Testwert der S- oder F-Verteilung
t_0	Berechneter Testwert der S- oder F-Verteilung
f	Freiheitsgrad
S (%)	Statistische Sicherheit
K, M, P	Endzahlwerte
$G1$—$G4$	γ-werte
$k1$—$k4$	k-Transformationskonstanten

Subskripten

i, j, q	Bedeuten immer eine Reihenfolge von Werten
X	Bezieht den Wert auf eine analytische Linie oder auf deren Untergrund
R	Bezieht den Wert auf eine Bezugslinie oder auf deren Untergrund
L + U	Bezieht den Wert auf eine nichtkorrigierte Linie (Bruttowert)
U	Bezieht den Wert ausschliesslich auf der Untergrund

TABELLE 2

Schema der vier möglichen Anfangsmatrices

Bezeichnung	Matrixstruktur	Bestimmung
($T = 0$)	$\{c_{X,j}, S_{X,L+U,i,j}, S_{R,L+U,i,j}\}$	Ohne Untergrundkorrektur
($T = 1$)	$\{c_{X,j}, S_{X,L+U,i,j}, S_{X,U,i,j}, S_{R,L+U,i,j}\}$	Untergrundkorrektur bei X
($T = 2$)	$\{c_{X,j}, S_{X,L+U,i,j}, S_{X,U,i,j}, S_{R,L+U,i,j}, S_{R,U,i,j}\}$	Untergrundkorrektur bei X und R
($T = 3$)	$\{c_{X,j}, S_{X,L+U,i,j}, S_{R,L+U,i,j}, S_{R,U,i,j}\}$	Untergrundkorrektur nur bei R

Die als ($T = 0$) bezeichnete Matrix der Tabelle 2 gilt ausschliesslich für jenen Auswertungsfall, bei dem an den Y-Werten keine Untergrundkorrektur vorgenommen wird ($\Delta Y_{X,R} = Y_{X,L+U} - Y_{R,L+U}$). Bei der Matrix ($T = 1$) wird die analytische Linie auf die Untergrundintensität korrigiert ($\Delta Y_{X,R} = \log [I_{X,L+U} - I_{X,U}] - Y_{R,L+U}$), und die Matrix ($T = 2$) erlaubt sogar die vollkommene Untergrundkorrektur ($\Delta Y_{X,R} = \log [I_{X,L+U} - I_{X,U}] - \log [I_{R,L+U} - I_{R,U}]$). Die Matrix ($T = 3$) dagegen ermöglicht lediglich die Untergrundkorrektur bei der Bezugslinie ($\Delta Y_{X,R} = Y_{X,L+U} - \log [I_{R,L+U} - I_{R,U}]$).

Berechnung der Grundparameter der Eichgeraden

Die Berechnung der Grundparameter $A_{X,R}$ und B_X, die eindeutig den Verlauf der Eichgeraden festlegen, fusst in der Minimalisierung der Gl. (1) anhand der Methode der kleinsten Quadrate:

$$F[A_{X,R}, B_X] = \sum_{1}^{K} \sum_{1}^{M} (\Delta Y_{X,R,i,j} - A_{X,R} - B_X \cdot \log c_{X,j})^2 = \sum_{1}^{K} \sum_{1}^{M} (eF_{i,j})^2 = \text{MIN} \tag{2}$$

Die Prozedur sieht eine konstante Zahl K für alle Eichkonzentrationen j vor. Dies ist für eine programmgesteuerte Berechnung sehr günstig. Schon bei der Eingabe der Werte der Anfangsmatrixes erleichtert diese Konzeption die Organisation des ganzen Input-Systems, ebenso auch die Durchführung der Linearitätsprüfung [5]. Die gesuchten Grundparameterwerte ergeben sich nach einer Serie von mathematischen Operationen [1, 5, 9] in Gl. (3) und (4):

$$A_{X,R} = \frac{\sum_{1}^{M} \log c_{X,j} \cdot \sum_{1}^{K} \sum_{1}^{M} \log c_{X,j} \cdot \Delta Y_{X,R,i,j}}{K[(\sum_{1}^{M} \log c_{X,j})^2 - M \sum_{1}^{M} (\log c_{X,j})^2]} - \frac{\sum_{1}^{K} \sum_{1}^{M} \Delta Y_{X,R,i,j} \cdot \sum_{1}^{M} (\log c_{X,j})^2}{K[(\sum_{1}^{M} \log c_{X,j})^2 - M \sum_{1}^{M} (\log c_{X,j})^2]} \tag{3}$$

$$B_X = \frac{\frac{1}{M} \sum_{1}^{K} \sum_{1}^{M} \Delta Y_{X,R,i,j} \cdot \sum_{1}^{M} \log c_{X,j} - M.K \sum_{1}^{M} \log c_{X,j}}{K \left[\frac{1}{M} \sum_{1}^{M} (\log c_{X,j})^2 - \left(\sum_{1}^{M} \log c_{X,j}\right)^2\right]} \tag{4}$$

Weiter ist es notwendig, eine Reihe von Standardabweichungen zu ermitteln. Erstens ist es die Standardabweichung $s_{\Delta Y_j}$, die für die einzelnen j-Gruppen der $\Delta Y_{X,R,i,j}$-Werte massgebend ist (5a), und die Standardabweichung $\overline{s_{\Delta Y}}$, die aus der gesamten Gruppe der $\Delta Y_{X,R,i,j}$-Werten abgeleitet wird (5c):

$$s_{\Delta Y_j} = [1/(K-1) \sum_{1}^{K} (\Delta Y_{X,R,i,j} - \overline{\Delta Y_j})^2]^{1/2} \tag{5a}$$

$$\text{wo } \overline{\Delta Y_j} = (1/K) \sum_{1}^{K} \Delta Y_{X,R,i,j} \tag{5b}$$

$$\overline{s_{\Delta Y}} = \left[\frac{1}{K-1} \sum_{1}^{K} \frac{1}{M-1} \sum_{1}^{M} (\Delta Y_{X,R,i,j} - \overline{\Delta Y_j})^2\right]^{1/2} \tag{5c}$$

Anhand dieses letztgenannten Wertes (5c) wird die relative Präzision der Konzentrationsbestimmung (5d) nach Prokofjev [14] berechnet

$$s_{c_{X,r}} = 230 \,.\, \overline{s_{\Delta Y}} \,.\, 1/B_X \tag{5d}$$

Weiterhin ermöglicht der $\overline{s_{\Delta Y}}$-Wert die Ermittlung der Standardabweichungen $s_{A_{X,R}}$ (6a) und s_{B_X} (6c), die für die Beurteilung der Präzision der Aufstellung der Eichgeraden [2, 5] sowie für die Ermittlung der "totalen" Präzision der Konzentrationsbestimmung [17] notwendig ist.

$$s_{A_{X,R}} = (1/\overline{s_{\Delta Y}}) \left[\sum_{1}^{M} (\log c_{X,j})^2 / (KM(\log c_{X,j} - \log \overline{c_X})^2)\right]^{1/2} \tag{6a}$$

$$\text{mit } \log \overline{c_X} = 1/M \,.\, \sum_{1}^{M} \log c_{X,j} \tag{6b}$$

$$s_{B_X} = (1/\overline{s_{\Delta Y}}) \left[K \sum_{1}^{M} (\log c_{X,j} - \log \overline{c_X})^2\right]^{1/2} \tag{6c}$$

Schliesslich ist es wünschenswert für die komplexe Bewertung auch den Wert der Korrelationskoeffizienten r, dessen Standardabweichung s_r sowie den Wert des Bestimmtheitsmasses R zu berechnen [18]

$$r = \left\{\frac{\sum_{1}^{K}\sum_{1}^{M} (\log c_{X,j} - \log \overline{c_X}) \,.\, (\Delta Y_{X,R,i,j} - \overline{\Delta Y_j})}{K \left[\sum_{1}^{M} (\log c_{X,j} - \log \overline{c_X})^2 \sum_{1}^{K}\sum_{1}^{M} (\Delta Y_{X,R,i,j} - \overline{\Delta Y_j})^2\right]}\right\}^{1/2} \tag{7a}$$

$$s_r = (1 - r^2)/KM \tag{7b}$$

$$R = r^2 \; 100 \tag{7c}$$

Testprüfungen

Da die ermittelten Werte aus einer stochastisch zusammenhängenden Matrix der $\{\Delta Y_{X,R,i,j}, c_{X,j}\}$-Werte entstanden, ist es berechtigt, einige Werte durch statistische Testverfahren überprüfen zu lassen [19—21]. Erstens muss der Wert des Parameters B_X, der gleichzeitig die relative Empfindlichkeit der Methode darstellt [22], auf die signifikante Ablehnung der Hypothese $B_X = 1$ geprüft werden [5, 18]. Die zuständige Formel stützt sich auf das Student'sche Testverfahren [19—21]:

$$t_c = |(B_X - 1)|/s_{B_X} \tag{8}$$

Diese Testprüfung wird zweckmässig für zwei statistische Sicherheiten (95% sowie 99%), und für den Freiheitsgrad $f = (KM) - 1$ durchgeführt. Der betreffende t_0-Wert wird entweder den Tabellen des Studenttestverfahrens (t_{tab}) entnommen, oder kann durch ein Unterprogramm STUDIN ermittelt werden, der diesen Wert aufgrund der theoretischen Grundlagen [20, 21] berechnet. Falls $t_c \leqslant t_0$ findet die geprüfte Hypothese ihre Bestätigung, B_X ist praktisch gleich Eins. Im Gegenfall, wenn $t_c > t_0$, wird die Hypothese abgelehnt, da B_X von Eins signifikant verschnieden ist.

Der Wert des Korrelationskoeffizienten muss auf die Ablehnung der Hypothese $r = 0$, für den Freiheitsgrad $f = (KM) - 1$, und die statistische Sicherheit $S = 99.9\%$, geprüft werden

$$t_c = [r/(1 - r^2)^{1/2}]\ [(KM) - 2]^{1/2} \tag{9}$$

Hier gilt wiederum, dass bei $t_c > t_0$ die Hypothese abgeleht, bei $t_c \leqslant t_0$ jedoch angenommen wird. Leider gibt der Test (9) auf linearen Zusammenhang der Grundmatrixwerte ungenügende Information [3, 18] die deswegen auf anderem Wege ermittelt werden, muss vorzugsweise durch die Prüfung der Dichte der experimentell ermittelten $\Delta Y_{X,R,i,j}$-Werte um den rechnerisch (10) ermittelten $\widehat{\Delta Y_j}$-Wert (Abb. 1):

$$\widehat{\Delta Y_j} = A_{X,R} - B_X \log c_{X,j} \tag{10}$$

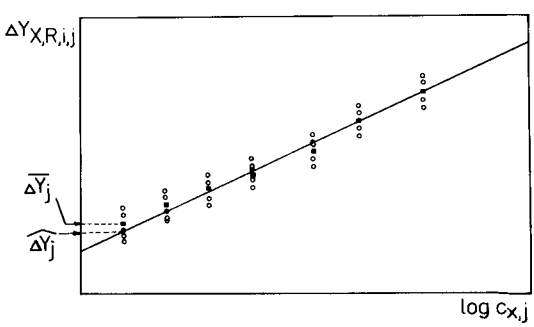

Abb. 1. Veranschaulichung der Lage der $\overline{\Delta Y_j}$- und $\widehat{\Delta Y_j}$-Werte auf einer analytischen Eichgeraden.

Die Berechnung des Testwertes $t_{c,LIN}$ verlangt die Ermittlung zweier spezieller quadratischer Abweichungswerte: der erste

$$(s_1)^2 = [K \sum_{1}^{M} (\overline{\Delta Y_j} - \widehat{\Delta Y_j})^2] / (M - 2) \tag{11a}$$

wird für den Freiheitsgrad $f_1 = M - 2$ und der zweite für den Freiheitgrad $f_2 = M\,(K - 1)$ sowie beide für zwei statistische Sicherheitswerte $S = 95\%$ und $S = 99\%$ ermittelt:

$$(s_2)^2 = \left[\frac{1}{M} \sum_{1}^{M} \sum_{1}^{K} (\Delta Y_{X,R,i,j} - \overline{\Delta Y_j})^2 \right] / (K - 1) \tag{11b}$$

Bei der Bildung der Quotienten $t_{c,LIN}$ wird jeweils der höhere Wert durch den kleineren dividiert, so das $t_{c,LIN} \geqslant 1$ wird. In der Regel gilt $(s_1)^2 \geqslant (s_2)^2$:

$$t_{c,LIN} = (s_1)^2 / (s_2)^2 \tag{12}$$

Der Testwert $t_{c,LIN}$ wird im weiteren entweder mit dem aus Tabellen der F-Verteilung entnommenen t_{tab}-Wert, oder mit dem durch das Unterprogram STUDIN ermittelten t_0-Wert, für zwei statistische Sicherheiten verglichen. Falls $t_c \leqslant t_0$ hält man die getestete Hypothese für bestätigt, und die Eichgerade entspricht den experimentellen $\Delta Y_{X,R,i,j}$-Punkten. Für $t_c > t_0$ hingegen wird man die Hypothese ablehnen. Die Gerade hat dann keine analytische Bedeutung, und die Grundeingangsmatrix muss weiter optimalisiert werden.

Programmierte Lösung der Aufstellung von analytischen Eichgeraden

Der verallgemeinerte Ablauf des Programms CANCAL ACL-MO-78 findet sich in Abb. 2. Zuerst werden die Befehlsangaben L und T eingegeben. Weiter werden die Zahlen K und M sowie die γ- und k-Werte abgespeichert. Diese letztgenannten Werte werden getrennt für die analytische Linie ($G1$, $k1$), deren Untergrund ($G2$, $k2$), sowie für die Bezugslinie ($G3$, $k3$) und deren Untergrund ($G4$, $k4$) angegeben. Der erste Teil der Eingabe (INPUT) endet mit dem Einlesen der Eich-Konzentrationswerte $c_{X,j}$. Die Programmeinheit enthält noch weitere drei Eingeban. Die erste nimmt die Informationen (Transparenz- oder Schwärzungswerte) über die analytische Linie, inbegriffen der Untergrundwerte, und die zweite die Informationen über die Bezugslinie. Die dritte Eingabe ist für den Spezialfall bestimmt, wenn man direkt mit ΔY-Werten, die schon früher getrennt gebildet wurden, in die Programme eingehen will. Die Sequenz der Eingabe dieser Werte muss aber der Reihenfolge der Eingabe der Konzentrationswerte streng entsprechen. Falls der Befehl ($L = 1$) ist, wird das Program die Eingabedaten als Schwärzungswerte betrachten; für ($L = 2$) ist es möglich, direkt mit ΔY-Werten zu rechnen. Wenn aber ($L = 0$) ist (Abb. 3), betrachtet die Anlage die Eingabedaten als Transparenzwerte a_i und berechnet sofort die entsprechenden Schwärzungs-

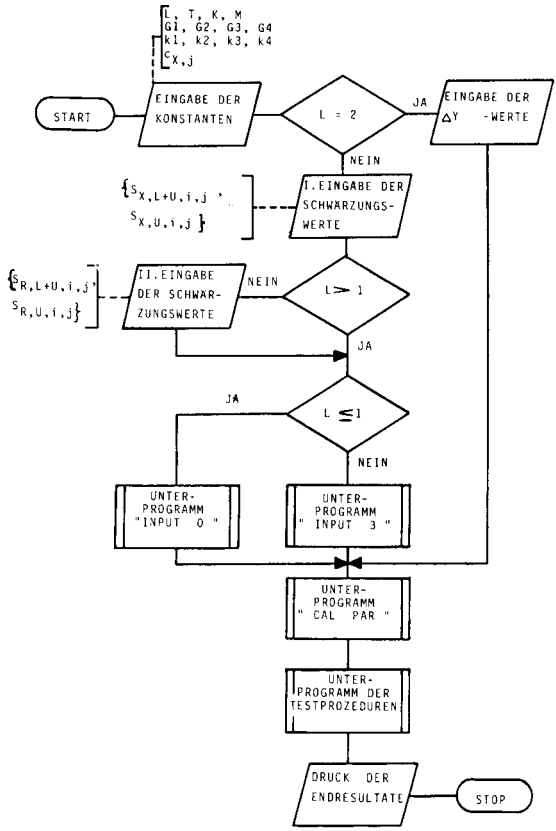

Abb. 2. Allgemeines Flussdiagramm des Programms CANCAL ACL-MO-78.

werte. Die Befehle (L = 3) und (L = 4) ermöglichen unter Anwendung des Unterprogramms INPUT 3 ohne Bezugslinienmethode zu arbeiten (Abb. 4). Im Fall (L = 3) wird der ΔY-Wert wie folgt gebildet: $\Delta Y = Y_{X,L+U} - Y_{X,U}$, wobei der Untergrundwert als Bezugswert $Y_{X,U}$ verwendet wird. Der Befehl (L = 4) schliesslich ruft die folgende Bildung der ΔY-Werte hervor: $\Delta Y = \log(I_{X,L+U} - I_{X,U}) - Y_{X,U}$. Dadurch werden die Intensitätswerte der analytischen Linien auf die Untergrundintensität korrigiert und gleichzeitig wird die Untergrundintensität als Bezugswert ($Y_{X,U} = \log I_{X,U}$) betrachtet.

Durch die T-Befehle (Abb. 3) werden die vier Berechnungsvarianten der ΔY-Werte geregelt, und deswegen ist dieser Teil als Organisations-Unterprogramm INPUT O zusammengefasst. Es enthält zwei weitere selbständige Unterprogramme. Das Unterprogramm TRANSL (Abb. 5) ist für die Schwärzungstransformation bestimmt und verwendet die l-Transformation [12], die aber gegen die P-Transformation auswechselbar ist. Weiterhin beinhaltet der INPUT O Programmteil (Abb. 3) auch des Unterprogramm

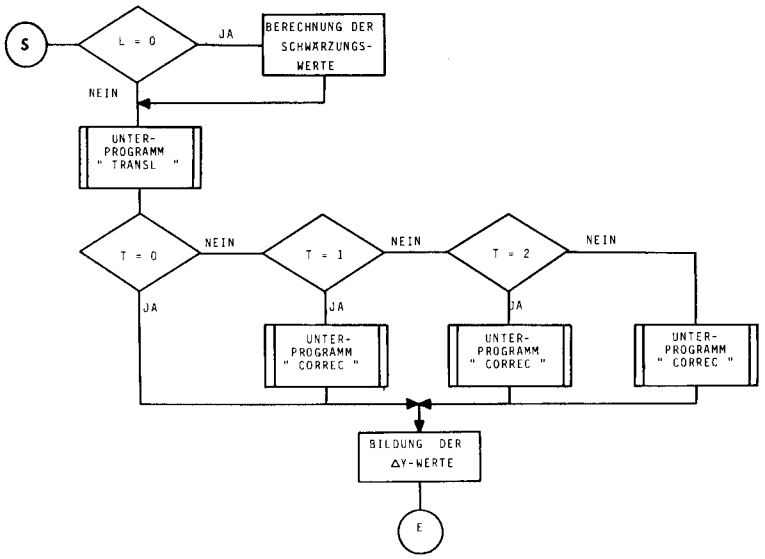

Abb. 3. Flussdiagramm des Unterprogramms INPUT O, und die Verknüpfung mit den Unterprogrammen TRANSL und CORREC.

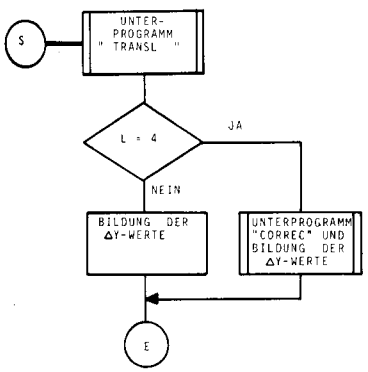

Abb. 4. Flussdiagramm des Unterprogramms INPUT 3 und der Bildung der ΔY-Werte.

CORREC (Abb 6), das für die Untergrundkorrektur bestimmt ist. Schliesslich sei noch erwähnt, dass für die Berechnung der Parameter der Eichgeraden ein integriertes Unterprogramm CAL PAR aufgestellt wurde, das auf den im ersten Kapitel genannten Beziehungen beruht.

LINEARISIERUNG UNZUVERLÄSSIGER EINGANGSMATRICES

Die Linearisierung der unzuverlässigen Eingangsmatrices richtet sich nach der folgenden Sequenz: es muss erstens der Einfluss der Untergrundkorrektur optimiert werden; weiter wird der Einfluss der eventuellen Linien-oder Band-

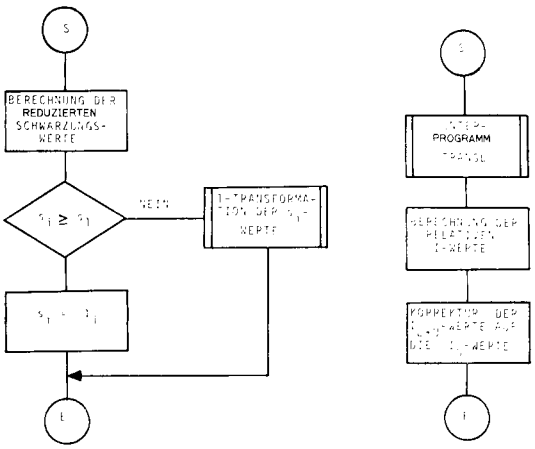

Abb. 5. Flussdiagramm des Unterprogramms TRANSL.

Abb. 6. Flussdiagram des Unterprogramms CORREC.

Interferenzen (auch Blindwertkorrektur) untersucht; schliesslich müssen manchmal von der Grundmatrix diejenigen $I_{X,L+U,i,j}$-Werte oder aber auch Gruppen von I-Werte entfernt werden, die im Untergrund untertauchen.

Die Entscheidung über die geeignetste Variante der Untergrundkorrektur [23, 24] kann ausschliesslich aufgrund der Ermittlung aller erwähnten Parameterwerte der Eichgeraden getroffen werden. Der komplexeste Wertungsparameter ist dabei der $s_{cX,r}$-Wert, da dieser in gleichem Masse die Werte der Parameter B_X sowie den Standardabweichungswert $\overline{s_{\Delta Y}}$ in Betracht zieht [5].

Die Blindwertkorrektur der analytischen Linien [25] beruht auf der Subtraktions des Intensitätswertes der Blindprobe I_{bl} vom Bruttointensitätswert der analytischen Linie:

$$Y_X = \log(I_{X,L+U} - I_{bl}) \tag{13a}$$

da der störende Intensitätswert I_{bl} auch eine Untergrundintensität $I_{X,U}$ beinhaltet. Diese Operation, die nur seltener zur Anwendung kommt, ist eigentlich überflussig und fehlt daher im Grundprogramm. Falls es sich bei der Bewertung der Resultate zeigt, dass eine analytische Linie durch das erwähnte Phänomen gestört ist, werden nachträglich die $Y_{X,L+U}$-Werte einer Korrektur unterworfen. Die Gl. (13a) kann im Fall $I_{X,U} \neq I_{bl}$ wie folgt modifiziert werden:

$$Y_X = \log(I_{X,L+U} - I_{X,U}) - \log(I_{bl} - I_{bl,U}) \tag{13b}$$

Bei der Aufstellung der analytischen Eichgeraden ist es in diesem Spezialfall möglich, anstatt der $Y_{R,L+U}$- und $Y_{R,U}$-Werte direkt die Y_{bl}- und $Y_{bl,U}$-Werte, oder aber die entsprechenden S-Werte, einzusetzen und die Berechnung auf konventionellem Weg durchzuführen.

Hautpsächlich ist es bei der Aufstellung von analytischen Eichgeraden für

die Spurenelementebestimmungen empfehlenswert, ausschliesslich mit solchen Schwärzungswerten der analytischen Linien zu arbeiten, die sich signifikant von der Untergrundschwärzung abheben. Da aber die Schwärzungswerte prinzipiell nicht addierbare Werte sind, ist es notwendig, die ganze Begrenzungsprozedur anhand der relativen Intensitätswerte und gleichzeitig unter Berücksichtigung der Bezugslinienintensitäten zu lösen [2]. Diese Prozedur verlangt zuerst in einem bestimmten i,j-Spektrum, wo $i = Z$ und $j = Q$ ist, in der unmittelbaren Nähe der analytischen Linie eine Reihe von Untergrund-Schwärzungswerten $S_{X,U,q}$ zu ermitteln, wo $q = 1, \ldots, P$ und $P \in \langle 15, 30 \rangle$. Weiter ist es notwendig, in demselben Z,Q-Spektrum auch die Schwärzung der Bezugslinie $S_{R,L+U,Z,Q}$ und eventuell auch deren Untergrundschwärzungswert $S_{R,U,Z,Q}$ auszumessen. Alle Schwärzungswerte müssen weiterhin aufgrund der l-Transformationsprozedur in die relativen Intensitätswerte umgerechnet werden. Aus der so definierten Matrix wird dann der Mittelwert $\bar{I}_{X,U}$ (14a) und dessen Standardabweichungswert $s_{I_{X,U}}$ (14b) berechnet

$$\bar{I}_{X,U} = (1/P) \sum_{1}^{P} I_{X,U,q} \tag{14a}$$

$$s_{I_{X,U}} = [1/(P-1) \sum_{1}^{P} (I_{X,U,q} - \bar{I}_{X,U})^2]^{1/2} \tag{14b}$$

Anhand dieser zwei Werte ist es möglich, einen Grenzwert zu formulieren. Dieser muss aber getrennt für die erwähnten Varianten der Untergrundkorrekturen gebildet werden.

Für die Fälle ($T = 0$) sowie ($T = 3$), wenn die analytische Linie nicht korrigiert wird, erhält man laut Gl. (15a) den Grenzwert Y_G

$$Y_G = \log(\bar{I}_{X,U} + 6s_{I_{X,U}}) \tag{15a}$$

Der Multiplikationsfaktor 6 garantiert, ähnlich wie bei den Garantiegrenzenbestimmungen [26, 27], die 99.9%-ige statistische Sicherheit, dass das analytische Signal höher liegt als der Mittelwert $\bar{I}_{X,U}$. Falls aber $P < 30$ ist, wird es notwendig, den $s_{I_{X,U}}$ Wert nachträglich noch mit einem gewissen τ-Wert zu multiplizieren [21], der die eventuelle Nicht-Gauss'sche Verteilung in Betracht zieht. Für die Fälle ($T = 1$) sowie ($T = 2$), wenn die analytische Linie auf die Untergrundintensität korrigiert wird, berechnet man den Grenzwert Y_G^X laut Gl. (15b)

$$Y_G^X = \log(6s_{I_{X,U}}) \tag{15b}$$

Das Ausschliessungskriterium, aufgrund der im ersten Kapitel definierten Voraussetzung, lautet entweder $Y_{X,L+U,i,j} < Y_G$ (für die nichtkorrigierten analytischen Linien), oder aber $Y_{X,i,j} < Y_G^X$ (für die auf Untergrund korrigierten Linien). Die erläuterten zwei Kriterien sind besser in ΔY-Werte auszudrücken, da diese den korrigierenden Einfluss der Bezugsintensität beinhalten.

Allgemein wird das Ausschliessungskriterium wie folgt festgelegt:

$$Y_{X,R,i,j} < Y_{min} \tag{16}$$

Der ΔY_{min}-Wert muss für die vier Auswertungsvarianten wie folgt angegeben werden

$$(T = 0)\ \Delta Y_{min} = Y_G - Y_{R,L+U,Z,Q} \tag{17a}$$

$$(T = 1)\ \Delta Y_{min} = Y_G^X - Y_{R,L+U,Z,Q} \tag{17b}$$

$$(T = 2)\ \Delta Y_{min} = Y_G^X - Y_{R,Z,Q} \tag{17c}$$

$$(T = 3)\ \Delta Y_{min} = Y_G - Y_{R,Z,Q} \tag{17d}$$

Programmierte Lösung der Begrenzungsprozedur

Die programmierte Ausschliessung der nichtzuverlässigen ΔY-Werte sowie die Aufstellung von linearisierten analytischen Eichgeraden beginnt (Abb. 7) mit dem Programm CANCAL wobei aber die ganze Anfangseingabe-Matrix gespeichert werden muss. Zuerst werden mit dem Programm COLINANCAL die Grundparameter berechnet, sowie weitere zusammenhängende Werte, und schliesslich auch die Testwerte. Falls die Linearität nicht bestätigt wurde, müssen sukzessive die Werte $S_{R,L+U,Z,Q}$ und $S_{R,U,Z,Q}$, die aus bestimmten (Z,Q)-Spektrum zu entnehmen sind, und schliesslich auch eine Reihe von $S_{X,U,q}$-Werten, die ähnlich in dem (Z,Q)-Spektrum ausgemessen wurden, eingespeichert werden. Alle Schwärzungswerte werden wiederum anhand der P-Transformation mittels Unterprogramm TRANSL in die P- sowie in relative I-Werte umgerechnet. Aus dieser Matrix werden die Werte $\bar{I}_{X,U}$, $s_{I_{X,U}} \cdot Y_G$, Y_G^X und ΔY_{min}-Werte ermittelt. Danach folgt die Ausschliessung (Abb. 7, Punkt 1) laut den definierten Kriterien wobei die angegebenen T-Befehle berücksichtigt werden. Nach der Ausschliessung der ausreissenden $\Delta Y_{X,R,i,j}$-Werte wurden (Abb. 7, Punkt 2) mit dem Unterprogramm CAL PAR-M die kompleten Parameter der analytischen Gerade berechnet, sowie mit dem Unterprogramm TEST PROCEDURE-M die entsprechenden Parameter getestet. Diese beiden Unterprogramme unterscheiden sich von dem Unterprogrammen des Programms CANCAL nur dadurch, dass sie nicht mit einem für jede j-Konzentration konstanten K-Zahl der $\Delta Y_{X,R,i,j}$-Werte arbeiten. Die Zahl K kann für die einzelnen j-Konzentrationswerte abgeändert werden.

Die Linearität der Eichgeraden kann aber auch im Gebiete höherer Konzentrationswerte durch eine einzige Gruppe von $\Delta Y_{X,R,i,j}$-Werte gestört werden (Abb. 8). Diese Störgruppe muss aber anhand eines statistischen Verfahrens festgestellt werden. Der entsprechende t_c-Testwert wird anhand der Vergleichsprozedur zweier arithmetischer Mittelwerte [19—21] berechnet (18)

$$t_c = |\Delta \overline{Y_j} - \widehat{\Delta Y_j}|/s_{\Delta Y_j} \tag{18}$$

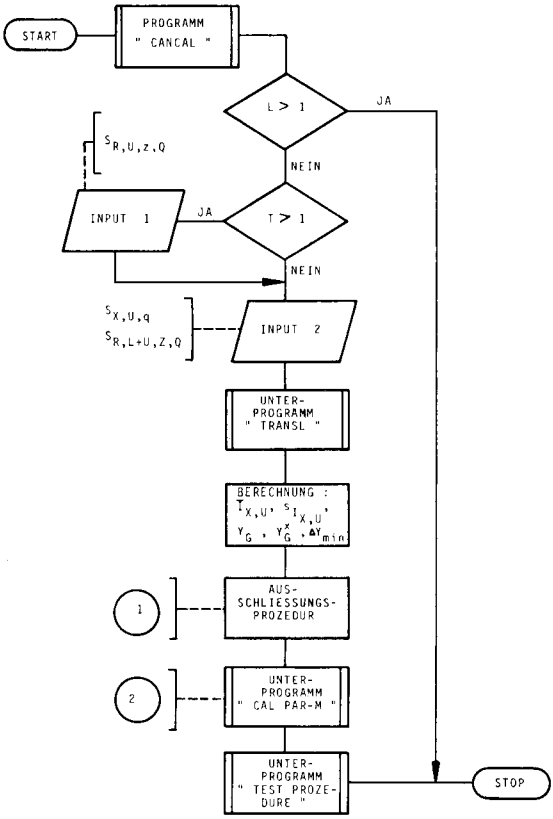

Abb. 7. Allgemeines Flussdiagramm des Programms COLINALCAL ACL-MO-78.

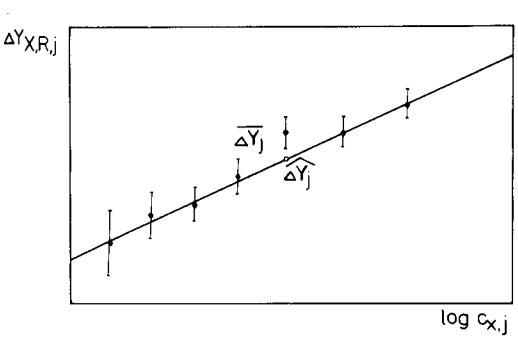

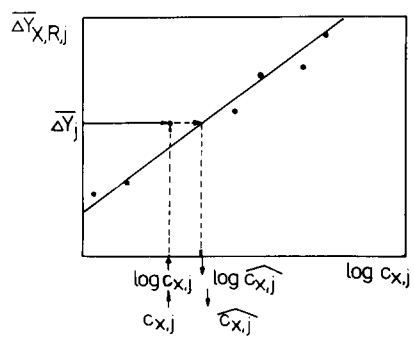

Abb. 8. Veranschaulichung eines signifikant ausreissenden $\overline{\Delta Y_j}$-Wertes.

Abb. 9. Schematische Darstellung der Ermittlung des $\widehat{c_{X,j}}$-Wertes.

Die Glieder der Gl. (18) erhält man aus den Gl. (5b), (5c) und (10). Da aber dieser Störeffekt nur seltener vorkommt, ist er in den angegebenen Programmen noch nicht eingebaut. Wenn bei einer Eichgeraden, die $s_{\Delta Y}$-Werte einer einzigen Gruppe stark streuen, ist es aber zu empfehlen, alle $\overline{\Delta Y_j}$-Werte anhand der angegebenen Prozedur prüfen zu lassen. Nach der Reduzierung der Glieder der $\{\Delta Y_{X,R,i,j},\ c_{X,j}\}$-Matrix um die Gruppe wo der $\overline{\Delta Y_j}$-Wert signifikant ausreisst, wird die ganze Rechenprozedur von Anfang an wiederholt.

BEWERTUNG DER VERLÄSSLICHKEIT DER EICHKONZENTRATIONSWERTE

Die Anwendung von verlässlichen Eichkonzentrationswerten ist die erste und unumgängliche Voraussetzung für das Aufstellen einer analytischen Eichgeraden. Bei der Anwendung von natürlichen Bezugsproben sind aber die Eichkonzentrationswerte durch die Streuung der angewendeten analytischen Methoden stark belastet. Diese Ungewissheit kann anhand der eventuell vorhandenen zuverlässigen Etalons getestet werden. Leider sind solche Etalons für die breite und bunte Skala von elektrisch nichtleitenden Materialien (Erzen, technische Halbprodukte usw.) meistens nicht vorhanden. Deswegen wurde eine Ersatzprozedur aufgebaut, die es teilweise erlaubt, das gegebene Problem zu lösen. Diese Prozedur sieht aber vor, dass nur einige wenige Eichkonzentrationswerte falsch sind.

Anhand der laut Gl. (5b) ermittelten $\overline{\Delta Y_j}$-Werte kann durch die Gl. (19) auch ein $\widehat{c_{X,j}}$-Hilfswert ermittelt werden (Abb. 9)

$$\widehat{c_{X,j}} = 10^{(\overline{\Delta Y_j} - A_{X,R})1/B_X} \tag{19}$$

Aus der Differenz der $\widehat{c_{X,j}}$- und $c_{X,j}$-Werte wird weiterhin die Standardabweichung s_{c_X} berechnet:

$$s_{c_X} = 1/(M-1) \sum_{1}^{M} (\widehat{c_{X,j}} - c_{X,j})^2]^{1/2} \tag{20}$$

Gleichzeitig muss man aber anhand der Gl. (19) und (20) auch für die einzelnen $\Delta Y_{X,R,i,j}$-Gruppen, die zu einem gewissen $c_{X,j}$-Konzentrationswert gehören, auch den Standardabweichungswert $s_{c_{X,j}}$ ermitteln. Bei diesem Rechengang werden aber in der Gl. (19) anstatt der $\overline{\Delta Y_j}$-Wert die einzelnen $\Delta Y_{X,R,i,j}$-Werte angewendet, und bei der Gl. (20) anstatt der $\widehat{c_{X,j}}$-Wert, die ermittelten $\widehat{c_{X,i,j}}$-Werte.

Falls ein $s_{c_{X,j}}$-Wert signifikant vom s_{c_X}-Wert abweicht, muss die entsprechende $c_{X,j}$-Eichkonzentration als unzuverlässiger Wert betrachtet werden. Für die Testprüfungen werden die Gl. (11a), (11b) und (12) angewendet. Selbstverständlich müssen dabei nicht die Standardabweichungen, sondern die quadratischen Abweichungswerte eingesetzt werden. Die Unterprogramme CAL PAR und CAL PAR-M beinhalten diese Rechengänge, aber die endgültige Entscheidung über die Reduzierung der Zahl von

Eichkonzentrationen muss von Hand gemacht werden. Danach wird die ganze Rechenprozedur wiederholt.

SCHLUSSBEMERKUNG

Die Aufstellung von analytischen Eichgeraden für die Emissionspektrochemie, die für eine im voraus definierte Konzentrationsspannweite $\langle c_{X,min}, c_{X,max} \rangle$ erfolgt, muss auf die Linearität geprüft werden. Die entsprechenden statistischen Methoden beruhen auf der Prüfung der Dichte der experimentell gewonnenen ΔY-Werte um die durch Rechnung ermittelte Gerade. Falls die Linearität bei der ersten Aufstellung nicht erreichbar ist, müssen weitere Bemühungen unternommen werden. Es sind dies die Auswahl, die wirksamste Art der Untergrundkorrektur, die eventuelle Blindwertkorrektur, sowie eine Begrenzung der Zahl der Glieder der ursprünglichen Eingangsmatrix $\{\Delta Y_{X,R,i,j}, c_{X,j}\}$.

Für die Berechnung der Grundparameter der analytischen Eichgeraden und deren statistische Bewertung wurde das Grund-Programm CANCAL entworfen, und für die weitere Linearisierung wurde dieses Programm ergänzt mit einer Ausschliessungsprozedur der nichtzuverlässigen $\Delta Y_{X,R,i,j}$-Werte. Das Programm COLINANCAL sowie das Grundprogramm CANCAL sind FORTRAN IV geschrieben.

LITERATUR

1 K. Flórián, A. Lavrín und M. Matherny, Chem. Zvesti, 27 (1973) 623.
2 M. Matherny, Wiss. Z. Karl-Marx-Univ. Leipzig, Math.-Naturwiss, R., 28 (1979) 449.
3 H. Kaiser, Optica, 21 (1964) 309.
4 M. Matherny, Chem. Anal. (Warszawa), 21 (1976) 339.
5 M. Matherny, Kém. Közlemények, 52 (1979) 49.
6 B. A. Lomakin, Z. Anorg. Chem., 187 (1930) 75.
7 G. Scheibe und O. Schnettler, Naturwissenschaften, 19 (1931)
8 J. T. M. Malpica, Gen. Elec. Rev., 43 (1940) 288.
9 E. Geges und A. Dombi, Acta Chim. Hung. (Budapest), 94 (1977) 295.
10 H. Hohnerjäger-Sohn und H. Kaiser, Spectrochim. Acta, 2 (1944) 396.
11 M. Matherny, Anal. Chim. Acta, 112 (1979) 277.
12 T. Török und K. Zimmer, Quantitative Evaluation of Spectrograms by Means of l-Transformation, Akadémiai Kiadó, Budapest, and Heyden, London, 1972.
13 H. Kaiser, Spectrochim. Acta, 3 (1947) 159.
14 V. K. Prokofjev, Spektralní analysa kovů a slitin, SNTL, Praha, 1954.
15 M. Matherny, Chem. Zvesti, 24 (1970) 112.
16 M. Matherny, Spectrosc. Lett., 6 (1973) 711.
17 M. Matherny, Spectrosc. Lett., 5 (1972) 227.
18 K. Flórián, V. Juričková und M. Matherny, Chem. Zvesti, 25 (1971) 421.
19 J. Swiętosławska, in Spektralna analiza emisyjna: Kap. VII, PAW, Warszawa, 1957.
20 R. S. Burrington und D. C. May, Handbook of Probability and Statistics with Tables, 2nd edn., McGraw-Hill, New York, 1970.
21 A. Hald, Statistical Theory with Engineering Application, Wiley, New York, 1962.
22 IUPAC, Nomenclature, Symbols, Units and their Usage in Spectrochemical Analysis. II. Terms and Symbols Related to Analytical Functions and their Figures of Merit. IUPAC Information Bulletin No. 26, 1972.

23 E. Krakovská und M. Matherny, Chem. Zvesti, 29 (1975) 177.
24 M. Matherny, Chem. Zvesti, 30 (1976) 153.
25 T. Török, J. Mika und E. Gegus, Spectrochemical Analysis, Akadémiai Kiadó, Budapest and Heyden, London, 1978.
26 H. Kaiser, Fresenius Z. Anal. Chem., 209 (1965) 1.
27 M. Matherny, Fresenius Z. Anal. Chem., 271 (1974) 101.

Analytica Chimica Acta, 133 (1981) 67—84
Computer Techniques and Optimization

USER-ORIENTED SOFTWARE FOR DETERMINATION OF THE PRECISION OF SIGNAL-INTEGRATING ANALYTICAL METHODS

R. P. J. DUURSMA and H. C. SMIT*

Laboratory for Analytical Chemistry, University of Amsterdam, Nieuwe Achtergracht 166, 1018 WV Amsterdam (The Netherlands)

(Received 4th February 1980)

SUMMARY

A software package for the determination of the uncertainty in signal-integrating analytical techniques is presented. The program can be used to calculate detection limits and to determine baseline drift properties, the influence of drift-correcting procedures and integration time, etc. Complete analytical procedures, e.g., chromatography or atomic emission spectrometry, or parts of a system can be tested. No profound theoretical knowledge is required by the user; confidence intervals are calculated where necessary. The theoretical basis and the structure of the program are evaluated.

Integrated signals are often used in analytical chemistry as a measure of an amount of substance. Inevitably, noise will be present and is also integrated, giving rise to an uncertainty in the determination of the time-integral of the analytical signal. The variance (σ_I^2) of the integral of noise with well-defined (statistical) properties can be determined; σ_I^2 is a function of the integration time [1] and can be used to determine a confidence interval of the integral with an arbitrarily chosen uncertainty. Furthermore, an optimal choice of the integration time can be made, because the random error increases and the systematic error decreases with increasing integration time.

The variance of the integrated signal can be calculated directly with the equations derived by Smit and Walg [1], only if the statistical properties of the baseline noise are completely known. No attention is paid, however, to the possibility of an incorrect description of the baseline noise, for example, because of a limited measuring time. Besides, in practice, baseline corrections (offset, drift) are applied, affecting the noise. In particular, the influence of very low frequencies as present in $1/f$ noise cannot properly be described.

In practice, the statistical properties of the noise, obtained from a limited piece of baseline or background, are estimated. Therefore, it is necessary to calculate the confidence interval of the results of the earlier equations [1]. Before σ_I^2 is estimated, it is necessary to correct the raw data in the same way as is done by data processing programs (smoothing, drift correction). Corrections of a higher order than second order are rarely used. The computer is indispensable for these calculations. The final result can be a graphical repre-

sentation of σ_I^2 as a function of the integration time. Such plots are useful in analytical chemistry because the precision (uncertainty) in signal-integrating methods can be estimated very simply. Detectors, complete analytical instruments, data processing programs, filter procedures, etc., can be specified or compared with respect to their precision and detection limit.

A computer program based on these considerations has been developed in this laboratory. The program also supplies information about the baseline drift. Conclusions concerning this drift can be drawn from the applied baseline drift corrections as calculated from the noise record. Because of the field of application, such a program has to be user-oriented. In this case, the user is generally not skilled in computer techniques and has no profound mathematical knowledge. However, it remains possible to achieve advanced statistical interpretation of the data obtained.

THEORETICAL BASIS

An extensive treatment of the underlying theory has been published [1]. Here, a summary of the theory is supplemented with considerations mainly concerned with estimation of autocovariance functions from noise records of limited time duration and the propagation of the resulting errors. (For convenience, the symbols used are defined in Table 1.)

Suppose, the operation

$$\int_0^T x(t)\,\mathrm{d}t = I \tag{1}$$

on the random function $x(t)$ has an expected value:

$$\mathrm{E}\{I\} = \int_0^T \mathrm{E}\{x(t)\}\mathrm{d}t = 0 \tag{2}$$

The variance of the integral, σ_I^2, can be calculated from the autocovariance function (ACVF or C_{xx}) of the random varying signal $x(t)$:

$$\sigma_I^2 = \mathrm{Var}\{I\} = \int_0^T x(t_1)\mathrm{d}t_1 \int_0^T x(t_2)\mathrm{d}t_2 \tag{3}$$

$$\sigma_I^2 = \int_0^T \int_0^T C_{xx}(t_1,t_2)\mathrm{d}t_1\mathrm{d}t_2 \tag{4}$$

Assuming ergodicity, eqn. (4) can be developed to:

$$\sigma_I^2 = 2\int_0^T (T-\tau)\,C_{xx}(\tau)\mathrm{d}\tau \tag{5}$$

TABLE 1

List of symbols and definitions

$x(t)$	function, varying randomly in time
I	integrated time signal
$x_c(\tau)$	uncertainty, superposed on $C_{xx}(\tau)$
σ_I^2	the variance of a piece of integrated $x(t)$
$\sigma^2_{\sigma_I^2}$	the variance of the variance of a piece of integrated $x(t)$
$E\{\ \}$	the expected value or the first normalised moment of the expression in the brackets
$Var\{\ \}$	the variance or the second centralised and normalised moment of the expression in the brackets
$COV[t,u]$	the estimated covariance for the lags t and u
$\gamma_{xx}(\tau)$	the theoretical autocovariance function (ACVF) of the function $x(t)$, as a function of the lag τ
$C_{xx}(\tau)$	the estimated ACVF ($\gamma_{xx}(\tau)$)
PDF	probability density function
T	the measuring time
T_T	total measuring time
T_p	partial measuring time or the correction time of a piece of baseline
T_i	the time duration per degree of freedom of the baseline
τ	the variable in the covariances; also the integration time
τ_m	maximal lag of an ACVF
u,v,t,r	variables representing time
λ	inverted time constant of a first-order filter
T_x	correlation time; for first order systems equal to τ
A,B,C	the terms of the baseline polynomial
ω	the angular velocity
n	order of a system
k	degrees of freedom
χ^2	Chi Square, representing a sum of squares
α,β	dimensionless constants, resp. $\tau\lambda$ and $T\lambda$

This last operation gives the desired relation σ_I^2 versus integration time T. Although this relation is expressed as a deterministic function, it is possible to distinguish between a deterministic and a random part:

$$C_{xx}(\tau) = \gamma_{xx}(\tau) + x_c(\tau) \tag{6}$$

where $\gamma_{xx}(\tau)$ is the theoretical ACVF, as calculated from a noise record with infinite time duration, and $x_c(\tau)$ is a superimposed random function, which is due to the limited time duration of the record $x(t)$. Equation (5) can be written as

$$\sigma_I^2 = 2\int_0^T (T-\tau)\gamma_{xx}(\tau)\,d\tau + 2\int_0^T (T-\tau)\,x_c(\tau)d\tau \tag{7}$$

The expected value is

$$E\{\sigma_I^2\} = \int_0^T E\{2(T-\tau)\gamma_{xx}(\tau)\}d\tau + \int_0^T E\{2(T-\tau)x_c(\tau)\}d\tau \tag{8}$$

$$E\{\sigma_I^2\} = 2\int_0^T (T-\tau)\gamma_{xx}(\tau)\,d\tau + 0 \tag{9}$$

In practice, $C_{xx}(\tau)$ is known at fixed intervals of the lag τ, so formula (4) becomes:

$$\sigma_I^2 = (\Delta t)^2 \sum_{i=1}^{n}\sum_{j=1}^{n} C_{xx}(i\Delta t, j\Delta t) \quad (\text{for } n = 1 \ldots\ldots N) \tag{10}$$

Jenkins and Watts [2] have described another approach, based on a linear combination of random variables and giving positive results for σ_I^2. The transformation of coordinates used in eqn. (5) does not influence this result, so that eqn. (9) should also be positive.

The variance of eqn. (7) can be calculated in a similar way as in eqns. (3)–(5):

$$\text{Var}\{\sigma_I^2\} = \int_0^T 2(T-\tau_1)x_c(\tau_1)\,d\tau_1 \int_0^T 2(T-\tau_2)\,x_c(\tau_2)\,d\tau_2 \tag{11}$$

$$\text{Var}\{\sigma_I^2\} = \int_0^T\int_0^T \text{E}\{4(T-\tau_1)(T-\tau_2)x_c(\tau_1)\,x_c(\tau_2)\}\,d\tau_1 d\tau_2 \tag{12}$$

$$\text{Var}\{\sigma_I^2\} = \sigma_{\sigma_I^2}^2 = 4\int_0^T\int_0^T (T-\tau_1)(T-\tau_2)\,\text{COV}\,[C_{xx}(\tau_1), C_{xx}(\tau_2)]\,d\tau_1 d\tau_2 \tag{13}$$

For COV $[C_{xx}(\tau_1), C_{xx}(\tau_2)]$ Jenkins and Watts [2] give the following expression:

$$\text{COV}\,[C_{xx}(\tau_1), C_{xx}(\tau_2)]\,\frac{1}{T^2}\int_0^T\int_0^T \{\gamma_{xx}(\nu-t)\gamma_{xx}(\nu-t+\tau_2-\tau_1) + \gamma_{xx}(\nu-t+\tau_2)\gamma_{xx}(\nu-t-\tau_1)\}\,dt\,d\nu \tag{14}$$

The ACVF of first-order band-limited white noise,

$$\gamma_{xx}(\tau) = \sigma_x^2\,e^{-\lambda\tau} \tag{15}$$

substituted in eqn. (4) results in (see Appendix 1):

$$\text{COV}\,[C_{xx}(\tau_1), C_{xx}(\tau_2)] = \frac{\sigma_x^4}{T^2}\left\{e^{-\lambda|\tau_2-\tau_1|}\left[-\tfrac{1}{2}(\tau_2-\tau_1)^2 + \left(T-\frac{1}{2\lambda}\right)|\tau_2-\tau_1| + \left(T-\frac{1}{2\lambda}\right)\frac{1}{\lambda}\right] + e^{-\lambda(\tau_2+\tau_1)}\left[-\tfrac{1}{2}(\tau_2^2+\tau_1^2) + \left(T-\frac{1}{2\lambda}\right)(\tau_2+\tau_1) + \left(T-\frac{1}{2\lambda}\right)\frac{1}{\lambda}\right] + e^{-2\lambda T}\,\frac{1}{2\lambda^2}\,[e^{-\lambda(\tau_2-\tau_1)} + e^{-\lambda(\tau_1-\tau_2)}]\right\} \tag{16}$$

After tedious calculations, the variance of the variance is now given by:

$$\sigma^2_{\sigma^2_I} = \frac{4\sigma_x^4}{\beta^2\lambda^4}\left[\left\{\alpha^3\left(\frac{4}{3}\beta - \frac{4}{3}\right) + 5\alpha^2 - \alpha(8\beta + 4) + 15\beta - 21.5\right\}\right.$$

$$+ e^{-\alpha}\{2\alpha^3 + 10\alpha^2 + \alpha(-4\beta + 26) - 20\beta + 18\} + e^{-2\alpha}\{\alpha^2 + \alpha(2\beta + 3)$$

$$\left. + 5\beta + 3.5\} + e^{-2\beta}\{e^{-\alpha}(-\alpha - 1) - \alpha^2 + 2 + e^{\alpha}(\alpha - 1)\}\right] \quad (17)$$

where α and β are the dimensionless units: $\alpha = \lambda\tau$; $\beta = \lambda T$; τ = integration time; T = measuring time. The calculation of $\sigma^2_{\sigma^2_I}$ for higher-order ACVF's is hardly possible.

Any drift (deterministic or stochastic) of the baseline can give rise to problems during the estimation of the ACVF. If we consider, for example, a distortion $A + Bt + Ct^2$ superimposed on $x(t)$

$$x'(t) = x(t) + A + Bt + Ct^2 \quad (18)$$

then $C'_{xx}(\tau)$ can be calculated as:

$$C'_{xx}(\tau) = C_{xx}(\tau) + A^2; B = 0, C = 0 \quad (19)$$

$$C'_{xx}(\tau) = C_{xx}(\tau) + A^2 + \frac{T^2}{12}B^2 - TAB\tau; C = 0 \quad (20)$$

$$C'_{xx}(\tau) = C_{xx}(\tau) + A^2 + (B^2T^2/12) + (C^2T^4/160) + (AC\,T^2/6)$$

$$+ \tau\,(ABT + BC\,T^2/4) + \tau^2\,(AC + C^2T^2/12) \quad (21)$$

Because it is impossible to distinguish, in general, between the cases (19), (20) and (21), it is necessary to remove the distortions mentioned before calculating $C_{xx}(\tau)$. These distortions are described by the least-squares estimates of eqn. (18), as described by Bevington [3]. In practice, these corrections are applied on a part of the baseline, which is large enough to distinguish a peak from the baseline. The part of the baseline to be corrected has a time duration T_p. From this part an ACVF $C_{xx,p}(\tau)$ is calculated. The total measuring time T_T is divided into parts T_p, which are combined into the final ACVF. This ACVF is used in eqn. (5).

A partial ACVF can be calculated in three ways (after correction with eqn. (18):

$$C_{xx,p}(\tau) = T_p^{-1}\int_0^{T_p-\tau} x(t)\,x(t+\tau)\mathrm{d}t \quad (22)$$

$$C'_{xx,p}(\tau) = (T_p - \tau)^{-1}\int_0^{T_p-\tau} x(t)\,x(t+\tau)\mathrm{d}t \quad (23)$$

$$C''_{xx,p}(\tau) = T_p^{-1} \int_0^{T_p} x(t)x(t+\tau)dt \tag{24}$$

Jenkins and Watts [2] pointed out that eqn. (22) yields a variance of $C_{xx,p}(\tau)$, converging to zero for a large τ, but with a bias. In eqn. (23) this bias is removed, but then the variance increases with increasing time τ. Neither expression is therefore usable. Equation (24) has no bias and the variance is given by

$$\mathrm{Var}[C''_{xx,p}(\tau)] = \sigma_x^4 \{2\beta - 1 + 2e^{-\beta} + [(2\alpha+1)(2\beta-1) - 2\alpha^2]e^{-2\alpha}\}/2\beta^2 \tag{25}$$

For large α ($\alpha \gg 1$) this may be expressed as:

$$\mathrm{Var}[C''_{xx,p}(\tau)] = \sigma_x^4 (\beta - \tfrac{1}{2} + e^{-2\beta})/\beta \tag{26}$$

This is independent of the integration time τ, and is considered as the most usable expression by the present authors. A drawback is that a baseline of length $T_p + \tau$ is used. Careful inspection of the procedure reveals that the points between T_p and $T_p + \tau$ are not used in other partial ACVF's with the same lag τ. A remaining drawback is that the baseline corrections of eqn. (18) are applied to $T_p + \tau_{max}$. However, in our opinion this is acceptable.

An advantage inherent to the procedure of estimating the final ACVF by averaging the partial ACVF's is the possibility of estimating the final distribution of each point of the ACVF. The first point of the ACVF ($\tau = 0$) is calculated from a sum of dependent squares. For independent squares, however, the following equations are valid:

$$E\{\chi^2\} = k/\sigma_x^2 \tag{27}$$

$$\text{and } \mathrm{Var}\{\chi^2\} = 2k/\sigma_x^4 \tag{28}$$

where k is the number of degrees of freedom and σ_x^2 the variance of the independent (virtual) distribution. A number of degrees of freedom can be attached to the measured ACVF's:

$$k = 2[E\{\chi^2\}]^2/\mathrm{Var}\{\chi^2\} = 2[E\{C_{xx}(\phi)\}]^2/\mathrm{Var}\{C_{xx}(\phi)\} \tag{29}$$

Now the accuracy of the estimate of the ACVF can be specified as a function of k. An impression of the applied baseline correction is obtained if

$$T_i = (T_{total} - \tau_{max})/k \tag{30}$$

(where τ_{max} is the maximal lag of the ACVF) is compared with T_p, the correction time. If $T_i < T_p$, the partial ACVF is a correct sample of the entire baseline. The other case, $T_i > T_p$, necessitates corrections of the highest order in order to remove the lowest frequencies and thereby the character of non-stationarity.

PRACTICAL CONSIDERATIONS

Generally, analytical signals are manipulated in various ways before they are integrated to give the final analytical information. An example is the background (baseline drift) correction mentioned above. In many data handling programs, e.g. those applied in chromatography, a background function is fitted outside the regions of peaks, interpolated under the peaks and subtracted. A general description of these operations is unnecessary, but the same procedure as executed by, for instance, a data handling program has to be applied to the data obtained prior to the determination of the uncertainty of the peak area caused by integrated noise. The suggested procedure is as follows: (1) raw analytical signals are sampled and converted from an analog to a digital value; (2) these values are transferred to a digital computer; (3) they are processed appropriately; and (4) combined to give an ACVF; (5) this is integrated to give the desired results.

Steps 1 and 2 can be done in many ways, but some demands must be fulfilled. The sampling and in particular the (constant) sampling interval (sampling frequency) are very important. Most analytical signals vary relatively slowly, and so can be sampled adequately with 1—10 Hz. However, spectroscopic signals may need higher sample frequencies, up to several hundred Hertz. For a reliable estimate, several thousands of data points may be required. Concerning the specification of the A/D converter, the same considerations as used earlier [4] are valid.

Various ways of collecting the data can be used, as indicated by the following examples. Digital cassettes, as sometimes found in data loggers, are useful. Problems of compatibility can arise with other play-back apparatus. A digital cassette recorder may need extensive electronics for interfacing to the A/D converter. The A/D conversion can be done by a digital voltmeter (accurate, slow) or by ready-made conversion circuits. The speed of a standard digital (compact) cassette limits the sampling frequency to ca. 200 Hz, which is generally fast enough for most spectroscopic data. Papertape is old-fashioned but still often applied; in practice, it is fast enough for chromatographic data, and a digital voltmeter can function as an A/D converter. Transient recorders are often necessary to collect fast output of data. Although generally not suitable for permanent storage, they are often useful for the conversion of analog data to papertape or cassette; the number of samples is limited. Direct coupling to a computer with built-in A/D converters is possible. The IEEE 488 bus of a computer can be coupled to an appropriate apparatus. Finally, floppy discs are often incorporated in microcomputer development systems. They are relatively expensive, but an enormous flexibility is added to the measurements. A/D converters are commercially available.

In this laboratory, a microcomputer system is used for collecting data. Sample frequencies can vary from 0.001 to 5 Hz. The analog data are converted to a 12-bit binary code. The binary code is converted to a decimal

value, represented in ASCII and punched on papertape. The system can also be used as a transient recorder by first storing the binary code and converting/punching afterwards. Sample frequencies can increase to 1000 Hz. The system consists of a GNC-80 system with the following extensions (see Fig. 1): A/D converter, sample frequency generator and sample counter, interrupt controller for maximum efficiency, and punch interface.

Steps 3—5 of the suggested procedure are covered by a Fortran IV program, developed in this laboratory. The entire program consists of six overlays plus a main program, controlling the flow through the overlays (Fig. 2). To facilitate the transfer of data to a digital computer, the input part of the program is designed to accept all kinds of integers and real numbers, including the internal (binary) notation of the computer. The nature and the expected number of data as well as the processing necessitates an internal computer storage, which can be a magnetic tape or a disc unit. Extensive error checking is necessary, while the sampling time, number of data points, identification, etc. are also stored. All these functions are performed by the first overlay.

The second overlay reads in the way of correcting the baseline. Parameters to be introduced are: the time duration of the part of the baseline over which one correction has to be effective; the order of the correction; and the maximal integration time (maximal 70% of the correction time).

In addition to these vital data, the way of presenting the final results can be chosen. The three ways of representation are as follows.

(1) Only σ_I^2 versus integration time is shown. The following functions are performed by the program. After correction of the baseline the final ACVF is calculated. This ACVF is roughly approximated by fitting with the function: correction = $A + Be^{-\tau\lambda}$. Any d.c. offset is removed by subtraction of the term A. The ACVF, now completely drift- and d.c.-corrected, is inte-

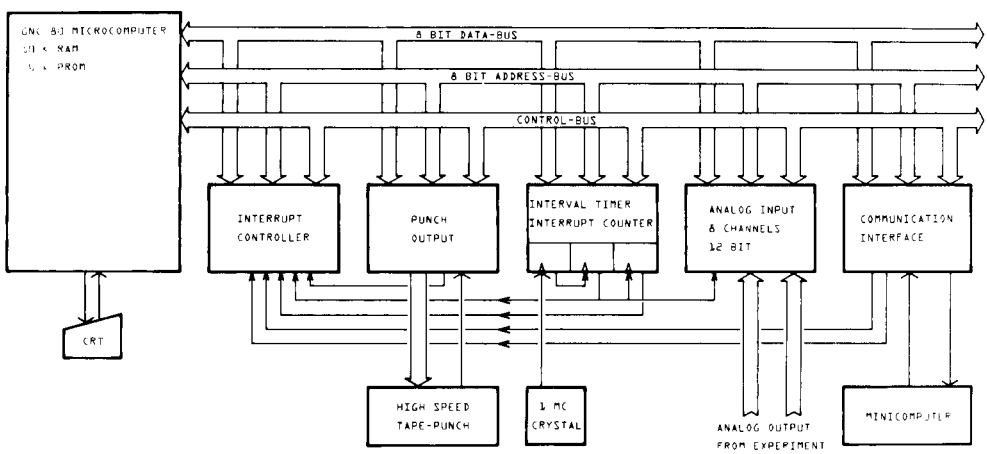

Fig. 1. Configuration of the microcomputer system used for data collecting. The bus structure facilitates extending the system with generally available LSI circuits.

grated to supply values of σ_I^2 versus integration time τ. The fit of the ACVF and in particular the single time constant are only used to give an estimate of the reliability of the final results. A plot of σ_I^2 versus time plus confidence interval and an overview of the corrections applied are displayed.

(2) Results for routine determinations. This is an extension of the first representation and consists of a plot of the PDF of all input data, a plot of the final ACVF with its population interval (based on a Student t distribution), and a listing of the individual steps of the fit of the ACVF, with the function $A + Be^{-\tau\lambda}$. A plot of the corrected ACVF and the fitted function are also presented.

(3) Extended check at all processing stages. To facilitate statistical interpretation of the input data and the effect of each individual baseline correction, a PDF and an ACVF of all drift-corrected parts of the baseline are shown. The possibility of cancelling or controlling the fit of the ACVF with the function mentioned is also included. A survey of the applied baseline corrections is always included. The average squared deviations of the baseline and the corrections are presented as well as the first and second moment of the coefficients of these corrections. From the data it is possible to specify the drift properties.

The third overlay generates the ACVF. The baseline is therefore divided into pieces of a length as required by the calculation of the baseline corrections. This correction is calculated by means of a least-squares estimate [3]. Partial ACVF's are calculated over the time $(T_p + \tau_m)$. To prevent loss of information, the succeeding correction starts at the point $(T_p - \tau_m)$. The final ACVF is calculated by averaging all ACVF's. The 90% distribution interval is calculated from the variance and is based on a Student t distribution.

The fourth overlay produces a plot and a list of the ACVF and stores the ACVF for further computation such as spectrum calculations as discussed previously [5].

The fifth overlay takes care of the fitting of the estimated ACVF with the function $A + Be^{-\tau\lambda}$. The fitting procedure is essentially as described by Bevington [3]. To obtain a starting point for the fitting procedure and to make it possible to give a confidence interval for unfitted functions, the correlation time T_x is calculated, which is assumed to be the time constant $T_x = \int_0^\infty [C_{xx}(\tau)d\tau/C_{xx}(\phi)]$. Finally, the variance as given by eqn. (17) is calculated. To elucidate the procedure, the flow chart of this overlay is given in Fig. 3.

The last overlay converts the variance from eqn. (17) to a 90% confidence interval, assuming a chi-square distribution for σ_I^2 (see Results). The main result is a plot of σ_I^2 versus τ. The confidence interval is shown only if the interval exceeds 5% of σ_I^2.

Although it may look superfluous to determine the uncertainty of an uncertainty, it is absolutely necessary to calculate this quantity and include it in the plot. It is the only precaution against misuse of the final data. How-

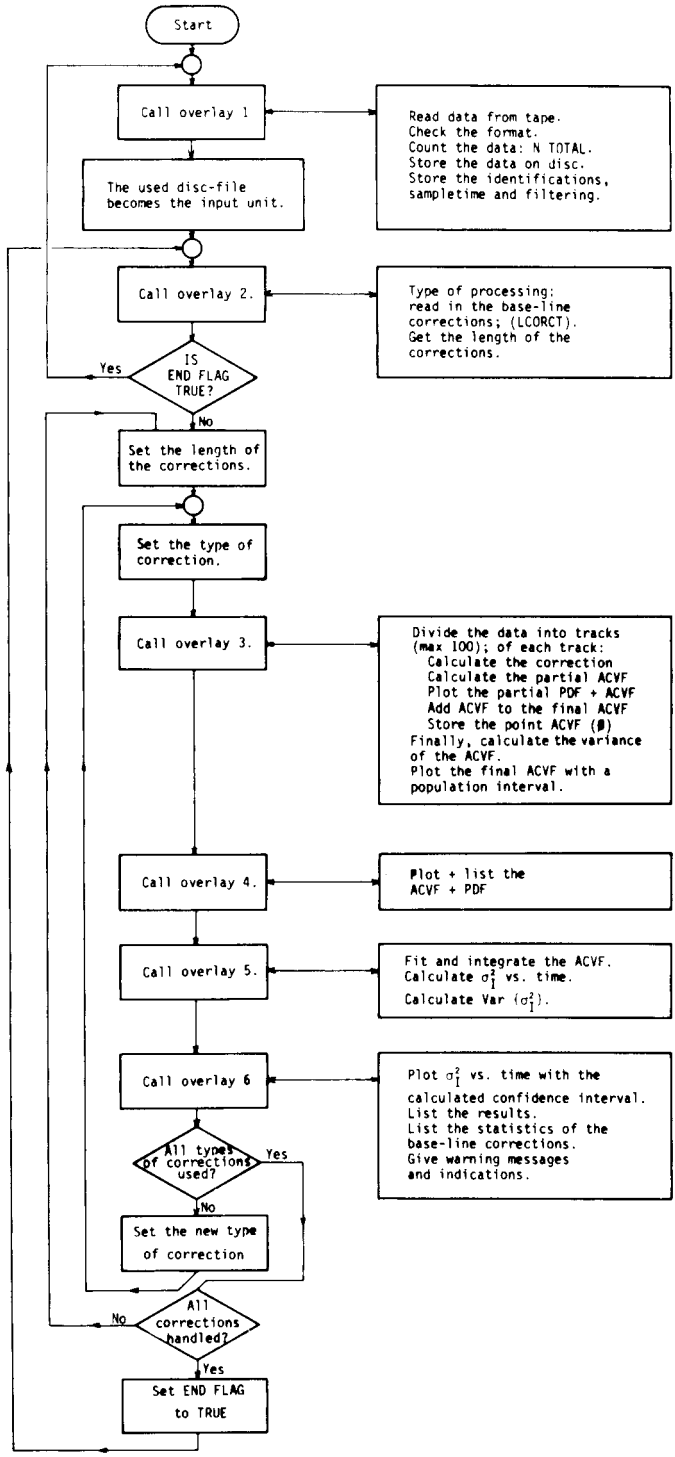

Fig. 2. Flow chart of the main program. The various functions are carried out by overlays. Several baseline corrections are performed by repetitive calls to overlays 2—6.

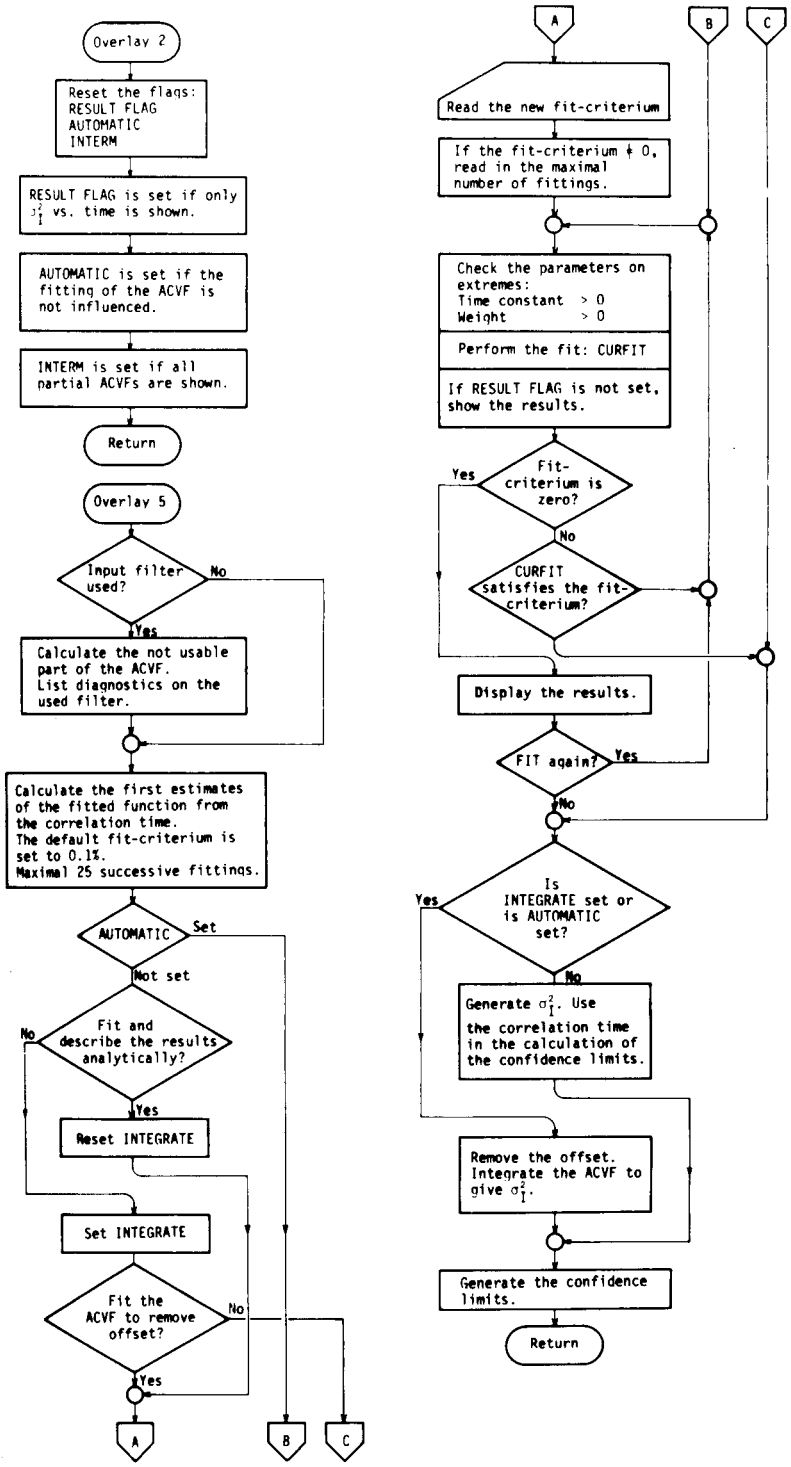

Fig. 3. Flow chart of the fifth overlay. This overlay is entirely controlled by the variables "RESULT FLAG", "AUTOMATIC" and "INTERM", which are read in overlay 2.

ever, only the σ_I^2 values need to be precise, even for high-order systems. The calculated uncertainty of the uncertainty, based on the assumption of first-order band-limited noise, is used only to indicate the reliability.

The following precautions are implemented in the program to ensure correct operation. First, eqns. (29) and (30) are used to determine a minimal recording time of the data, which serves to verify the baseline correction time applied. Secondly, at least 5 points are necessary to produce a correct exponential function for the fitting procedure. Thirdly, an (anti-aliasing) filter can be present in the data-collecting chain. This can be considered as an independent operation on the noise-generating process and changes the shape of the ACVF by adding a second ACVF to the original. The magnitude of the ACVF is lowered, as is expected from a filter operation.

The distortion can be approximated assuming a maximally flat filter, with the transfer function [6]: $H(\omega^2) = [1 + (T_x\omega)^{2n}]^{-1}$ (n = order of the filter). When operating on white noise, this gives the correlation time T_x of the ACVF: $T_x \approx \omega_0^{-1}$, where ω_0 = —3 dB cut-off frequency. The correlation time of a higher-order filter diminishes, compared with a first-order filter with the square root of the order: $T_{x,n} = (\omega_0 n^{1/2})^{-1}$. If the distortion introduced dominates the ACVF, i.e. if the next criterion is fulfilled, a warning is given on the filter used: $C_{xx}(2T_{x,n}) \leqslant \frac{1}{2} C_{xx}(0)$.

EXPERIMENTAL

To verify the theory, artificial noise was used (Hewlett-Packard 3722A). The high-order band-limited white noise was converted to first-order band-limited white noise by filtering with a dominant first-order system, simulated on an analog computer (Telefunken RA 742). The ACVF's were calculated in a digital correlator (Hewlett-Packard 3721A) and punched on papertape (Facit 4070). The data were processed in a minicomputer (Varian V75, operating under Vortex II).

The chromatographic data were recorded on papertape with a system (Fig. 1) consisting of a microcomputer (Great Northern Computers, Canada) with a monitor in 6 kbyte PROM, 2 kbyte RAM memory for programs and pointers, and 8 kbyte RAM for storage of data when the system is used as a transient recorder. The system is extended with an 8228/8224 (Intel) combination of microcomputer components to accommodate the following devices: (1) programmable interrupt controller (8259, Intel), used in data sampling programs and for interfacing a papertape punch; (2) A/D converters (Analog Devices, type 1128); (3) interval timer and sample counter (8253, Intel). Program development was done in the minicomputer mentioned with the aid of a TSS-subsystem and a cross-assembler.

The examples of results obtainable originated from the following apparatus.

(1) High-performance liquid chromatography. Orlita pump, DMP 1515; column, 5-μm silica gel; eluent, methanol/isopropanol; detector, Zeiss u.v. The PDF, ACVF, fitted ACVF and the σ_I^2 vs. time were plotted.

(2) Gas chromatography. Perkin-Elmer 900 with FID; column, Porapak Q, 100—120 mesh. σ_I^2 vs. time was plotted.

(3) Inductively coupled plasma. This was used as an emission detector (Jarrell-Ash) and was equipped with a monochromator, tuned at the Fe-II line; nebulization rate, 72 ml h^{-1}. Essentially, the data were the same as earlier [7], but with different scaling. σ_I^2 vs. time was plotted.

RESULTS

In the first place, the formulation of the covariance (eqn. 16) was checked: 156 autocovariance functions were recorded on an HP 3721 A correlator and converted to papertape. Before the conversion to disc storage, the average ACVF was calculated and a d.c.-correction determined from the least 40 points of the ACVF. The average covariance of two lags was calculated after correction of the ACVF with the average ACVF. The error in the result was within the experimental uncertainty (Table 2).

Secondly, the covariance was integrated, with the algorithm

$$\sigma_I^2 = \Delta t \sum_{i=1}^{n} \left[\frac{n}{2} \left\{ C_{xx}(i) + C_{xx}(i+1) \right\} - \left\{ \left(\frac{i}{2} + \frac{1}{6} \right) C_{xx}(i) + \left(\frac{i}{2} + \frac{1}{3} \right) C_{xx}(i+1) \right\} \right]$$

This algorithm yields an error in σ_I^2, which is 20 times smaller than straightforward trapezium integration. The differences between the estimated and theoretical integral (eqn. 17) were less than 0.1%. The next step was the integration of the recorded ACVF's with the algorithm. From the distribution, the second moment of the integrals was estimated. The results are shown in Table 3. It was confirmed by these integrations that the resulting distribution was one-side limited. It was approximated with a χ^2-distribution.

Finally, a number of noise signals were recorded. From the results, too many to display here, three examples are taken, which are representative of most of the results obtained. The program was run in the routine mode, so that the results displayed are a PDF of all data after correction, an ACVF with estimated population interval, a fit of the ACVF and finally an integrated ACVF with calculated uncertainty limits. Figures 4—10 show the results.

DISCUSSION AND CONCLUSIONS

Concerning the use of the program, it is important to realize that the method of correcting the baseline drift, as applied in almost every chromatographic data-processing program, is certainly not optimal. A good estimation of the baseline under the peak requires a polynomial fit of a very large part of the baseline on both sides of the peak, combined with an interpolation procedure. The usual first-order, or at best second-order, approximation performed on relatively small parts of the baseline can result in rather

TABLE 2

The covariances of an estimated first-order ACVF: $C_{xx}(\tau) = \sigma_x^2 e^{-\tau\lambda} \cdot \lambda^{-1}$ is 10 ms theoretical and 9.38 ms estimated. $\sigma_x^2 = 2.82\ V^2$. Listed are the average and s.d. of 156 points as a function of two times: τ_1 and τ_2, as well as the theoretical values.

τ_2 (ms)	Value of τ_1 (ms)					
	0	1	3	10	30	99
0	2.735 E-3 ±2.7 E-4 2.884 E-3	2.693 E-3 ±2.7 E-4 2.868 E-3	2.567 E-3 ±2.7 E-4 2.763 E-3	1.910 E-3 ±2.0 E-4 2.041 E-3	2.071 E-4 ±1.4 E-4 4.832 E-4	−1.03 E-4 ±1.6 E-4 7.910 E-7
1		2.676 E-3 ±2.7 E-4 2.884 E-3	2.563 E-3 ±2.7 E-4 2.755 E-3	1.904 E-3 ±2.0 E-4 2.043 E-3	1.83 E-4 ±1.4 E-4 4.85 E-4	−9.21 E-5 ±1.6 E-4 7.955 E-7
3			2.503 E-3 ±2.6 E-4 2.688 E-3	1.898 E-3 ±2.0 E-4 2.047 E-3	1.678 E-4 ±1.4 E-4 4.97 E-4	−6.24 E-5 ±1.6 E-4 8.271 E-7
10				1.829 E-3 ±1.8 E-4 1.974 E-3	2.712 E-4 ±1.1 E-4 6.329 E-4	−1.49 E-4 ±1.3 E-4 1.2 E-6
30					1.305 E-3 ±1.4 E-4 1.46 E-3	−1.59 E-4 ±1.3 E-4 7.25 E-6
99						1.552 E-3 ±1.7 E-4 1.442 E-3

inexact corrections. The baseline correction in the present program is based on the usual corrections and is not the optimal method.

It is possible to use noise spectra for determining the uncertainty in signal-integrating procedures. However, the use of spectra as reported in literature is impractical. The influence of a priori data manipulations like offset and drift correction is not taken into account. A least-squares estimate of the correction results in an ACVF, which has an integral of zero. A noise spectrum with a d.c. value of zero is not realistic, however.

The chosen solution, a least-squares fit of the ACVF with $A + Be^{\tau\lambda}$ results in an ACVF approaching zero for a large lag and gives a more realistic estimate of the averaged squared deviations from the baseline. This idealisation of the non-ideal methods is necessary to produce coherent data for different correction times. It should be remembered that a baseline correction over a consecutive time interval, as is carried out in the program, is generally impractical in chromatography. Two time intervals, one on each side of a peak, are used, which affects only the reliability of the correction.

The program has been tested on a number of detectors, both in spectroscopy and chromatography. Our experience is that, after correction, noise from many sources can be described adequately by a first-order ACVF.

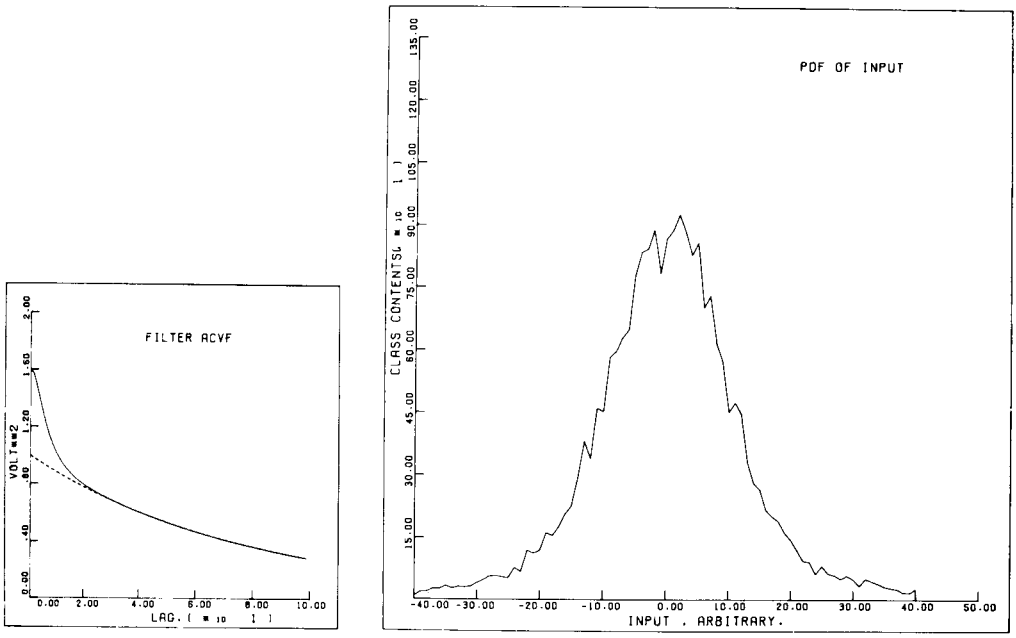

Fig. 4. Example of the effect of filtering on a first-order ACVF. The smaller amplitude after filtering is not taken into account, in order to reveal the difference in shape. (---) Without filtering.

Fig. 5. The PDF of all samples of a piece of baseline noise after application of a 2nd order correction. (Experimental, example 1).

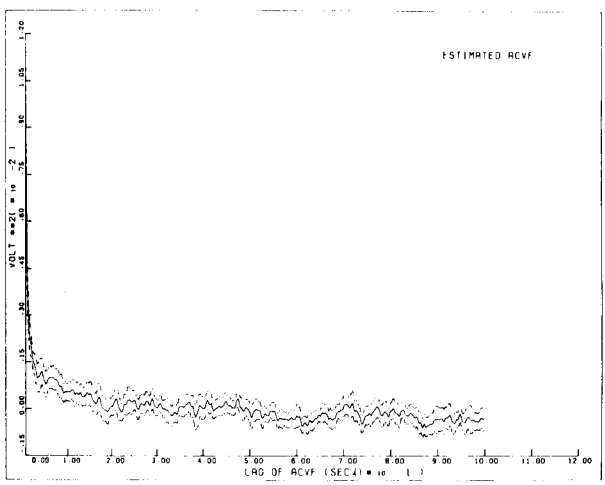

Fig. 6. The ACVF of the same data as used for Fig. 5, together with the 90% confidence interval, calculated from partial ACVFs.

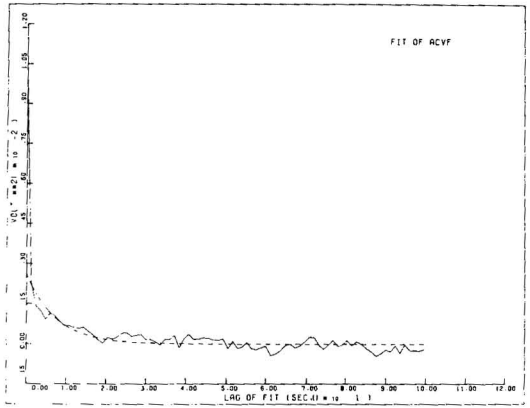

Fig. 7. The final fit of the estimated ACVF with a first-order approximation. The distortion caused by an anti-aliasing filter is not taken into account in the fit.

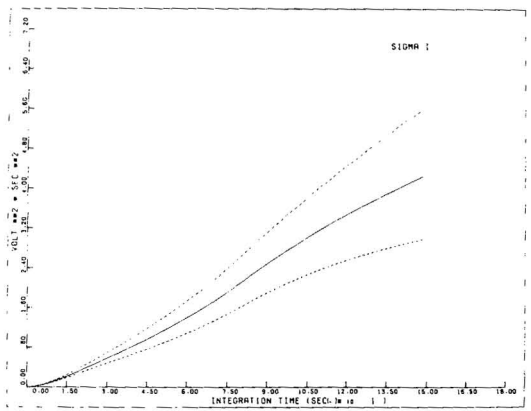

Fig. 9. The final result for the variance of a piece of integrated baseline with a 90% confidence interval. Noise source: flame ionization detector (Experimental, example 2).

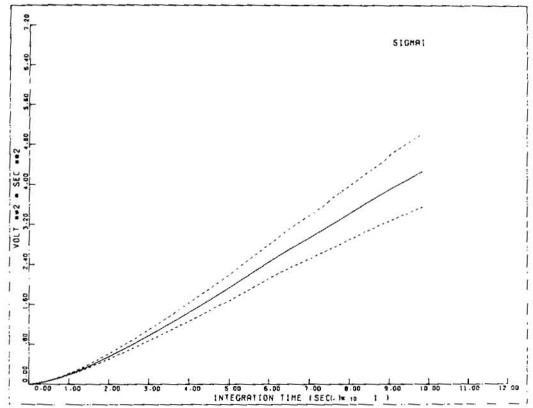

Fig. 8. The final result for the variance of a piece of integrated baseline with a 90% confidence interval. The integration took place after application of a 2nd order correction. Noise source: u.v. detector (Experimental, example 1).

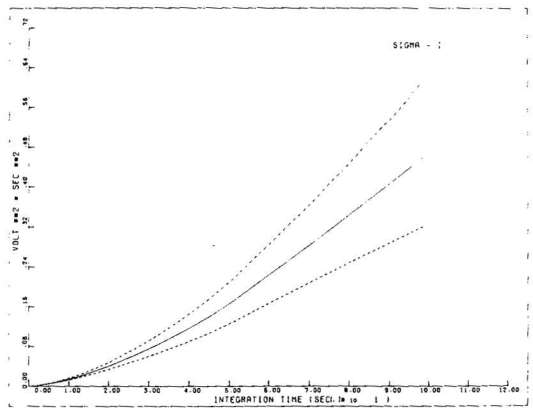

Fig. 10. The final result for the variance of a piece of integrated baseline with a 90% confidence level. Noise source: i.c.p.-a.e.s. detector (Experimental, example 3).

TABLE 3

The second moment of the integral over the ACVF (cf. eqn. 5) as a function of integration time for various ACVF's ($\Delta\tau$ is the sampling time and is multiplied by the number of points in the first column to yield the integration time. T is the measuring time of each ACVF. τ or λ^{-1} is the estimated time constant of the ACVF; for the higher-order system it corresponds to the correlation time. σ_x^2 is the variance of the noise. N is the number of repetitions of each integration.)

No. of points	$\Delta\tau$ = 1 ms T = 512 ms τ = 9.4 ms σ_x^2 = 0.28 V² N = 156	$\Delta\tau$ = 1 ms T = 2.0 s τ = 11 ms σ_x^2 = 0.29 V² N = 176	$\Delta\tau$ = 1 ms T = 128 ms τ = 8.0 ms σ_x^2 = 0.27 V² N = 177	$\Delta\tau$ = 3.3 ms T = 1.7 s τ = 8.8 ms σ_x^2 = 0.28 V² N = 162	$\Delta\tau$ = 0.33 ms T = 0.17 s τ = 8.8 ms σ_x^2 = 0.28 V² N = 84	$\Delta\tau$ = 1 ms T = 512 ms τ = 9.6 ms σ_x^2 = 0.35 V² N = 174
2	4.29 E-14 4.58 E-14	1.27 E-14 1.38 E-14	1.79 E-13 2.06 E-13	1.52 E-12 1.29 E-12	1.44 E-15 1.48 E-15	7.31 E-14 7.13 E-14
5	1.62 E-12 1.74 E-12	4.89 E-13 5.26 E-13	6.86 E-12 7.88 E-12	4.69 E-11 4.04 E-11	5.6 E-14 5.77 E-14	2.79 E-12 2.71 E-12
10	2.42 E-11 2.5 E-11	7.33 E-12 7.9 E-12	1.03 E-10 1.18 E-10	5.38 E-10 4.47 E-10	8.84 E-13 9.11 E-13	4.14 E-11 4.02 E-11
20	3.17 E-10 3.4 E-10	9.66 E-11 1.07 E-10	1.36 E-9 1.60 E-9	4.74 E-9 4.15 E-9	1.37 E-11 1.39 E-11	5.32 E-10 5.33 E-10
50	6.31 E-9 7.76 E-9	1.98 E-9 2.56 E-9	2.92 E-8 3.78 E-8	5.63 E-8 6.86 E-8	4.69 E-10 4.47 E-10	1.06 E-8 1.22 E-8
99	4.54 E-8 6.66 E-8	1.31 E-8 2.24 E-8	2.07 E-7 3.28 E-7	2.36 E-7 5.37 E-7	5.52 E-9 4.91 E-9	7.29 E-8 1.05 E-7

APPENDIX

The basic method of calculating the covariance of an ACVF has been described [2]. The following definitions and notations are used:

time series: $x(t)$

estimated ACVF:
$$C_{xx}(\tau) = \begin{cases} \frac{1}{T}\int_0^T x(t)\,x(t+\tau)\mathrm{d}t, & |\tau| \leqslant T \\ 0, & |\tau| > T \end{cases}$$

theoretical ACVF: $\gamma_{xx}(\tau) =$ in this case $\sigma_x^2 e^{-\lambda|\tau|}$, $\lambda > 0$

covariance of the estimated ACVF:
$$\mathrm{COV}\,[C_{xx}(u_1), C_{xx}(u_2)] = \frac{1}{T^2}\int_0^T\int_0^T \{\gamma_{xx}(\nu - t)\gamma_{xx}(\nu - t + u_2 - u_1) + \gamma_{xx}(\nu - t + u_2)\gamma_{xx}(\nu - t - u_1)\}\mathrm{d}t\mathrm{d}\nu$$

The integral, representing the covariance of the estimated ACVF, is split into parts for the conditions $u_1 \geqslant 0 \wedge u_2 \geqslant 0$, integrated for all cases and combined to give:

$$\mathrm{COV}\,[C_{xx}(u_1), C_{xx}(u_2)] = \frac{\sigma_x^4}{T^2}\left\{e^{-\lambda|u_2-u_1|}\left(-\tfrac{1}{2}\,|u_1-u_2|^2 + \left(T-\frac{1}{2\lambda}\right)|u_1-u_2\right.\right.$$

$$\left. + \frac{T}{\lambda} - \frac{1}{\lambda^2}\right) + e^{-\lambda(u_1+u_2)}\left(-\tfrac{1}{2}\,(u_1^2+u_2^2) + \left(T-\frac{1}{2\lambda}\right)(u_1+u_2) + \frac{T}{\lambda} - \frac{1}{\lambda^2}\right)$$

$$\left. + e^{-2\lambda T}\,\frac{1}{2\lambda^2}\left(e^{-\lambda(u_2-u_1)} + e^{-\lambda(u_1-u_2)}\right)\right\}$$

If $u_1 = u_2$, Var $\{C_{xx}(u)\}$ is obtained (eqn. 25). This is equivalent to the formulation in Bendat and Piersol [8, eqn. 31].

The integral (eqn. 5) $\sigma_I^2 = 2\int_0^T (\tau - t)C_{xx}(t)\mathrm{d}t$ has a variance, given by:

$$\sigma^2_{\sigma_I^2} = \int_0^T \int_0^T 2(\tau - t_1)2(\tau - t_2)\mathrm{COV}\,[C_{xx}(t_1), C_{xx}(t_2)]\;\mathrm{d}t_1\mathrm{d}t_2$$

For the first-order case, with $\gamma_{xx}(\tau) = \sigma_x^2 e^{-|\tau|\lambda}$, we define: $\alpha = \lambda\tau$ (τ = integration time) and $\beta = \lambda T$ (T = measuring time). This yields

$$\sigma^2_{\sigma_I^2} = \frac{4\sigma_x^2}{\beta^2\lambda^4}\left[\left\{\alpha^3\left(\frac{4}{3}\beta - \frac{4}{3}\right) + 5\alpha^2 + \alpha(-8\beta - 4) + 15\beta - 21.5\right\} + e^{-\alpha}\{2\alpha^3\right.$$

$$+ 10\alpha^2 + \alpha(-4\beta + 26) - 20\beta + 18\} + e^{-2\alpha}\{\alpha^2 + \alpha(2\beta + 3) + 5\beta - 3.5\}$$

$$\left. + e^{-2\beta}\{e^{-\alpha}(-\alpha - 1) - \alpha^2 + 2 + e^{\alpha}(\alpha - 1)\}\right]$$

REFERENCES

1 H. C. Smit and H. L. Walg, Chromatographia, 8 (1975) 311.
2 G. M. Jenkins and D. G. Watts, Spectral Analysis and its Applications, Holden-Day, San Francisco, 1969.
3 P. R. Bevington, Data Reduction and Error Analysis for the Physical Sciences, McGraw-Hill, New York, 1969.
4 T. T. Lub and H. C. Smit, Anal. Chim. Acta, 112 (1979) 341.
5 H. L. Walg and H. C. Smit, Anal. Chim. Acta, 103 (1978) 43.
6 J. Vlach, Computerized Approximation and Synthesis of Linear Networks, J. Wiley, New York, 1969.
7 C. H. Gast, J. C. Krook, H. Poppe and F. J. M. J. Maessen, J. Chromatogr., 185 (1979) 549.
8 J. S. Bendat and A. G. Piersol, Measurement and Analysis of Random Data, J. Wiley, New York, 1968.

Analytica Chimica Acta, 133 (1981) 85—97
Computer Techniques and Optimization

SOME CONSIDERATIONS ON BATCH ARRIVAL AND BATCH ANALYSIS IN ANALYTICAL LABORATORIES

J. G. VOLLENBROEK and B. G. M. VANDEGINSTE*

Department of Analytical Chemistry, University of Nijmegen, Toernooiveld, Nijmegen (The Netherlands)

(Received 28th April 1980)

SUMMARY

The mean delay of analytical results is an important parameter in the performance of analytical laboratories. The modes of sample arrival and processing influence that delay. By the application of queueing theory and digital simulation, the effects of batch arrival and batch processing on the delay are estimated.

Various aspects of the organisation of an analytical laboratory for structural analysis have been considered previously [1, 2]. The effects of various dispatching rules on the performance, i.e., the delay of the analytical result, of the laboratory were estimated. For instance, the effects of (i) the introduction of an adaptable routing procedure of the samples, (ii) various analyst assignment decisions, and (iii) different strategies on the priorities of the samples, were simulated with a computer model of an actual laboratory for structural analysis, using spectroscopic methods [2]. In addition to these decisions, the laboratory must also decide about the number of samples that will be analyzed simultaneously in one batch. Moreover, the effects of alternative policies for sample arrival at the laboratory should be known. In the present paper these effects are computed, starting from the simplest single-server queueing model having exponentially distributed inter-arrival and analysis times (M/M/1 system). That model has been extensively studied, and Kleinrock [3] has given a good survey of its properties. Thereafter, the estimated effects are validated for the laboratory investigated by means of the earlier simulation model [1, 2]. In the model, a batch arrival and/or batch analysis of the samples can be generated. The batch size of the arriving samples and the inter-arrival times of the batches can be distributed according to various probability density functions (Gaussian, constant, Poisson, exponential).

The laboratory investigated receives about 3000 samples per year, which can be analyzed in four sections: infrared (i.r.), proton magnetic resonance (^{1}H-n.m.r.), mass (m.s.) and carbon-13 nuclear magnetic resonance (^{13}C-n.m.r.) spectrometry. The analytical procedure consists of two consecutive steps: the measurement and interpretation of the spectrum. On average, 1.28

analyses are done per sample. Under normal operation, the samples arriving at the laboratory have a Poisson distribution, which is equivalent to exponentially distributed inter-arrival times [3].

In the model an upper and lower limit of the batch size for analysis is introduced. Before starting the measurements, the analyst should wait until the required batch size (lower limit) has been reached. When the lower limit equals one, the analyst starts the measurements whenever there are samples waiting. Spectra are interpreted after the measurement of a batch has been completed. In order to account for the decrease in the analysis time by performing batch analysis, an overhead factor lying between 0 and 1 is introduced.

CALCULATIONS ON M/M/1 MODELS

Batch input systems

An alternative to separate arrivals of samples at the laboratory is to collect the samples during a given period and send them in a batch. In that model, the delay for a sample consists of two independent components: the delay for the first member of the batch and the delay caused by the analysis times of the preceding samples in the batch. Queues are described by a shorthand notation A/B/m, where A, B and m represent the distributions for inter-arrival time (iAT) and analysis time (AT), and the number of channels. For example, in the M/M/1 system, both the inter-arrival time and service time are exponentially distributed, and there is only one service channel.

Consider the transformation of an M/M/1 system to a system where batches of samples arrive with a mean size $\bar{r}$. When batch analysis does not affect the mean analysis time ($\overline{AT}$) of the samples, the mean process time of a batch equals $\bar{r} \times \overline{AT}$. Clearly, the mean inter-arrival time of the batches equals $\bar{r} \times \overline{iAT}$. Consequently, the transformation of the M/M/1 system to a batch arrival system does not alter the utilization factor (ρ) of the system as $\rho = \bar{r}.\overline{AT}/\bar{r}.\overline{iAT} = \overline{AT}/\overline{iAT}$. When two models are compared having an equal sample flow, one with and the other without batch arrivals, then the ratios (Table 1) between the mean system times of both systems can be calculated (see Appendix A for the derivation of the equations). At first sight, one might expect that batch arrivals would result in lower delays. However, the equations presented in Table 1 indicate that the mean delay time will only be improved under certain conditions. It is easily seen that for exponentially distributed inter-arrival times of the samples, the outcome of eqns. (5)—(8) is greater than one. Therefore, for such systems no improvement can be obtained, and the performance becomes even worse as the batch size becomes larger. When the batches arrive at equidistant times, it depends on the distribution of the batch size whether an improvement will be obtained or not. In that case, systems with Poisson or exponentially distributed batch sizes have longer delays than systems with individual arrivals. In contrast, when all batches are of equal size, lower delays are obtained when $\bar{r} < 1/(1 - \rho)$. However, the lowest delay is found for $r = 1$, as then the original M/M/1

TABLE 1

Ratio between the delay in an M/M/1 system with and without batch arrivals

P.d.f. of the batch size	Probability density function (p.d.f.) of the inter-arrival time of the batches								
	Equations				Verification by simulation[a]				
	Constant		Exponential		Constant			Exponentia	
					σ_r	calc.	sim.	calc.	sim
Poisson	$0.5\bar{r}(1-\rho)+1$	(1)	$1+0.5\bar{r}$	(5)	2.8	2.1	2.8	5	8.5
Constant	$0.5\bar{r}(1-\rho)+0.5$	(2)	$0.5+0.5\bar{r}$	(6)					
Exponential	$0.5\bar{r}(2-\rho)+0.5$	(3)	$0.5+\bar{r}$	(7)	8	4.6	3.8	8.5	5.6
Gaussian	$0.5\frac{\sigma_r^2}{\bar{r}}+0.5\bar{r}+0.5-0.5\bar{r}.\rho$	(4)	$0.5\frac{\sigma^2 r}{\bar{r}}+0.5\bar{r}+0.5$	(8)	1	1.7	1.7	4.5	4.9
					2.8	2.2	2.0	5.0	4.7
					4	2.7	2.1	5.5	5.2
					0[b]	0.8	0.8		

[a] M/M/1 system with $\overline{iAT} = 1$, $\overline{AT} = 0.7$ transformed to a batch arrival system with $\bar{r} = 8$ and $\overline{iAT} = 8$.
[b] Same system, transformed to $\bar{r} = 2$ and $\overline{iAT} = 2$.

system has been transformed to a D/M/1 system (D stands for deterministic arrival). Substituting $r = 1$, in eqn. (2) (Table 1), the ratio between the delay with and without batch arrivals is $(1 - 0.5\ \rho)$. That is exactly the ratio between the delay of a D/M/1 and M/M/1 system having the same utilization factor (ρ).

Furthermore, for Gaussian-distributed batch sizes, improvement is only achieved under certain conditions of the variation coefficient of the batch size (σ_r^2/r^2). The outcome of eqn. (4) in Table 1 is only smaller than one, when $\sigma_r^2/r^2 < 1/r - (1 - \rho)$. That means that with increasing mean batch sizes, the variation coefficient of the batch size should be decreased in order to achieve better operation. The number of arrivals per unit of time in an M/M/1 system has a Poisson distribution. In the alternative situation, where all samples enter the laboratory simultaneously, e.g. once or twice per day, the batch sizes will also have a Poisson distribution. Here, no enhancement of the system performance is obtained (eqn. 5 in Table 1), and the results become even worse when the sample flow (λ) to the system is high $(\bar{r} = \lambda)$.

The equations presented in Table 1 were verified by simulation for an M/M/1 system with $\overline{iAT} = 1$, $\overline{AT} = 0.7$ and $\bar{r} = 1$, which was transformed to a batch input system with $\bar{r} = 8$ and $\overline{iAT} = 8$. The results compiled in Table 1 demonstrate that the outcome of the simulations agrees reasonably well with the theoretical forecast. Simulation experiments as described later in this paper were conducted with the laboratory model in order to validate these theoretical results on the practical situation.

Batch analysis systems

Two main batch analysis systems can be established in analytical laboratories. The analyst (or instrument) can handle a batch of r samples simultaneously. If the instrument becomes free while less than r samples are

waiting, the analysis of the batch is not started until r samples have been collected in total (rule 1). However, because it seems a waste to wait until a batch of r samples is present, a discipline can be chosen where the analyst starts the analysis even when less than r samples are waiting (rule 2).

The effect of batch analysis on the mean delay depends on the relative effect of waiting until a batch of a given size becomes available and the decrease of the utilization factor as a result of a decrease of the mean analysis time. In spectroscopic analysis, samples of a batch are measured sequentially. In that case, a sample can be prepared during the scan of the preceding one. This decreases the mean analysis time by a factor depending on the overlap of the manipulations on the sample, which is called the overhead factor (f).

Exact calculations on an M/M/1 system with batch analysis as a function of the utilization factor (ρ), the overhead factor (f) and the mean batch size ($\bar{r}$) are rather complicated. A good approximating relation, however, can be obtained starting from the point that the system time is much more affected by the mean of the analysis time than its variation coefficient [1]. The mean analysis time ($\overline{AT_r}$) of the samples in a system where exactly r samples are analyzed sequentially can be calculated by using eqn. (9) if it is assumed that the analysis time of the second and next samples in the batch equals $(1-f)AT_2$; $(1-f)AT_3 \ldots$

$$\overline{AT_r} = (\overline{AT}/r)\,[1 + (1-f)(\bar{r}-1)] \tag{9}$$

Consequently the utilization factor of the batch system (ρ_r) is

$$\rho_r = (\rho/r)\,[1 + (1-f)(r-1)] \tag{10}$$

where ρ is the utilization factor ($\rho = \overline{AT}/\overline{iAT}$) of the original M/M/1 system.

By substituting eqns. (9) and (10) in the relation (11) between the delay and utilization factor for an M/M/1 system, and adding a term accounting for the mean time the analyst should wait before having a batch of r samples, an approximation of the mean delay of a batch service system is found (eqn. 12)

$$\overline{T} = \overline{AT}/(1-\rho) \tag{11}$$

$$\overline{T_r} = \overline{AT}[1 + (1-f)(\bar{r}-1)]/\bar{r}\left\{1 - \frac{\rho[1 + (1-f)(\bar{r}-1)]}{r}\right\} + \overline{iAT}(\bar{r}-1) \tag{12}$$

where $\overline{iAT}$ is the mean inter-arrival time of the samples, and ρ is the utilization factor of the original M/M/1 system. Substituting the value $r = 1$ in eqn. (12) yields the mean delay of an M/M/1 system.

For $f = 0$, the analyses of the samples do not overlap, and therefore no reduction of the analysis time is obtained. As a result, in that case, the delay is increased with the mean time the analyst has to wait to obtain a batch of r samples: $iAT(\bar{r}-1)$. For $f = 1$, the situation of an analyzer with r parallel channels is obtained. Because in such systems, r samples may be analyzed

simultaneously in an average time $\overline{AT}$, the utilization factor (ρ) of the system is $\rho/\bar{r}$. For that system eqn. (12) forecasts that

$$T_r = \overline{AT}[1/(r - \rho) + (r - 1)/\rho] \tag{13}$$

For large batches $(r - 1)/\rho \gg 1/(r - 1)$, most of the time is spent waiting until r samples are present.

The accuracy of eqn. (12) was checked against simulations of an M/M/1 system with batch analysis. The results of these simulations, presented in Fig. 1, demonstrate clearly that for small overhead factors ($0 < f < 0.4$), close agreement is obtained. For high overhead factors ($f > 0.4$) and large batches, an excessive response of the delay on the batch size is obtained. More interesting is the observation that for $f \neq 0$, an optimal batch size (N_{opt}) can be obtained, yielding a minimal delay. In Fig. 2, the optimal batch size is plotted as a function of the overhead factor (f) and utilization factor (ρ), which can be found by differentiating eqn. (12)

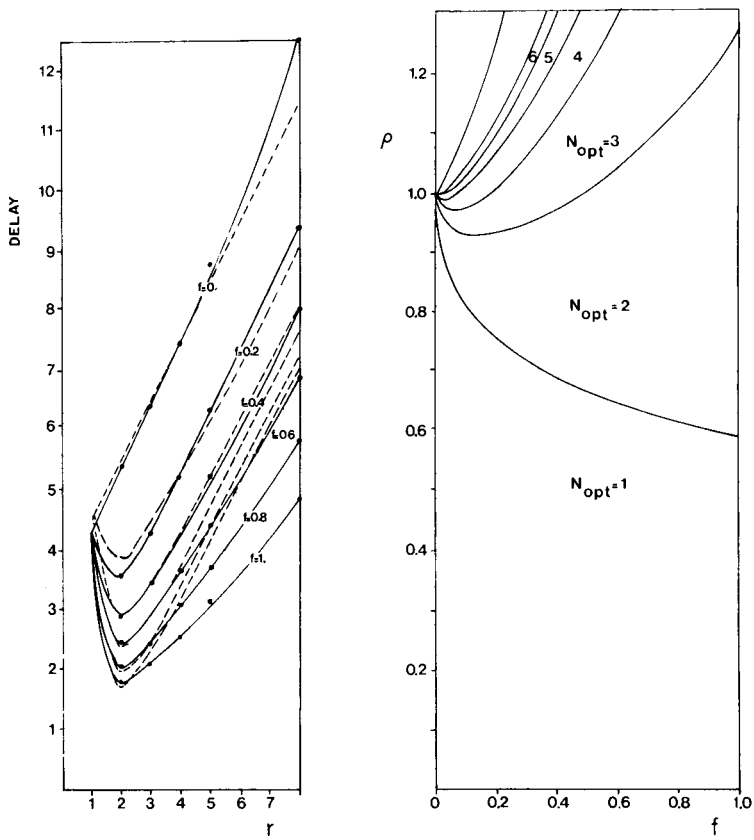

Fig. 1. The influence of the batch size (r) for analysis on the mean delay (rule 1: see text). (—) Simulated data; (---) calculated data.

Fig. 2. The optimal batch size (N_{opt}) as a function of the overhead factor (f) and utilization factor (ρ) (rule 1: see text).

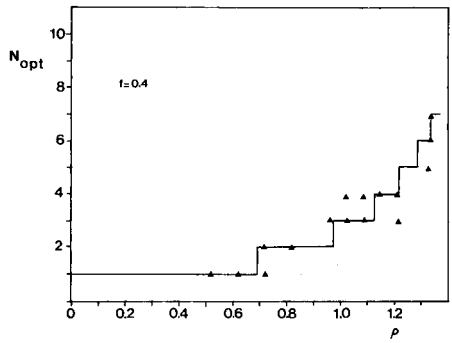

Fig. 3. Comparison of the calculated and simulated optimal batch size (N_{opt}) as a function of the utilization factor (ρ) for an overhead factor $f = 0.4$ (rule 1: see text). (—) Calculated data; (▲) simulated data.

$$N_{opt} = (f + f^{1/2}/\rho)/(f - 1 + 1/\rho) \tag{14}$$

This calculated optimal batch size agrees reasonably well with the simulated observations for $f = 0.4$ (Fig. 3). In both cases, the N_{opt} increases asymptotically with the utilization factor (ρ), approaching a value greater than 1. In such a system, more samples enter the system than can be analyzed if reduction of the analysis time is not obtained by simultaneous analysis. For $f = 1$ (i.e. parallel analysis), the optimal batch size is $\rho + \rho^{1/2}$. Thus parallel analysis in an M/M/1 system becomes advantageous only if $\rho > 0.6$. Clearly, for $\rho > 1$, batch analysis becomes necessary in order to avoid system congestion. For the M/M/1 system considered, the simple rule is obtained that the optimal batch volume for parallel analyzers, in terms of delay, is somewhat greater than the ratio between the analysis time of a single sample and the inter-arrival time of the samples. For saturated systems ($\rho > 1$) with smaller overhead factors, the batch size should be increased further, in order to obtain a sufficient decrease of the mean analysis time so as to remove system congestion. In contrast, the optimal batch volume for systems with low utilization factors ($\rho < 0.9$) decreases with decreasing overhead factors. Apparently, in that situation, the time needed to collect the samples becomes greater than the reduction of the delay by batch analysis. If the condition that analysts should wait until r samples are available is abandoned, i.e., they are permitted to start measurements when less than r samples are waiting, a totally different situation appears. For this particular instance, the change in delay time on increasing the batch size, assuming parallel analysis ($f = 1$), can be calculated exactly from the equations given by Kleinrock [3] (see Appendix B). The results (Fig. 4) indicate here that the delay is a monotonic decreasing function of the batch size, which approaches $\overline{AT}$ asymptotically for large batches. In that case, it is always advantageous to analyze batches, instead of separate samples. However, the graphs for $\rho < 1$ ($\rho = 0.5$ and 0.9) clearly demonstrate that there is little sense in processing more than

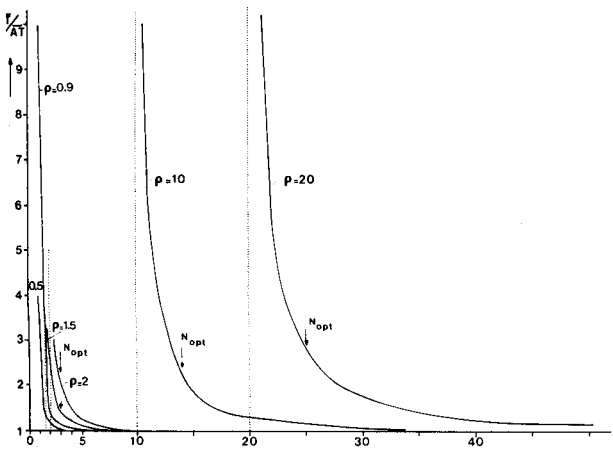

Fig. 4. The mean delay as a function of the batch size (r) for parallel analysis, for various utilization factors (ρ) (rule 2: see text). N_{opt} is the optimal batch size for the same system operating under rule 1.

three samples at once in systems with spare capacity, as 98.7 or 98.3%, respectively, of the obtainable effect is already acquired. For systems where batch analysis is necessary in order to avoid system congestion ($\rho > 1$), the absolute reduction of the delay becomes very small for $r > 1.7\ \rho$. The underlying system is identical to the above-mentioned model having an upper (N_u) and lower (N_l) limit to the batch size (r), where $N_l = 1$ and $N_u = r$. In Fig. 4, the optimal batch sizes (N_{opt}) are marked as found for the model where $N_l = N_u = r$. Here, it should be noted that for the system with $N_l = 1$, the upper limit of the batch size has only a minor influence on the performance of the system, provided that this limit is greater than the optimal batch size found for the system with $N_u = N_l = r$. For systems with spare capacity ($\rho < 0.6$), the optimal batch size is one. Therefore, it can be expected that a very loose rule can be applied in the laboratory studied: the analysts may start simultaneously the analysis of as many samples as they like, provided that they do not wait until some particular number of samples is present.

Simulations carried out on an M/M/1 system with $N_l = 1$ confirm these theoretical expectations (Fig. 5). In summary, the following effects can be forecast on batch analysis in analytical laboratories.

Rule 1. The analyst should wait until a batch of r samples is available ($N_u = N_l = \bar{r}$). An optimal batch size (N_{opt}) can be calculated, for which a minimal delay is found. For systems with spare capacity ($\rho < 0.6$), $N_{opt} = 1$; that value is independent of the overhead factor (f). For highly saturated (but not congested) systems ($0.7 < \rho < 1$), the optimal batch size is less than 3, except for very small overhead factors ($f < 0.1$). For congested systems ($\rho \gg 1$), the optimal batch size for parallel analysis ($f = 1$) is somewhat greater than the ratio between the mean analysis time of a sample and the mean inter-arrival time.

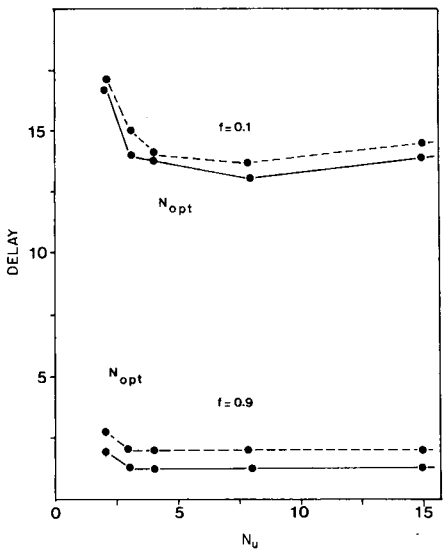

Fig. 5. The mean delay as a function of the upper limit (N_u) of the batch size. (---) Lower limit (N_l) of the batch size = 2; (—) lower limit (N_l) of the batch size = 1. N_{opt} is the optimal batch size for the same system when $N_l = N_u$.

Rule 2. The batch size is confined between an upper (N_u) and lower limit (N_l). The analyst starts the analyses as soon as there are N_l samples present in the system. Only systems with $N_l = 1$ and $f = 1$ were considered. The delay is a monotonic decreasing function of the batch size. It is always advantageous to analyze batches whatever their size; for systems with $\rho < 1$, almost all obtainable reduction of the delay is acquired for $N_u = 3$ whereas for congested systems ($\rho \gg 1$) the absolute reduction of the delay becomes small when $N_u > 1.7\,\rho$.

SIMULATIONS

The first part of this paper forecast the effects of batch arrival and batch analysis on the delay. However, as stated above, an M/M/1 model is too simple a representation of a complex system such as a real laboratory. The analytical procedure consists of two steps: measurement and interpretation. Therefore, a batch of samples is measured first, whereafter the interpretation commences. Only during the measurement step is a reduction of the analysis time obtained by batch analysis. Also the batch arrival process to the laboratory is more complex than is supposed in the M/M/1 model. Samples arrive in the laboratory investigated from two main origins at a ratio of 1:3. Moreover, 20% of all submitted problems are not solved after the first analysis, which causes a circulation of unfinished samples in the laboratory, and complicates the description of the arrival process [2]. The non-analytical activities of the analysts, while samples are waiting, have a very strong impact

TABLE 2

Effect of the mean batch size ($\bar{r}$), probability density function of the batch sizes, and the minimal required batch size (N_1) before starting the measurements. Analysis of variance of a 2×3^2 design
(Factor levels: (A) minimal batch size (N_1) = 1 (loose rule), maximal batch size (tight rule); (B) p.d.f. of the batch size: constant, Poisson, exponential; (C) batch size = 1, 2 batches/day, 1 batch/day. P.d.f. of the inter-arrival times of the batches is constant.)

Source of variation	Sum of squares	Degrees of freedom	Mean square	Effect (days)
Main effects				
A	7.16	1	7.16[a]	+1.26
B	0.55	2	0.27	
C	1.08	2	0.54[b]	+0.59
Two-factor interactions				
A × B	0.24	2	0.12	
A × C	1.25	2	0.62[b]	
B × C	2.30	4	0.57[b]	
Residual	0.21	4	0.05	

[a]Significant $P < 1\%$. [b]Significant $1\% < P < 5\%$.

on the delays, which is comparable to the influence of the utilization factor. The simulated delay in the laboratory without non-analytical activities and without instrument failure was 3.9 days, with a maximum delay of 24 days. Under normal conditions, the delay is 6.9 days with a maximum of 40 days. For this reason, the influence of batch arrival and analysis was simulated, using the previously described digital simulation model of the laboratory.

Batch arrivals

The effect of the mean batch size of the arriving samples and its probability density function was investigated by means of a 2×3^2 factorial design. The results (Table 2) demonstrate that the delay in the simulation model is considerably less sensitive to the arrival process than is the M/M/1 system. The introduction of a batch arrival (once per day) of samples increases the delay by 10% only, whereas the distribution of the batch size does not affect the mean delay significantly.

In this factorial design, the effect of the introduction of batch arrivals was compared to the effect of the lower limit (N_1) of the batch size, required for analysis. It was found that this latter factor is considerably more important. The best operation is to process the samples individually. This agrees with the theoretical calculations on an M/M/1 system as the utilization factors of the instruments and personnel are about 0.6 and only small overhead factors (f = 0.1) were introduced. In theory, according to Fig. 2, no improvement of the delay could be expected by the introduction of batch analysis. The effect of batch analysis can be expected to depend on the

arrival process of the samples. However, relatively small interactions were observed.

Batch analysis

The effects of the upper (N_u) and lower (N_l) limits on the batch size for analysis, and the overhead, were investigated by means of a 2×3^2 factorial design. As expected from the calculations presented in Fig. 2, the results (Table 3) show that the overhead factor and lower limit of the batch size have a significant effect on the mean delay. A minimal delay is found for $N_l = 1$. In terms of laboratory organization, this means that the loose rule, where the analyst should not wait until a sufficiently large batch of samples is present, performs better than the tight rule, where the analyst should wait.

No significant effect was found for the upper limit of the batch size. For this reason, the conclusion is confirmed that the analyst may analyze simultaneously as many samples as he likes, provided that he does not wait until some definite number of samples is present. Simulation results where the upper and lower limits of the batch size are equal show that the optimal size depends on the sample flow and the overhead factor (Table 4). This agrees with the calculations on an M/M/1 system (Fig. 2) where the optimal batch size increases with increasing overhead factor and number of arrivals. An interesting property is that the optimal batch size is hardly dependent on the overhead factor at the level of the sample flow to the laboratory.

TABLE 3

Effects of the minimal batch size (A), overhead (B) and maximal batch size (C). Analysis of variance of a $2^1 \times 3^2$ design
(Factor levels: (A) minimal batch size = 1 (loose rule), maximal batch size (tight rule); (B) overhead = 1.0, 0.9, 0.8; (C) maximal batch size, 0.5λ, λ, 1.5λ, where λ is the input density to the section.)

Source of variation	Sum of squares	Degrees of freedom	Mean square	Variance ratio	Effect
Main effects					
A	2.6	1	2.6	54.1[a]	+0.8
B	5.24	2	2.6	54.1[a]	−1.3
C	0.32	2	0.16	3.3	
Two-factor interactions					
A × B	0.07	2	0.034	0.7	
A × C	0.25	2	0.125	2.6	
B × C	1.43	4	0.36	7.5[b]	
Three-factor interactions					
A × B × C	0.01	4	0.0025	—	
var ($\overline{T}$)			0.048		

[a]Significant $1\% < P < 5\%$. [b]Significant P 21%.

TABLE 4

Simulated flow dependency of the optimal batch size (N_{opt}) in the actual laboratory

Sample flow Actual situation = 100	Overhead factor (f)	
	$f = 0.1$	$f = 0.9$
118	3	4
100	2	2—3
78	1	2
64	1	1

CONCLUSIONS

Calculations on a simple M/M/1 model forecast that the introduction of batch arrivals to the laboratory will improve the system performance (mean delay) only when three conditions are fulfilled: (i) the batches enter the system at equal intervals; (ii) the variation coefficient of the batch size lies between 0 and $1/r - (1 - \rho)$; (iii) the batch size is less than $1/(1 - \rho)$. The delay in the simulation model, however, is considerably less sensitive to the arrival process than in an M/M/1 system. This is probably because the non-analytical activities of the analysts influence the delay in the laboratory considerably. The best operation of sample processing (batches or single samples) is strongly dependent on the utilization factor (ρ), and the overhead factor (f).

For systems with fixed batch sizes, where the analyst waits until a batch of r samples is present, an optimal batch size can be calculated. For systems having a low utilization factor ($\rho < 0.6$) the best operation is to analyze the samples individually. If for such systems, the analyst should not wait until r samples are present, but may analyze all waiting samples collectively up to a maximum of r samples, the mean delay decreases monotonically with increasing batch size. However, 98% of the obtainable reduction of the delay is already acquired when $r = 3$.

Simulations of the laboratory demonstrated that application of the loose rule "that the analysts may analyze as many samples simultaneously as they like, if they do not wait until some number of samples is present" does not augment the delay significantly. One may generally conclude that the simulated effects obtained with the laboratory model are less pronounced than for simple queueing systems.

APPENDIX A. CALCULATION OF THE DELAY IN SYSTEMS WITH BATCH ARRIVALS

According to Burke [4], the average delay ($\overline{T}$) of a sample equals the sum of the delay of the first member of the batch ($\overline{T}_1$) and the delay caused by the analysis times of the members of the same batch analyzed before it:

$$\overline{T} = \overline{T_1} + \frac{\overline{AT}}{2}\left[\frac{E(r^2)}{E(r)} - 1\right] = \overline{w_1} + \frac{\overline{AT}}{2}\left[\frac{E(r^2)}{E(r)} + 1\right] \tag{A1}$$

where $\overline{w_1}$ is the waiting time of the first member of the batch ($\overline{w_1} = \overline{T_1} - \overline{AT}$), $\overline{AT}$ is the mean analysis time per sample and $E(r^2)$ is the second moment of the probability density function (p.d.f.) of the batch size. The second term in eqn. (A1) gives the average delay from the analysis times of the members of the batch analyzed before the sample. Table 5 gives the expressions for the first two moments of the various considered p.d.f. of the batch size (r).

(A) When the inter-arrival times of the batches are exponentially distributed, $\overline{w_1}$ can be calculated using the Pollaczek—Khinchin formula:

$$\overline{w_1} = (\overline{AT_b}/2)(1 + C^2_{AT_b})\rho/(1-\rho) \tag{A2}$$

with AT_b as the mean analysis time of a batch and $C^2_{AT_b}$ as the variation coefficient of the analysis time. For the batch system, $C^2_{AT_b} = \text{var}[AT_b]/[\overline{AT_b}]^2$. Because $\overline{AT_b} = \bar{r} \times \overline{AT}$, $\text{var}[AT_b] = \text{var}[AT]\{\bar{r} + \text{var}(\bar{r})\}$. Thus $C^2_{AT_b} = \text{var}[AT]\{\bar{r} + \text{var}(\bar{r})\}/[\bar{r}^2\,\overline{AT}^2]$. For exponentially distributed analysis times: $\text{var}[AT] = \overline{AT}^2$. Thus

$$\overline{w_1} = \rho\bar{r}\overline{AT}[1 + 1/\bar{r} + \text{var}(r)/\bar{r}^2]/[2(1-\rho)] \tag{A3}$$

(B) When the inter-arrival times are equidistant, $\overline{w_1}$ can be calculated using the heavy-traffic approximation of Kingman [5]:

$$\overline{w_1} = \{\text{var}[iAT_b] + \text{var}[AT_b]\}/2(1-\rho)\overline{iAT_b} \tag{A4}$$

where $\text{var}[iAT_b]$ is the variance of the inter-arrival times of the batches, and $\text{var}[AT_b]$ is the variance of the analysis time of the batches. For the batch system considered, $\text{var}[iAT_b] = 0$, $\overline{iAT_b} = r\,\overline{iAT}$, and $\text{var}[AT_b] = \text{var}[AT]\{r + \text{var}(r)\}$. Thus

$$w_1 = \overline{AT}\rho\{\bar{r} + \text{var}(r)\}/2\bar{r}(1-\rho) \tag{A5}$$

(C) The delay of an M/M/1 system is $\overline{T} = \overline{AT}/(1-\rho)$. The ratio between the delay of an M/M/1 system modified to a batch system and the original M/M/1 system can now easily be calculated by substituting the values of Table 5 in eqns. (A1), (A3) and (A5).

APPENDIX B. CALCULATION OF THE DELAY IN SYSTEMS WITH BATCH ANALYSIS

According to Kleinrock, the following relations hold in a system with batch analysis, where the analyst can handle r samples simultaneously, but should start the analysis even when less than r samples are waiting: the mean number of samples in the system is $\overline{N} = (1/z_0)/(1 - 1/z_0)$, where z_0 is the only root of the equation $\rho z^{r+1} - (1+\rho)z^r + 1$ for which $|z_0| > 1$. The mean delay ($\overline{T}$) can be calculated from Little's [6] relation $\overline{N} = \overline{T}\lambda$, where λ is the input density (e.g., samples per day). The curves presented in Fig. 5 are calculated for $AT = 1$, and λ values ranging from 0.9 to 20.

TABLE 5

The two first moments for several p.d.f. of the batch size (r)

P.d.f.	$E(r)$	$E(r^2)$	$\overline{T}$
Constant	r	$\bar{r}^2$	$\overline{w}_1 + \overline{AT}(\bar{r} + 1)/2$
Exponential	$\bar{r}$	$2(\bar{r})^2$	$\overline{w}_1 + \overline{AT}(2\bar{r} + 1)/2$
Poisson	$\bar{r}$	$\bar{r} + \bar{r}^2$	$\overline{w}_1 + \overline{AT}(\bar{r} + 2)/2$
Gaussian	$\bar{r}$	$\sigma_r^2 + (\bar{r})^2$	$\overline{w}_1 + \overline{AT}[\sigma_r^2/\bar{r} + \bar{r} + 1]$

REFERENCES

1 B. G. M. Vandeginste, Anal. Chim. Acta, 112 (1979) 253.
2 B. G. M. Vandeginste, Anal. Chim. Acta, 122 (1980) 435.
3 L. Kleinrock, Queueing Systems, Vol. 1, Theory, Wiley, New York, 1975.
4 P. J. Burke, Oper. Res., 23 (1975) 830.
5 J. F. C. Kingman, J. Royal Stat. Soc., B24 (1962) 383.
6 J. D. C. Little, Oper. Res., 9 (1961) 383.

Analytica Chimica Acta, 133 (1981) 99—101
Computer Techniques and Optimization

Short Communication

THEORY OF ERROR APPLIED TO PURE TEST VECTORS IN TARGET FACTOR ANALYSIS

EDMUND R. MALINOWSKI

Department of Chemistry and Chemical Engineering, Stevens Institute of Technology, Hoboken, New Jersey 07030 (U.S.A.)

(Received 23rd June 1980)

Summary. In target factor analysis, errors from the data matrix mix into the target-testing procedure even when the target is pure, thus confusing the analysis. A theoretical study shows how the errors mix into the target procedure and is used to develop a criterion to judge the degree of acceptability of pure targets.

In target factor analysis [1] certain types of target vectors are pure, i.e. free from experimental uncertainty. The unity test, the uniqueness test, tests for the presence of certain functional groups, and structural vectors, such as the carbon number, represent a few examples of pure targets. Predicted vectors which result from testing pure targets invariably contain an admixture of error caused by experimental error in the data matrix. Hence, the decision to accept or to reject a pure target by comparing it with the predicted vector is not simple. The present communication is concerned with developing a criterion for making such a decision.

Theory

The theory of error for target factor analysis [2] shows that a Pythagorean relationship exists between the apparent error in the target (AET), the real error in the target (RET) and the real error in the predicted target (REP):

$$(\mathrm{AET})^2 = (\mathrm{RET})^2 + (\mathrm{REP})^2 \qquad (1)$$

The apparent error in the target is the root-mean-square (RMS) error between the raw target vector, $\overline{\overline{\mathrm{R}}}$, which contains experimental error, and the predicted vector, $\overline{\mathrm{R}}$, which results from least-squares target testing. The real error in the target is the RMS error between the raw target and the hypothetically pure target, $\overline{\mathrm{R}}^*$. The error in the predicted target is the RMS error between the predicted vector and the pure target vector. If the target test vector were pure, RET would be zero and AET would equal REP.

In the original work [2], the calculated target transformation vector T was assumed to be equal to the hypothetically pure transformation vector T^*. This assumption leads to the conclusion that the real error in the predicted vector emanates solely from the error in the data matrix (EDM). By removing

this assumption an additional error contribution, called the excess error, appears in the equations, giving a truer portrayal of the situation.

Specifically, the assumption that

$$[R^*]\ T \cong \overline{R}^* \tag{2}$$

in eqn. (17) of the original paper should be replaced by

$$[R^*]\ T = \overline{R}^* + E_x \tag{3}$$

where $[R^*]$ is the hypothetically pure abstract row-factor matrix and E_x is the excess error vector. Since $[R^*]\ T^* = \overline{R}^*$, eqn. (3) can be rearranged to yield

$$E_x = [R^*]\ T - [R^*]\ T^* \tag{4}$$

By carrying the excess error vector E_x through the derivation as described earlier [2], the following relationship is obtained:

$$(REP)^2 = (EXE)^2 + (EDM)^2 \tag{5}$$

Here EXE is the RMS of the excess error, defined by

$$EXE = (E_x \cdot E_x / r)^{1/2} \tag{6}$$

Furthermore, this line of reasoning leads to

$$EDM = (RE)\ (T \cdot T)^{1/2} \tag{7}$$

where RE is the real error in the data matrix, which can be calculated from the eigenvalues [1, 3]. Note that if EXE is assumed to be zero then REP = EDM and

$$REP = (RE)\ (T \cdot T)^{1/2} \tag{8}$$

This equation, which is identical to eqn. (33) in the original work, is an approximation whereas eqn. (7) represents the true situation.

According to eqns. (1) and (5), if the target is pure, RET = 0 and

$$(AET)^2 = (EXE)^2 + (EDM)^2 \tag{9}$$

Since values for AET and EDM are readily obtainable, eqn. (9) affords a method for calculating EXE when pure targets are involved.

Even if a true pure test vector were found for which $T = T^*$, an error would still appear in the predicted vector because of the error in the data matrix (see eqn. 7). Considering eqns. (4) and (9), the best that can be achieved is

$$(AET)^2 = (EDM)^2 \tag{10}$$

From eqns. (9) and (10) it becomes evident that the excess error is a measure of the deviation from the best possible situation.

Criterion

The ratio between the excess error and the smallest possible apparent error in the target, called SPOIL,

$$\text{SPOIL} = \text{EXE/EDM} \tag{11}$$

can be used as a criterion to judge the acceptability of the target. If the pure target is a real factor its SPOIL, calculated by means of eqn. (11), should be close to zero. As a rule of thumb, for pure targets, a SPOIL between 0 and 1.5 is indicative of a real factor and is acceptable; a SPOIL between 1.5 and 3.0 is moderately acceptable because there is an increasing degree of uncertainty; a SPOIL greater than 3.0 is not acceptable. This definition of a SPOIL is consistent with the earlier definition involving impure targets [2] except that the three regions for judging the degree of acceptability of a pure target are narrower by a factor of two.

REFERENCES

1 E. R. Malinowski and D. G. Howery, Factor Analysis in Chemistry, Wiley-Interscience, New York, 1980.
2 E. R. Malinowski, Anal. Chim. Acta, 103 (1978) 339.
3 E. R. Malinowski, Anal. Chem., 49 (1977) 606.

Analytica Chimica Acta, 133 (1981) 103—108
Computer Techniques and Optimization

Short Communication

THE USE OF THE MODIFIED SIMPLEX METHOD FOR AUTOMATIC PHASE CORRECTION IN FOURIER-TRANSFORM NUCLEAR MAGNETIC RESONANCE SPECTROSCOPY

MARSHALL M. SIEGEL

FMC Corp., Research and Development Center, Princeton, NJ 08540 (U.S.A.)

(Received 29th April 1980)

Summary. FT-n.m.r. spectra were automatically phase-corrected using the modified simplex method. Three optimization criteria for phase correction were investigated. Best results were obtained by maximization of the intensity minimum and maximization of the summed intensities below the baseline. The maximization of spectral area consistently failed to correct the spectral data satisfactorily.

Phase shifts create distortions in Fourier transform n.m.r. spectra. The three major causes for phase shifts [1] are: misadjustment of the phase dectector; delays between the initial r.f. pulse and the start of data acquisition; and phase shift caused by electronic filtering of the n.m.r. signal. The first of these phase errors is frequency-independent, whereas the other two errors generally vary linearly with frequency. Corrections for these phase shifts can be expressed for the absorption (real) mode of a FT-n.m.r. spectrum as

$$A_j' = A_j \cos\theta_j - D_j \sin\theta_j \tag{1}$$

where A_j' is the phase-corrected absorption mode intensity for data point j; A_j and D_j are the original absorption and dispersion mode intensities for data point j; and

$$\theta_j = \alpha + 2j\beta/N \tag{2}$$

where α is the frequency-independent phase correction angle; β is the frequency-dependent phase correction angle; and N is the total number of data points. It is assumed in eqn. (2) that data acquisition is such that the frequency interval between all adjacent points is equal and that the data points are counted starting from the irradiation frequency.

Phase correction in FT-n.m.r. can be achieved by spectrometer calibration [2], or by estimating the phase angles α and β that best fit the spectral data. In most commercial FT-n.m.r. spectrometers, the latter method is followed; the phase angles α and β are entered manually into the data system and

substituted into eqns. (2) and (1). This manual process is repeated until the desired phase-corrected absorption n.m.r. spectrum is obtained.

Especially when the irradiation frequency, sample insert and sample type are changed frequently, this popular manual iterative process often becomes tedious, because of the interaction of the α and β phase angles on the corrected spectrum. An automated procedure was therefore sought which would be applicable under general operating conditions. The modified simplex method [3, 4] was considered to be useful for automating the iterative process to establish optimum values for α and β. Three different optimization criteria were evaluated: maximization of the absorption mode summed intensities (integrated area) [5]; maximization of the summed absorption mode intensities (integrated area) below the baseline (this can also be expressed as minimization of the absolute area below the baseline); and maximization of the minimum spectral absorption mode intensity.

Application of the modified simplex method

The modified simplex method [3, 4] is an iterative optimization method suitable for computer automation in which all the variables are changed simultaneously. When applied to the FT-n.m.r. phase correction problem, the simplest version is appropriate as there are only two independent variables, α and β, which have no boundary conditions. The simplex converges very rapidly and requires little computer memory for computation and storage. The modified simplex algorithm is illustrated in Figs. 1 and 2. Initially, three pairs of phase angles α and β are chosen, corresponding to points L, M and S, substituted into eqn. (2) and the summed absorption intensities (integrated area) $I = \Sigma_{j=1}^{N} A_j'(\alpha,\beta)$, or the summed intensities below the baseline, or

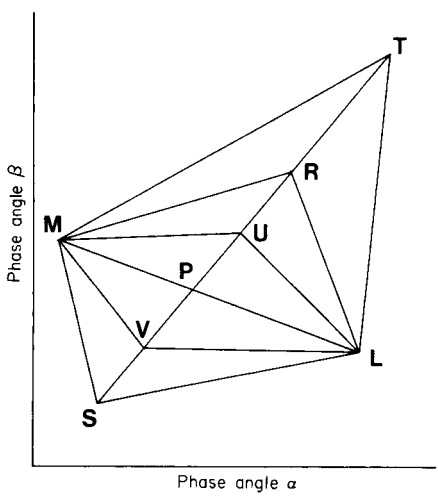

Fig. 1. Possible moves in the modified simplex method in α—β phase angle space.

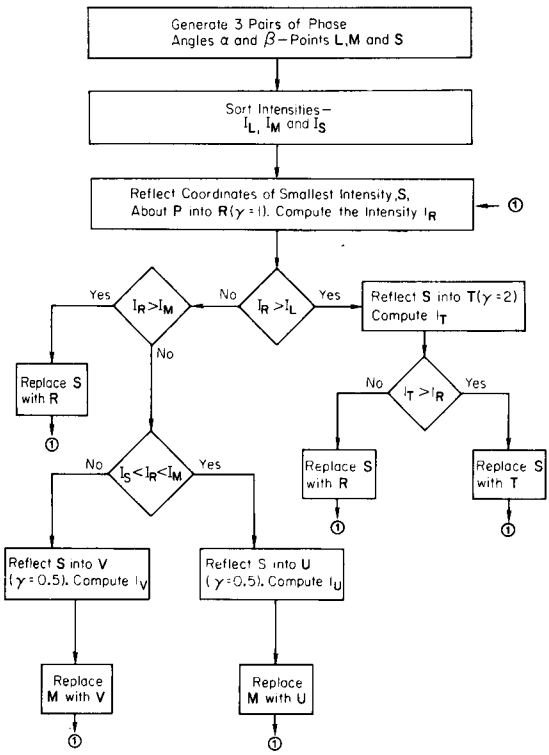

Fig. 2. Block flow diagram for applying modified simplex method to phase corrections in FT-n.m.r.

the minimum spectral absorption mode intensity is computed for each of the phase angle pairs, viz., intensities I_L, I_S and I_M, respectively. A two-dimensional plot of these points in an α—β coordinate system produces the triangular pattern ΔLMS illustrated in Fig. 1.

The modified simplex algorithm proceeds to generate new phase-angle coordinates by reflecting the point corresponding to the smallest intensity, S, and reflecting it about the midpoint, P, of the line $\overline{LM}$. This reflection process can include expansion or contraction to generate the new point, N, which can be computed from $N = P + \gamma\,(P - S)$, where $\gamma = 1$ for pure reflection, $\gamma = 2$ for an expanded reflection and $\gamma = 0.5$ or -0.5 for a contracted reflection. The new coordinates generated by the equation for N corresponding to $\gamma = 1$, 2, 0.5 and -0.5 are illustrated in Fig. 1 as points R, T, U and V, respectively. Initially, γ is set equal to 1 to generate point R with an intensity of I_R. If $I_R > I_L$, the reflection operation is expanded by setting $\gamma = 2$ to generate point T. If $I_T > I_R > I_L$, replace S with T and continue the iteration. If, however, $I_L > I_T > I_R > I_M$, replace S with R and proceed with another iteration. If $I_S < I_R < I_M$, the reflection operation is contracted by setting $\gamma = 0.5$ to generate point U. Compute I_U, replace point M with point U, and

iterate. This process changes the direction of motion of the simplex. If $I_R < I_S$, the reflection operation is contracted further by setting $\gamma = -0.5$ to generate point V. Compute I_V, replace point M with point V and iterate. This changes the direction of the iteration. The flow diagram is shown in Fig. 2.

The modified simplex iteration is ended when intensity changes become very small or zero for a preset number of consecutive iterations, or by limiting the number of iterations. Convergence of the simplex is assured when very different initial phase angle pairs produce similar spectra.

Experimental

Free-induction decay data (or n.m.r. spectra) were transmitted from a Varian FT-80A n.m.r. spectrometer to a Digital Equipment Corp. PDP 11/70 mini-computer equipped with an RSX-11M multi-user, multi-task operating system. The decay data were transformed using the Sande—Tukey Radix-2 fast Fourier transform algorithm [6] and phase-corrected either in segments or as a whole by the above modified simplex algorithms programmed in FORTRAN IV. The resulting spectrum was displayed on a Hewlett-Packard Model 2648A Graphics Terminal and a hard copy produced on a Hewlett-Packard Model 7221A Graphics Plotter. This experimental procedure was not optimized but was chosen for convenient demonstration of the automatic phase-correction procedure. Newer FT-n.m.r. data systems have higher-level operating systems in which the suggested simplex algorithms can be readily incorporated without resorting to a host data system.

The above algorithms were checked with synthetically generated phase-distorted spectra with and without noise. Also, a series of samples was run in the ^1H and ^{13}C modes under various operating conditions including cases where the frequency-dependent phase angle was systematically changed by varying the delay between the initial r.f. pulse and the start of data acquisition. In all cases checked, satisfactory phase corrections were obtained in reasonable time relative to that of an experienced operator.

Results and discussion

Typical criteria used in displaying phase-corrected FT-n.m.r. spectra are symmetrical line shapes and flat baselines with only random noise below the baseline. The improvements which can be achieved by the proposed automated method are illustrated for ethylbenzene. Figure 3 shows phase-corrected and uncorrected proton FT-n.m.r. spectra of ethylbenzene in DMSO-d_6. Spectrum A, which is the raw real component of the FT decay signal shows the phase distortions of the aliphatic proton signals. Spectrum B was obtained from maximization of the summed intensities as a function of the two phase angles. The integrated area is about 1.0% greater than that of the phase-uncorrected spectrum A. The unexpected feature of spectrum B is that area maximization occurred at the expense of additional phase distortion in each of the three absorption regions. Apparently, the algorithm optimized at a point where the positive and negative areas caused by phase

distortions were compensated so as to increase the net total intensity sum of the spectra. This effect produced an unacceptable phase-corrected spectrum. Spectrum C was obtained by maximizing the summed spectral intensities that are below the baseline as a function of the two phase angles. The ring and benzyl protons give symmetrical peaks and the methyl proton region is almost phase-corrected except for some intensity below the baseline. Spectrum D was obtained by adjusting the phase angles so as to maximize the lowest spectral intensity in the spectrum. All spectral lines appear to be phase-corrected. The peak shape of the ring protons is not symmetrical at the base. The manually obtained phase-corrected spectrum was identical to spectrum D.

Random noise was added to the proton free induction decay of ethylbenzene to study the effect of noise on the optimization procedures. As expected, the resultant spectra optimized as in Fig. 3, but the differences in the spectra between the maximum area below the baseline and maximum intensity minimum techniques were blurred by the baseline noise.

Similar results were obtained with various compounds. Maximization of integrated area generally failed to improve the spectra and on occasion created increased distortion; the main cause of these poor results is the effect of the phase correction in raising the baseline during the iterative optimization procedure about unsymmetrical line shapes to maximize the area.

In some cases, where the phase-angle correction is not satisfied by eqn. (2), corrections are best obtained by phase-correcting segments of the spectrum rather than the whole spectrum. This option was incorporated into the software and should be useful for phase-correcting spectra in which strong solvent absorptions are attenuated by a notch filter [7]. To increase the speed of iteration, the phase-correction procedure can be initiated using every second, third, or even fourth data point. After convergence, the optimization can then be fine-tuned using all the data points.

Fig. 3. Proton FT-n.m.r. spectra of ethylbenzene in DMSO-d_6. (A) Raw absorption mode data; (B) data phase-corrected using maximum area method; (C) data phase-corrected maximizing the summed intensities below the baseline; (D) data phase-corrected maximizing the intensity minimum.

Ernst [8] used the simplex method to optimize magnetic field homogeneity in n.m.r. spectrometers. In the near future, n.m.r. simplex software could be fully integrated with spectrometer hardware for automatically turning the spectrometer and phase correcting the spectrum.

REFERENCES

1 J. W. Cooper, The Computer in Fourier Transform NMR in G. C. Levy (Ed.), Topics in Carbon-13 NMR Spectroscopy, Vol. II, J. Wiley, New York, 1976, Chapt. 7.
2 B. L. Neff, J. L. Ackerman and J. S. Waugh, J. Magn. Reson., 25 (1977) 235.
3 J. A. Nelder and R. Mead, Comput. J., 7 (1965) 308.
4 S. N. Deming and S. L. Morgan, Anal. Chem., 45 (1973) 278A.
5 R. R. Ernst, J. Magn. Reson., 1 (1969) 7.
6 P. Bloomfield, Fourier Analyses of Time Series: An Introduction, J. Wiley, New York, 1976, pp. 75—76.
7 A. G. Marshall, T. Marcus and J. Sallas, J. Magn. Reson., 35 (1979) 227.
8 R. R. Ernst, Rev. Sci. Instrum., 39 (1968) 998.

Evaluation and Optimization of Laboratory Methods and Analytical Procedures

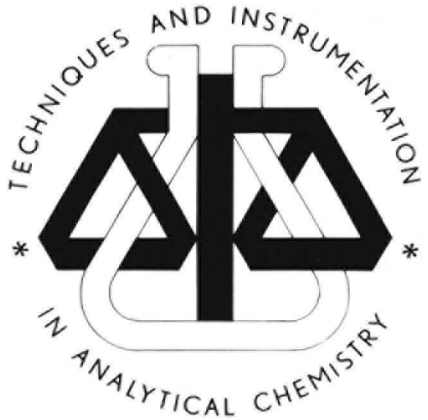

A Survey of Statistical and Mathematical Techniques

D.L. MASSART, A. DIJKSTRA *and* L. KAUFMAN.

with contributions by S. Wold, B. Vandeginste *and* Y. Michotte

Techniques and Instrumentation in Analytical Chemistry - Volume 1

This book provides detailed treatment, in a single volume, of formal methods for optimization in analytical chemistry. It is a comprehensive and practical handbook which no analytical laboratory will want to be without.

All aspects of optimization are discussed, from the simple evaluation of procedures to the organization of laboratories or the selection of optimal complex analytical programmes. Quantitative discrete analysis as well as qualitative and continuous measurement techniques are evaluated.

The book consists of 30 chapters divided into 5 main parts.The main sections are: Evaluation of the Performance of Analytical Procedures, Experimental Optimization, Combinatorial Problems, Requirements for Analytical Procedures, and Systems Approach in Analytical Chemistry.

This work will be of practical value not only to those involved with optimization problems in analytical chemistry, but also to those in related fields such as clinical chemistry or specialized fields such as chromatography. Because it discusses the application of many mathematical techniques in analytical chemistry, this book will also serve as a general introduction to the new field of Chemometrics.

1978 1st Reprint 1979 xvi + 596 pages US $68.25 / Dfl. 140.00
ISBN 0-444-41743-5

ELSEVIER

P.O. Box 211,
1000 AE Amsterdam
The Netherlands

52 Vanderbilt Ave
New York, N.Y. 10017

The Dutch guilder price is definitive. US $ prices are subject to exchange rate fluctuations.

7113

VOL. 133, No. 1 ANALYTICA CHIMICA ACTA February 1, 1981

(Computer Techniques and Optimization, Vol. 5, No. 1)

CONTENTS

Printed in The Netherlands